UNIVERSITA' DEGLI STUDI DI VERONA

DIPARTIMENTO DI
SCIENZE NEUROLOGICHE, NEUROPSICOLOGICHE,
MORFOLOGICHE E MOTORIE

SCUOLA DI DOTTORATO DI
SCIENZE INGEGNERIA MEDICINA

DOTTORATO DI RICERCA IN
NEUROSCIENZE

Con il contributo di
ISTITUTO DI CIBERNETICA "E.CAIANIELLO" C.N.R. POZZUOLI

CICLO XXIV

"ENDOCANNABINOID-CONTROLLED MODULATION OF OREXINERGIC NEURONS IN OBESITY: SWITCH FROM EXCITATORY TO INHIBITORY WIRING"

S.S.D. BIO/17

Coordinatore: Prof. Michele Tinazzi

Tutor: Dr. Luigia Cristino

Dottorando: Dr. Roberta Imperatore

INDEX

INTRODUCTION

ABSTRACT

Acute or chronic alterations in energy status lead to changes in the balance between excitatory and inhibitory synaptic transmission and associated synaptic plasticity, facilitating adaptation of energy metabolism to new homeostatic requirements. The impact of such changes, especially during obesity, on endocannabinoid signalling at CB1 receptors, a master modulator of synaptic transmission and strength, and a target for anti-obesity drugs, is not well understood. Endocannabinoids stimulate food intake and their synthesis and release increase after food-deprivation thus inducing activation of CB1 receptors. In particular, endocannabinoid levels increase in the hypothalamus and blood during short-term fasting (1, 2) and decrease after leptin administration and feeding (3, 4). Impairment of leptin signaling (db/db mice expressing a defective leptin receptor), leptin deficiency (ob/ob), and leptin resistance (acquired resistance due to diet-induced obesity, HFD mice) in mice showed elevated levels of Endocannabinoids in the hypothalamus and in adipose tissue (5). Recent papers show that leptin modulates also the axonal growth and synaptic plasticity within the hypothalamus (6,7). In particular, leptin increases neurite extension in the Arcuate Nucleus during mouse perinatal development, thus playing an early trophic role within those circuits that will be the target of leptin physiological actions in adult life (6). Leptin also may act on the Orexinergic-synthesizing (OX) neurons of the lateral hypothalamus, which send widespread projections to the brain (8) playing a strategic integrative role in the feeding. Leptin suppress the activity of OX neurons, the biosynthesis of OX or both. Moreover, an OX_1R-selective antagonist reduced food intake and ameliorated obesity of leptin-deficient ob/ob mice (9), suggesting that leptin deficiency at least partly activates the orexin pathway to increase food intake. On the other hand, pretreatment with subeffective doses of rimonabant, a selective CB1 antagonist, attenuates the orexigenic actions of OX (10), whereas electrophysiological data support the inhibitory role of cannabinoids on orexinergic neurons in physiological conditions (11). Staring from these bases, we investigated if a remodeling of orexinergic neuronal wiring occurs in the LH during a prolonged nutritional perturbation caused by, or resulting in, leptin signalling deficiency, as in ob/ob and HFD mice, respectively, and its impact on neuromodulatory function of the endocannabinoid system, since high neural plasticity occurs in this circuitry for adequate regulation of energy balance (12).

Alterazioni acute o croniche dello stato energetico provocano cambiamenti negli equilibri tra trasmissione sinaptica eccitatoria ed inibitoria e nella plasticità sinaptica ad essi associata, favorendo l'adattamento del metabolismo energetico alle nuove esigenze omeostatiche. L'impatto di tali cambiamenti, in particolare durante l'obesità, sul segnale degli endocannabinoidi sui recettori CB1, uno dei principali modulatori della trasmissione sinaptica, e uno dei target per i farmaci anti-obesità, non è ben compreso. Gli endocannabinoidi stimolano l'assunzione di cibo e la loro sintesi e rilascio aumentano dopo deprivazione di cibo, inducendo così l'attivazione dei recettori CB1. In particolare i livelli di endocannabinoidi aumentano nell'ipotalamo e nel sangue durante brevi periodi di digiuno (1, 2) e diminuiscono in seguito a somministrazione di leptina e dopo assunzione di cibo (3, 4). Topi con riduzione dei segnali della leptina (topi db/db che esprimono un recettore difettoso della leptina), con carenza di leptina (ob/ob), e con resistenza alla leptina (resistenza acquisita a causa dell' obesità indotta da dieta, topi HFD) presentano elevati livelli di endocannabinoidi nell'ipotalamo e nel tessuto adiposo (5). Lavori recenti mostrano che la leptina modula anche la crescita degli assoni e la plasticità sinaptica nell'ipotalamo (6,7). In particolare, la leptina incrementa l'estensione degli assoni nel Nucleo Arcuato durante lo sviluppo perinatale del topo, svolgendo così un ruolo trofico all'interno di quei circuiti che saranno oggetto delle azioni fisiologiche della leptina nella vita adulta (6). La leptina può anche agire sui neuroni sintetizzanti Orexina (OX) dell'ipotalamo laterale, i quali inviano proiezioni diffuse al cervello (8) svolgendo un ruolo integrativo strategico nell'alimentazione. La leptina sopprime l'attività dei neuroni OX, la loro biosintesi o entrambi. Inoltre, un antagonista selettivo del recettore OX_1R riduce l'assunzione di cibo e diminuisce l'obesità in topi ob/ob (9), suggerendo che la carenza di leptina, almeno in parte, attiva il patway dell'orexina per aumentare l'assunzione di cibo. D'altra parte, il pretrattamento con dosi sub-efficaci di rimonabant, un antagonista selettivo del CB1, attenua l'azione oressigenica dell'OX (10), mentre dati elettrofisiologici sostengono un ruolo inibitorio dei cannabinoidi sui neuroni orexinergici in condizioni fisiologiche (11). Partendo da queste basi, abbiamo studiato se un rimodellamento del wiring neuronale orexinergico si verifica nell'LH nel corso di una prolungata perturbazione nutrizionale causata da, o risultante in, carenza di segnalazione della leptina, come in topi ob/ob e topi HFD, rispettivamente, ed il suo impatto sulla funzione neuromodulatoria del sistema endocannabinoide, dato che un' alta plasticità neuronale si verifica in questo circuito per un' adeguata regolazione del bilancio energetico (12).

The Endocannabnoid System

Cannabis sativa has been used since antiquity to treat many ailments, including eating disorders. In 1964 a group of Israeli researchers was able to isolate and synthesize the delta-9-tetraidrocannabinolo (Δ9-THC), the most powerful of the numerous active ingredients in cannabis (13, 14). Since that time, there have been many dramatic breakthroughs in understanding the molecular mechanisms underlying the pharmacological action of Δ9-THC. More recently, in 1988, researchers discovered the presence in the body of a membrane receptor capable of being activated by Δ9-THC (15). These discoveries have opened new horizons to a possible therapeutic use of Cannabis sativa. Cannabis contains over 400 chemical compounds, of which 70 are structurally related to Δ9-THC and are collectively known as cannabinoids (16). Some of these compounds possess THC-like effects, though many act through different mechanisms of action and possess unknown pharmacology. The term cannabinoids usually displayed not only the cannabinoids from plant, but also all the ligands of cannabinoid receptors, i.e. those of plant origin, but also the endogenous molecules and some molecules of synthetic origin. These molecules are called, respectively, fitocannabinoids, endocannabinoids (ECs) and "classic cannabinoids" (to distinguish them from synthetic molecules, with a not cannabinoid structure but still able to activate the cannabinoid receptors). The chemical characterization of the Δ9-THC by Mechoulam and Gaoni in 1964 had allowed a number of important clarifications, especially regarding its mechanism of action (13,14). The studies focused more on Δ9-THC because of its clear psychotropic activity and the social implications of it. The strong hydrophobic nature of this compound suggested that its effects might be due to a general non-specific perturbation of cell membranes rather than to a specific interaction with selective binding sites. It was only thanks to the synthesis of enantiomers of THC and its synthetic analogues (17, 18), and to the subsequent discovery that its principal pharmacological actions were enantioselective, that the idea of a ‘cannabinoid’ receptor was put forward. The discovery of the cannabinoid receptor was a completely random event because it happened in the course of an accurate screening of the DNA of the rat to find the genes of receptors for the neurochinine. On that occasion, in fact, was found an "orphan ligand" receptor, whose distribution coincided with a known brain cannabinoid radiolabeled ligand ([3H]-CP-55940). The suspicion that it was the cannabinoid receptor, was finally confirmed in 1988, when subsequent investigations decreed that the isolated receptor in rat brain, was actually the

specific receptor through which cannabinoids mediate behavioral and pharmacological effects (15). This receptor was named CB1, because shortly after, was identified, by homology cloning, a second receptor, CB2, which explained the immunosuppressive effects of cannabis derivatives in the immune system. Subsequently, the two receptor subtypes were better characterized: the CB1 receptor has been cloned in 1990 (19) while the CB2 receptor has been cloned in 1993 (20). The two cloned receptor subtypes (CB1 and CB2) belong to the family of membrane receptors coupled to G proteins and, as such, they present a single polypeptide chain that crosses the plasma membrane seven times. The amino acid sequence has the amino terminus, with the sites of glycosylation, on the extracellular side and the carboxyl terminus, with the sites of phosphorylation, on the intracellular side. Both receptors are Gi/o protein-coupled receptors type, being able to inhibit adenylyl cyclase and to activate the mitogen-activated protein kinase (MAPK) (21). The activation of CB1 is also able to inhibit the L-, N-, and P/Q-type voltage-gated calcium channels (22, 23), while it has the opposite effect on A-type potassium channels and on inwardly-rectifying Kþ channels (24). In some cases, the activation of the CB1 stimulates phospholipase C, thus indicating its coupling with a protein of the type Gq or Gs (25). Studies carried out immediately after the molecular characterization of CB1 and CB2 receptors established the distribution of their mRNAs in several mammalian tissues, with a very high abundance of CB1 in the central nervous system (CNS) and in peripheral tissue (e.g., liver and adipocytes), and of CB2 in immunocompetent cells and tissues. We now know, however, that both receptors, and CB1 in particular, are much more widely distributed than originally believed. For example, the liver, initially used as a 'negative control' to validate probes and antibodies designed to detect the CB1 receptor, is now known to express a low but nevertheless functionally important amount of this protein (26). On the other hand, the CB2 receptors, the existence of which in the brain had been initially ruled out, have been shown to be expressed in low amounts also in this organ during neuroinflammatory conditions (27), and even in central neurons under physiological conditions (28, 29). As a consequence, the original idea that CB1 receptors played a role almost uniquely in the brain, and CB2 in the immune system, has now evolved into the concept that either cannabinoid receptor type might control several general central and peripheral functions, including neuronal development, transmission and inflammation, cardiovascular, respiratory and reproductive functions, hormone release and action, bone formation and energy metabolism, as well as cellular functions such as cell architecture, proliferation, motility,

adhesion and apoptosis (30-33). The wide distribution of CB1 throughout the CNS explains the plethora of physiological processes that this system modulates, including cognition, pain, memory, attention, reward, motor behavior, and feeding. Specifically, in terms of energy regulation and feeding behavior, CB1 receptors can be found in the hypothalamus, nucleus accumbens, vagus nerve, nodose ganglion, myenteric neurons, epithelial cells of the gastrointestinal tract, adipocytes, and the liver (34, 35). At the level of the peripheral nervous system, CB1 was found in peripheral sensory fibers and autosomal (interneurons in the spinal dorsal root ganglia, the myenteric neurons in the pre-junctional fibers of the bladder and in the superior cervical ganglion sympathetic fibers) in perfect agreement with some of the reported effects on nociception and functions of the vascular and gastrointestinal tract (34, 36-38). The CB2 receptor instead, at least in physiological conditions, turns out to be much more abundant in the immune system (mast cells, B cells, T lymphocytes) where it is implicated in the control of both humoral and cellular immune response (39, 40). The revelation of the existence of specific receptors for THC was quickly followed by the frantic search of endogenous ligands for these proteins (endocannabinoids, ECs). THC acts upon an endogenous cannabinoid system (ECS) that modulates a variety of physiological systems, including pain, inflammation, feeding, energy balance, memory, attention, and reward processing. This rather complex and pleiotropic endogenous signalling system was discovered in the late 1990s, starting from studies on the mechanism of action of Δ9-THC. This system includes: 1) at least two G-protein-coupled receptors, known as the cannabinoid CB1 and CB2 receptors; 2) the endogenous agonists at these receptors, known as endocannabinoids, of which anandamide (AEA) and 2-arachidonoylglycerol (2-AG) are the best known; and 3) proteins and enzymes for the regulation of endocannabinoid levels and action at receptors (Fig.1).

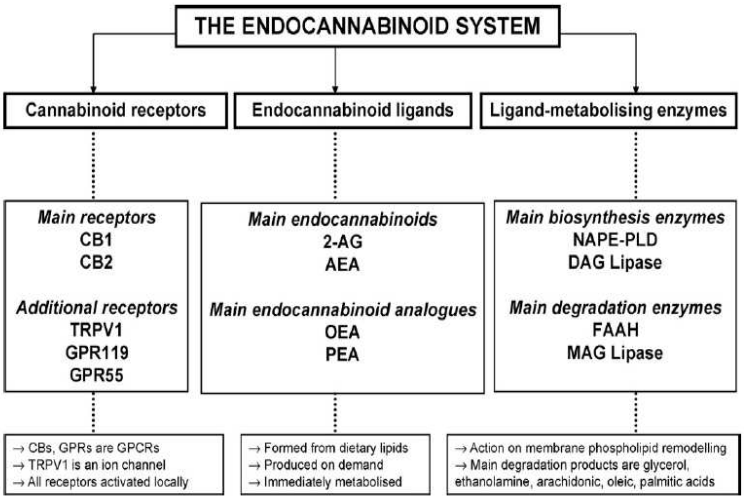

Fig. 1: *Overview of the molecular composition of the Endocannabinoid system*

The endocannabinoid system: biochemical and molecular aspects

The discovery of the CB1 receptor was followed, in 1992, by the isolation, from the pig brain, of the first endogenous metabolite able to bind selectively to this protein. The first such compound to be discovered was anandamide (AEA, arachidonoyl ethanolamide, from the Sanskrit word ananda for ‘bliss’) (41), and this finding was soon to be followed by the identification of the cannabimimetic properties of an already known endogenous metabolite, 2-arachidonoylglycerol (2-AG) (42, 43). The AEA is able to bind both receptor subtypes behaving as a partial agonist (44, 45); also the 2-AG is able to activate both receptor subtypes, however, behaving as a full agonist (42). The fact that there were endogenous molecules able to play a physiological role, necessarily imply the existence of biosynthetic pathways adjustable, or of specific molecular mechanisms able to synthesize these substances in the appropriate ways, places and times. Also, must necessarily exist a catabolic pathway can be adjusted to terminate the signal at the appropriate time. The ECs are considered as local neuromodulators that, unlike other neuromodulators, are not stored in secretory vesicles, but are produced on demand (on request) from the cells, from precursors of membrane before being released into the extracellular side, similarly to other eicosanoids such as prostaglandins. ECs are produced 'on demand' to help restore the levels and function of other mediators (including excitatory and inhibitory neurotransmitters) after acute or chronic alterations of the

physiological homeostasis of the cell (31). In the nervous system the ECs work as retrograde messengers from the post-synaptic to presynaptic terminals where they modulate (inhibit) neurotransmitter release through activation of CB1 receptors (46). Thus, endocannabinoids can either facilitate inhibitory or excitatory post-synaptic potentials depending upon the type of neurons on which their receptors are expressed. Moreover, they have been discovered to play a prominent role both in short-term and in long-term synaptic plasticity, as well as to directly control the rate of firing of presynaptic cells. The short-term inhibitory actions of cannabinoids on afferent GABAergic and glutamatergic transmission are respectively known as depolarization-induced suppression of inhibition, or DSI, and depolarization-induced suppression of excitation, or DSE. DSI/DSE are well characterized in the hippocampus and cerebellum and have been observed in other brain areas (47,48) (Fig.2).

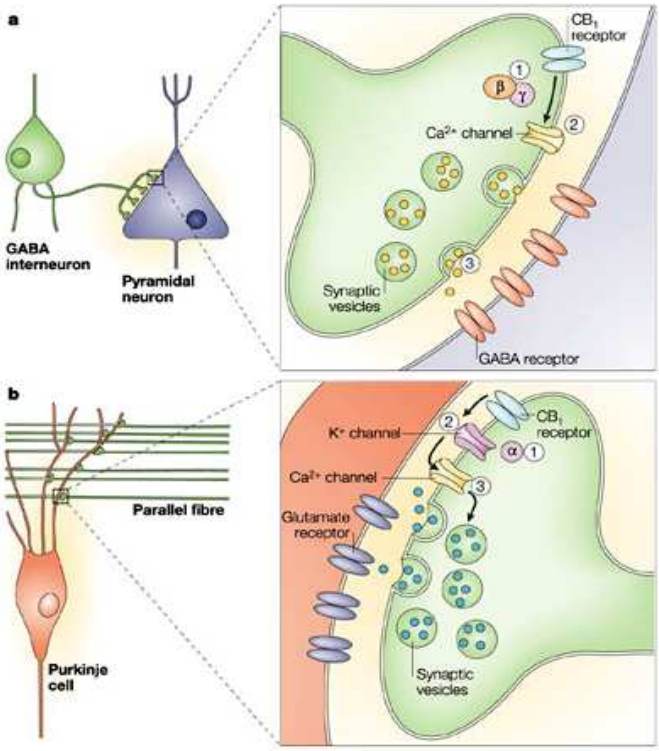

Fig. 2: *Regulation of presynaptic ion channel activities by CB1 cannabinoid receptors.* ***a)*** *At synapses between GABA (γ-aminobutyric acid) interneurons and pyramidal cells: activation of CB1 receptors can initiate a series of intracellular events, which include (1) activation of G-protein β–γ subunits, (2) closure of voltage-gated* Ca^{2+} *channels and (3) inhibition of GABA release.* ***b)*** *At parallel fibre–Purkinje cell synapses in the cerebellum: CB1 activation can (1) engage G-protein α-subunits that (2) cause the opening of* K^{+} *channels; the resulting membrane hyperpolarization can (3) reduce* Ca^{2+} *entry and inhibit glutamate release. Mechanisms similar to those illustrated above are thought to underlie cannabinoid-mediated inhibition of neurotransmitter release in other brain regions.*

Studies on the biosynthetic and catabolic pathways and enzymes for anandamide and 2-AG started immediately after their discovery. The AEA is biosynthesized by the hydrolysis of the corresponding N-acyl-phosphatidylethanolamine (NAPE) through the work of a specific phospholipase type D Ca^{2+}-dependent (NAPE-PLD) that shows peculiar properties than other known PLD, in fact it belongs to the family of zinc-metal hydrolase of the β-lactamase (49). NAPE was shown to be produced from the transfer of arachidonic acid from the sn-1 position of membrane phospholipids to the nitrogen atom of phosphatidylethanolamine (50). Whereas diacylglycerol (DAG) precursors for 2-AG were shown to be produced either from the phospholipase-C-catalysed hydrolysis of phosphatidylinositol or from the hydrolysis of phosphatidic acid (51, 52). Have recently been cloned and characterized two isozymes of DAG lipase (DAGLα and DAGLβ) responsible for hydrolysis of the ester bond selective present at position sn-1 of the DAGs (53). Once synthesized, the ECs are released outside the cell, where do they bind to receptors on neighboring cells or on the same cell that produced them, acting as autocrine or paracrine mediators. Their fat-soluble nature, in fact, not favors the spread in the extracellular matrix or in the blood. Turning off the signal ECs provides, therefore, the re-uptake by the cell, enzymatic hydrolysis and re-esterification of the products obtained in membrane phospholipids. The re-uptake of ECs acts through a transport mechanism of facilitated diffusion driven by a specific carrier of membrane that would be able to work in both directions (incoming and outgoing from the cell) according to the gradient concentration of ECs across the plasma membrane. The existence of a specific carrier is still debated. After being seized by extracelluar side, the ECs, within the cell, are subject to enzymatic hydrolysis. Both AEA and 2-AG were found to be inactivated mostly by enzymatic hydrolysis of the amide and ester bonds, respectively, and the major enzymes responsible for these reactions were cloned and named fatty acid amide hydrolase (FAAH) (54), and monoacylglycerol lipase (MAGL) (55, 56), respectively. The FAAH is an integral membrane protein of approximately 64kDa which works at alkaline pH (the optimum is at pH 9.0), is formed from 597 amino acids and has a highly conserved sequence amidase, rich in glycine and serine residues. Studies of immunohistochemical and in situ hybridization, have confirmed that the expression of this enzyme in the various brain areas is directly related to the density of the CB1 receptor (57). The MAGL is present both on cytosol and plasma membrane where recognize 2-monoacylglycerols AG as a substrate (58, 59). The MAGL is a protein of 33kDa which belongs to the family of serine hydrolases expressed

especially in those areas of the brain where the CB1 receptors are more present (Fig. 3).

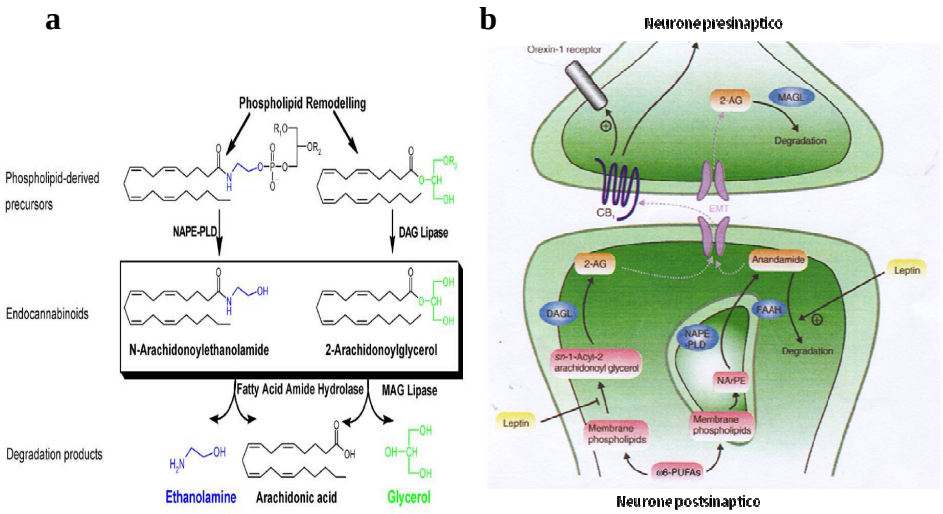

Fig. 3: ***a)*** *Biosynthesis and degradation pathways of Endocannabinoids.* ***b)*** *The endocannabinoid system in neurons. Diet-derived ω6-polyunsaturated fatty acids (ω6-PUFAs) are incorporated into membrane phospholipids, which can subsequently be metabolized into the two major endocannabinoids, 2-AG and anandamide, by membrane-associated enzymes. Degradative enzymes for endocannabinoids are localized to internal membranes. Leptin signaling can influence 2-AG biosynthesis in the hypothalamus and anandamide hydrolysis in T-lymphocytes. CB1 is located mostly presynaptically, allowing for retrograde action of endocannabinoids. DAGL: sn-1 selective diacylglycerol lipase; EMT: putative endocannabinoid membrane transporters; FAAH: fatty acid amide hydrolase; MAGL: monoacylglycerol lipase; NArPE: N-arachidonoyl-phosphatidyl-ethanolamine; NAPE-PLD: N-acyl-phosphatidylethanolamine selective phospholipase D. Blunt-ended line indicates inhibition.*

The endocannabinoid system: therapeutic effects

Considering the robust nature of cannabinoid activity, it is no surprise then that it is an area of interest for a wide range of potential therapeutic applications: the stimulation of this system reduces chemotherapy-induced nausea and emesis, increases appetite, and may stimulate lipogenesis. Nonetheless, a considerable amount of interest remains in understanding the role of the ECS in energy regulation. The effects of THC are mediated through the endocannabinoid system (ECS), which promotes a positive energy balance through stimulation of appetite as well as shifting homeostatic mechanisms toward energy storage. One of the best known pharmacological actions of THC on the brain is to reduce sensitivity to pain, for this is very useful as analgesic against diseases such as recurrent headaches or menstrual pain, but above all, by offering an anti-inflammatory is also useful in other types of pain such as those due to rheumatism (60-62). Cannabinoids are able to decontract the musculature, in fact, have an effect on muscle relaxant and antispastic. The first study on the effect of THC on beneficial muscle spasms of multiple sclerosis dates from the late ‘70 (63), recently, but was also shown the involvement of the ECS in the control of spasticity in some models animals of multiple sclerosis (64-67). The abundance of the EC and CB1 receptors in those regions of the basal ganglia (globus pallidus and substantia nigra), members of the movement, have prompted researchers to find out if the ECs were involved in the regulation of movement and, consequently, to take advantage of this involvement in related diseases. In an animal model of Parkinson's disease has been observed in increased levels of ECs in the reduction of movement in rats treated with reserpine, an animal model of Parkinson's disease (68); in another study was instead, demonstrated the possible involvement of ECs in the onset of dyskinesia, a troublesome side effect of levodopa therapy (69). The ECs are also involved in Alzheimer's disease, have been reported, in fact, the alterations in the ECS in tissues affected by this disease (70) and in addition, recently, it has been discovered that cannabinoids are able to counteract the effects of amyloid beta peptide (responsible for the neurodegeneration linked to Alzheimer's disease) (71, 72). Also as part of the neuro-degenerative diseases, studies have been conducted on Huntington's disease and has been observed a reduction of CB1 receptors in the globus pallidus and in the caudate-putamen in an animal model generated by the injection of 3-nitropropionic acid (73). The same group of researchers has realized, as a result, a work that demonstrates the therapeutic efficacy of THC in an animal model of Huntington

generated by injection of malonate (74). Other studies have been conducted in psychotic patients with schizophrenia, where it was observed that THC aggravates the symptoms of schizophrenia (75) suggesting that the basis of this disorder may be caused by malfunction of the ECS. The association of the latter with the circuits in the brain dopamine has been extensively investigated both from an anatomical point of view, that the biochemical and pharmacological (76) and confirmation of this, it was recently reported a study in which shows an alteration of the EC system in schizophrenic patients, not only in the central nervous system, but also in the blood (77). Cannabinoids also stimulate the appetite by acting through the activation of CB1 receptors, this observation suggested, therefore, the use of CB1 antagonists in the treatment of obesity. It is expected, in fact, the next marketing a selective antagonist of CB1 (Rimonabant, Acomplia) with the statement. In a study conducted on 48 mice genetically modified (deficient for the CB1), it was shown that the EC involved in fat metabolism by acting at the level of hepatic lipogenesis (26). The EC are also involved in some eating disorders because their blood levels are increased in anorexia nervosa (3). It was finally shown that malnutrition in pregnancy are decreased hypothalamic levels of AEA in the newborn, confirming that the ECs also play a crucial role in neonatal development (78).

The orexinergic system

In 1998, de Lecea et al. (79) discovered two mRNAs encoding for the same neuropeptides, named hypocretin-1 and -2. In the same year, Sakurai et al. (8) independently discovered the same neuropeptides while screening for ligands for orphan G-protein-coupled receptors, named orexin A and B (OX-A and OX-B). OX-A and OX-B constitute a novel distinct peptide family, showing no significant homology with any previously described peptides (80). These peptides have been called orexin, from the Greek word "orexis" meaning appetite, since the mRNA for the precursor of these peptides is expressed abundantly and specifically in the perifornical area of the LH, a region normally involved in the central regulation of feeding behavior and energy homeostasis (8, 80). Molecular cloning studies showed that both OX-A and OX-B are derived from a common precursor polypeptide of 131 amino-acid, prepro-orexin, with usual proteolytic processing presumably by pro-hormone convertases. OX-A is a 33-amino acid peptide of 3562 Da with two sets of intrachain disulfide bonds. It has an N-terminal pyroglutamyl residue and C-terminal amidation (8). The primary structure of OX-A predicted from the cDNA sequences is completely conserved among several mammalian species (human, rat, mouse, cow, sheep, dog, and pig). On the other hand, rat OX-B is a 28-amino acid, C-terminally amidated linear peptide of 2937 Da that is 46% (13/28) identical in sequence to OX-A. The C-terminal half of OX-B is very similar to that of OX-A (73%; 11/15), whereas the N-terminal half is variable. OX-B also has a high degree of sequence similarity among species. In the same year, by means of experiments, Sakurai et al. have also identified two subtypes of orexinergic receptors: orexin receptor-1 and orexin receptor-2 (OX_1R and OX_2R) (Fig.4). OX_1R was initially identified as an expressed sequence tag from human brain (8, 81). Subsequently, OX_2R was identified by searching an expressed sequence tag database by tBLASTn with the OX_1R sequence as a query (8). The amino acid identity between the fullength human OX_1R and OX_2R sequences is 64%. Amino acid identities between the human and rat counterparts of each of these receptors are 94% for OX_1R and 95% for OX_2R, indicating that both receptor genes are highly conserved between the species (8).

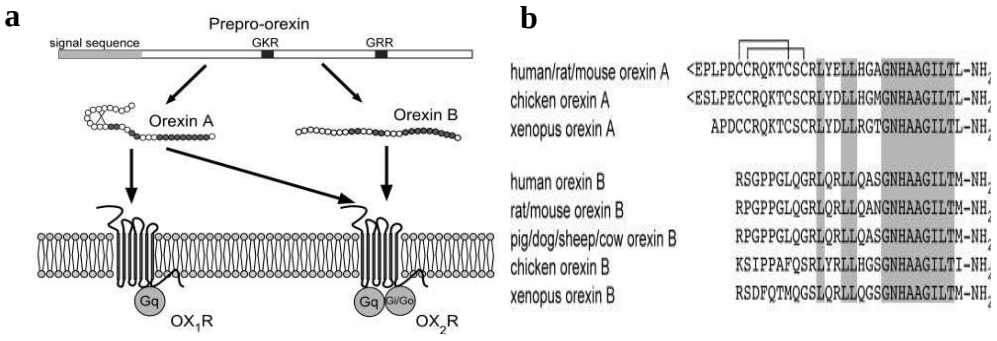

Fig. 4: *An overview of the orexin system.* ***a)*** *Orexins and their receptors. OX-A and OX-B are derived from a common precursor peptide, prepro-orexin. The actions of orexins are mediated via two G protein–coupled receptors OX_1R and OX_2R. OX_1R is selective for orexin A, whereas OX_2R is a nonselective receptor for both OX-A and OX-B. OX_1R is coupled exclusively to the Gq subclass of heterotrimeric G proteins, whereas OX_2R couples to Gi/o and /or Gq. It was revealed that the orexin receptors have different binding profiles for the respective orexinergic peptides: OX_1R has greater affinity for OX-A than OX-B by 1 order of magnitude; in contrast, OX_2R has similar affinity for both OX-A and OX-B (8). Furthermore, OX_1R is coupled to the Gq/11 class of G proteins, which results in activation of phospholipase C with subsequent triggering of the phosphatidylinositol cascade and influx of extracellular Na^+ and Ca^{2+}, presumably through TRP channels to cause depolarization of neurons. OX_2R is shown to be coupled to both Gq/11 and inhibitory Gi proteins when expressed in cell lines (82). So while OX-A and OX-B themselves are very similar, they may mediate distinct actions via binding to their receptors.* ***b)*** *Structure of mature OX-A and OX-B peptides. The topology of the two-intrachain bonds in OX-A is indicated above the sequence. Shadows indicate amino acid identity. Mammalian OX-A sequences thus far identified (human, rat, mouse, pig, dog, sheep, and cow) are all identical, whereas the sequences of OX-B show some differences among species.*

Distribution of orexinergic system

One of the most distinctive features of the orexinergic system is its restricted localization to a few thousand neurons in the lateral hypothalamus. The highest density of OX-immunoreactive fibres is observed within the hypothalamus, including the lateral hypothalamic area (LHA), perifornical area and posterior hypothalamus (83-85), with innervations in the lateral, dorsal and posterior areas, the paraventricular hypothalamic nucleus (PVN), arcurate nucleus (ARC) and supramammillary nucleus (83-85). Outside the hypothalamus, high OX terminal density can be observed in the following brain nuclei: locus coeruleus, septum, bed nucleus of the stria terminalis, thalamic paraventricular and reunion nuclei, periaqueductual grey, substantia nigra, raphe peribrachial pontine region, medullary reticular formation and the nucleus of the solitary tract. Less prominent projections are detectable in the cortex, amygdala, hippocampus and olfactory bulb (83, 85, 86). One of the primary reciprocal projection bundles innervates nuclei of the ascending arousal system such as the cholinergic pedunculopontine and laterodorsal tegmental nuclei, the serotonergic dorsal and median raphe nuclei, the noradrenergic LC, and the histaminergic tuberomammillary nucleus (83). By using conventional (87) and transgene-based (88) retrograde tracing several groups have shown that hypothalamic nuclei involved in circadian and metabolic integration such as the ARC nucleus, dorsomedial hypothalamus (DMH) and PVN nuclei send projections to OX cells. This anatomical structure suggests that the activity of OX neurons influences multiple brain areas. OX neurons were also showed to receive innervations from regions associated with energy homeostasis including neuropeptide Y- (NPY), agouti-related peptide, and α-melaninstimulating hormone-immunoreactive fibers, which presumably come from the ARC (89, 90). Despite colocalization of OX-A and OX-B in cell bodies (85), fibres immunoreactive for OX-A are more common in the brain than those immunoreactive for OX-B (91, 92). In the central nervous system, in situ hybridization studies have demonstrated that both OX receptor mRNAs are expressed in regions in which contain dense orexin innervations. OX_1R and OX_2R mRNAs show partially overlapping but largely distinct and complementary distribution patterns, suggesting that they play different physiological roles for each receptor subtype. OX_1R is expressed in many brain regions, such as the prefrontal and infralimbic cortex, hippocampus (cornu ammonis 2), amygdala, and bed nucleus of the stria terminalis (BST), paraventricular thalamic nucleus, anterior hypothalamus, dorsal raphe (DR), ventral tegmental area (VTA), LC, and

laterodorsal tegmental nucleus (LDT)/pedunculopontine nucleus (PPT) (93-95). OX_1R is also distributed in the peripheral tissues, such as kidney, adrenal, thyroid, testis, ovaries, and jejunum. OX_2R is expressed in the amygdala and BST, paraventricular thalamic nucleus, DR, VTA, and LDT/PPT (94, 95). On the other hand, OX_2R is abundantly expressed in the ARC, TMN, DMH, PVN nucleus, LHA in the hypothalamus, cornu ammonis 3 in the hippocampus, and medial septal nucleus (94, 95). OX_2R is found in adrenal glands, lung, and pituitary (96). The distribution of OX receptors is on the whole consistent with the location of the OX axons and OX mRNA-expressing neurons. Thus, the distribution patterns of OX_1R and OX_2R coincide in some regions but are distinct and complementary in some others. This suggests different physiological roles for each receptor subtype (fig. 5).

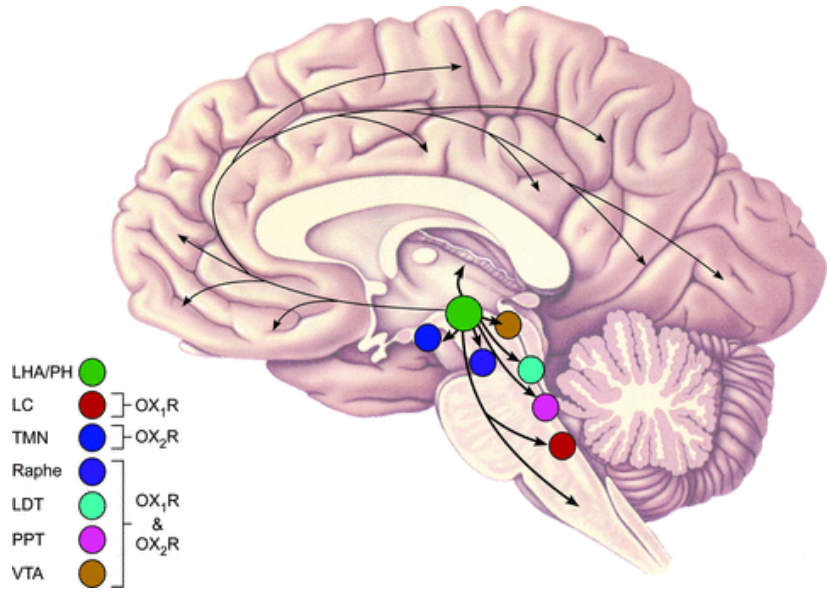

Fig. 5: *Major projections of orexin neurons. Circles show major target sites for orexins. Included in these are the LC (containing noradrenaline, NA), TMN (containing histamine, HA), raphe nuclei (Raphe, containing 5HT), VTA (containing dopamine, DA) and PPT/LDT (containing Ach).*

Functions of orexinergic system

The orexins were recognized as regulators of feeding behavior because of 1) their exclusive production in the LHA, a region known as the feeding center, and 2) their pharmacological activity since intracerebroventricular administration of OX induces food intake (8, 9, 97, 98). Supporting the physiological relevance of orexin in the control of feeding, ICV administration of an anti-orexin antibody or an OX_1R selective antagonist reduced food intake (98, 99). OX neurons are reciprocally connected to neurons of hypothalamic ARC for feeding regulation. The responsiveness of OX neurons to peripheral metabolic cues, such as leptin and glucose, suggest that these neurons have important role as a connection between the energy homeostasis and vigilance states. Consistent with the dense projection of OX neurons to the ARC (83, 84, 100), several studies have suggested that the increased food intake following OX-A administration is at least partly mediated by activation of NPY neurons in the ARC (100, 101). Other events involved in orexin-induced feeding behavior include inhibition of proopiomelanocortin (POMC) neurons in the ARC, which are thought to play an important role in leptin-mediated inhibition of food intake (101). Recent reports also showed that infusions of OX-A into the shell of the nucleus accumbens (NAc) increase feeding behavior (102). Moreover infusions of the GABAA receptor agonist muscimol into the NAc shell strongly induced food intake and simultaneously increased Fos expression specifically in OX neurons (103). These findings suggest that reciprocal interactions between the OX and limbic systems play a role in the regulation of feeding. In addition, the OX system stimulates feeding associated glucose utilization in skeletal muscle by activation of sympathetic nervous system through acting on the VMH (104). Although OX neurons are scarce, they have a profuse projection system to numerous brain regions involved in arousal and cortical activation and in sleep-wakefulness cycle regulation. In recent years it has become clear that these neuropeptides are involved in the regulation of many other organic functions, such as thermoregulation and neuroendocrine and cardiovascular control, whole-body energy expenditure, reward mechanisms as well as in the control of the sleep-wakefulness cycle. In particular dense sites of OX innervation include the locus coeruleus, DR, periacqueductal gray (PAG) and PVN of the thalamus, structures important for regulation of arousal and sleep. Indeed, OX deficiency in rodents and humans results in narcolepsy, and evidence suggests that OX crucially regulates the transition between sleeping and waking (105-109). OX neurons also send relays via the

hindbrain and spinal cord to regulate the autonomic and sympathetic nervous system (104, 110-112). Additionally, OX neurons innervate many regions involved in regulating behavior, including the amygdala, septal area, medial preoptic area, and substantia innominata as well as the VTA and the NAc, the main components of the mesolimbic dopaminergic (DA) system (113, 114). These histological findings suggest that orexins and their receptors are likely to play a broad regulatory role in the central nervous system and could regulate feeding, autonomic control, sleep, memory, and the reward system. Circadian modulation of OX cells is suggested by the presence of a small number of direct projections from the suprachiasmatic nucleus (SCN) (115), although most of the input is indirect through the DMH. In contrast, ascending projections mostly arrive from brainstem arousal centres. Histamine neurons in the tuberomammillary nucleus are also targets of OX neurones, and the reciprocal interactions between the histamine system and OX may have an important role in cortical arousal (116). These multifunctional neuropeptides modulate energy homeostasis, arousal, stress, reward, reproduction and cardiovascular function. OX neurons, in general, have a stimulatory effect on LH neurons, including melanin-concentrating hormone (MCH) neurons. Notably, OX neurons are rapidly activated by fasting and exhibit leptin-dependent synaptic plasticity during fasting. Elevated orexigenic output of the melanocortin system promote the activity of corticotropin releasing hormone (CRH)-producing neurons in the hypothalamus, which, in turn, can further activate OX neurons (117) (Fig 6).

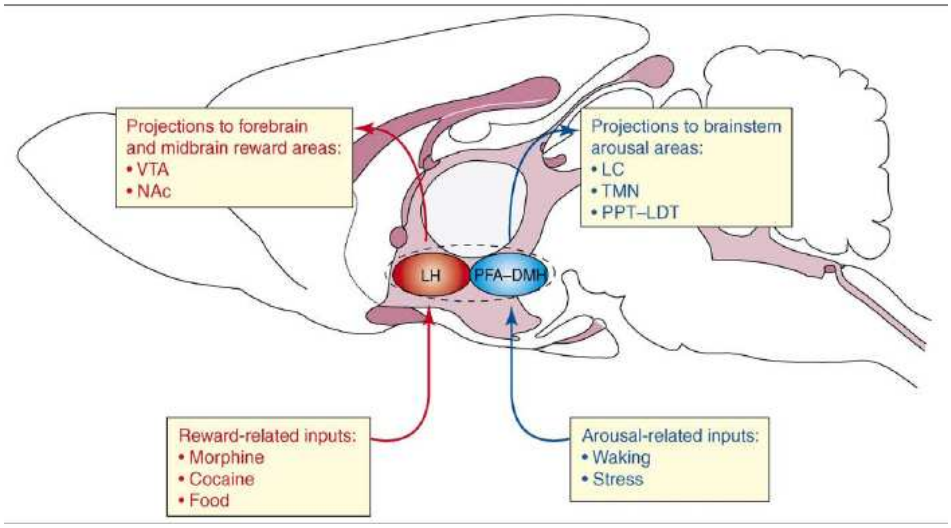

Fig. 6: *Orexin neurons in the lateral hypothalamic area (LHA) and posterior hypothalamus (PH) are anatomically well placed to provide a link between the limbic system, systems involved in energy homeostasis and monoaminergic and cholinergic neurons in the brain stem. Solid arrows show excitatory projections, and broken lines inhibitory ones. Wake-active regions, sleep-active regions and REM-active regions are shown by red, blue and green boxes, respectively. Orexin neurons promote wakefulness through the monoaminergic nuclei that are wake-active. Stimulation of dopaminergic centres by orexins can modulate reward systems (purple). Peripheral metabolic signals such as leptin, ghrelin and glucose influence orexin neuronal activity to coordinate arousal and energy homeostasis. The nucleus suprachiasmaticus (SCN), the central body clock, sends signals to orexin neurons via the dorsomedial hypothalamus (DMH). The DMH acts as a food-entrainable ossilator, and influences orexin neuronal activity. Input from the limbic system (amygdala and bed nucleus of the stria terminalis (BST)) might regulate the activity of orexin neurons upon emotional stimuli to evoke emotional arousal or fear-related responses. VLPO, ventrolateral preoptic area; DR, dorsal raphe; GABA, γ-aminobutyric acid; LC, locus coeruleus; LDT, laterodorsal tegmental nucleus; PPT, pedunculopontine tegmental nucleus; SNr, substantia nigra pars reticulata; TMN, tuberomammillary nucleus.*

Lateral hypothalamic area

The lateral hypothalamic area (LHA) is a large and heterogeneous area with several distinct nuclear groups and is one of the most extensively interconnected areas of the hypothalamus, allowing it to receive a vast array of interoceptive and exteroceptive information and to modulate cognitive, skeletal motor, autonomic, and endocrine functions. The LHA merges rostrally into the preoptic area and caudally into the ventral tegmental area. It borders medially to the dorsomedial, ventromedial, and arcuate nuclei and the anterior hypothalamic and medial preoptic areas, and laterally to the internal capsule, the optic tract, and more caudal to the subthalamic nucleus. There is no doubt that the LHA consists of numerous distinct nuclei (118, 119), but the function and connectivity of most of these subnuclei has not been systematically studied. Generally, the LHA can be divided into anterior, tuberal (roughly at the level of the ventromedial hypothalamus) and posterior portions based on its efferent connectivity as first described by Saper (119). Based on such verification, afferents to the lateral hypothalamic area have been demonstrated to originate from various cortico-limbic structures such as the prefrontal/orbitofrontal, insular, and olfactory cortex, amygdala, hippocampal formation, the shell of the nucleus accumbens, and from brainstem structures including most aminergic cell groups such as the nucleus of the solitary tract (120, 121). Afferents from medial portions of the hypothalamus, although generally sparse, are functionally highly significant, as for example, projections from the arcuate nucleus POMC/CART and NPY/AgRP neurons (90, 122, 123). Furthermore, given its size and structural complexity, there is considerable connectivity within the lateral hypothalamic area itself, particularly projections from anterior to more posterior portions (85, 90, 122, 123). Within the hypothalamus the lateral zone has efferent projections to most medial zone nuclei such as the arcuate, paraventricular, dorsomedial, ventromedial, and anterior hypothalamic nuclei (120). Another useful anatomic guide is the distribution pattern of two well studied neuronal populations that express either OX or MCH (118). OX neurons projection pattern is equally widespread throughout the brain but, in particular, OX neurons have been shown to project to the ARC and PVN nuclei (79, 85). MCH neurons project very broadly throughout the CNS (124, 125), and similarly MCH receptors are distributed equally broad in the brain. The LHA was originally described as a “feeding center” based on findings that LHA lesions produced extreme hypophagia (to the point of starvation) while electrical stimulation of the LHA promoted food intake even in sated

animals (124-129). Furthermore, MCH expression levels increase with fasting and are restored to fed levels with leptin injections (130). Intracerebroventricular MCH injections increase food intake (131), and MCH overexpression leads to obesity and insulin resistance (132), thus suggesting that MCH acts as a typical orexigenic neuropeptide that may regulate and integrate various aspects of feeding behavior (132). On the other hand, OX-A injections into the lateral ventricle increase food intake (133) and systemic injection of an OX receptor antagonist decreases food intake (134). OX gene expression does not increase by fasting but is strongly increased by leptin administration (130, 135, 136). Most neurons in the LHA express more than one peptide and in addition may express either one of the classical neurotransmitters glutamate or GABA (Fig. 7, 8).

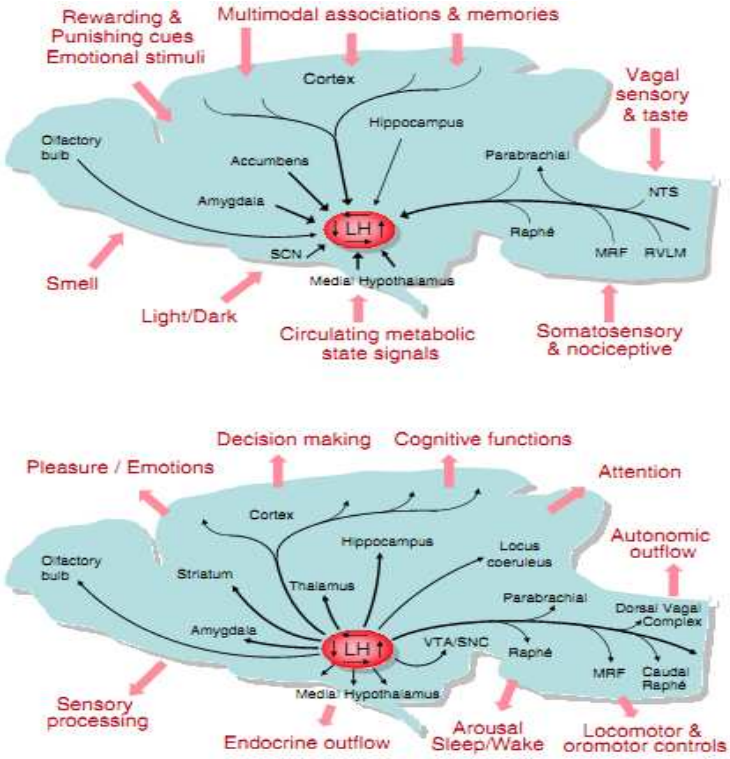

Fig. 7: *Schematic diagrams showing major inputs (top) and outputs (bottom) of the lateral hypothalamic area on an outline of the rat brain.*

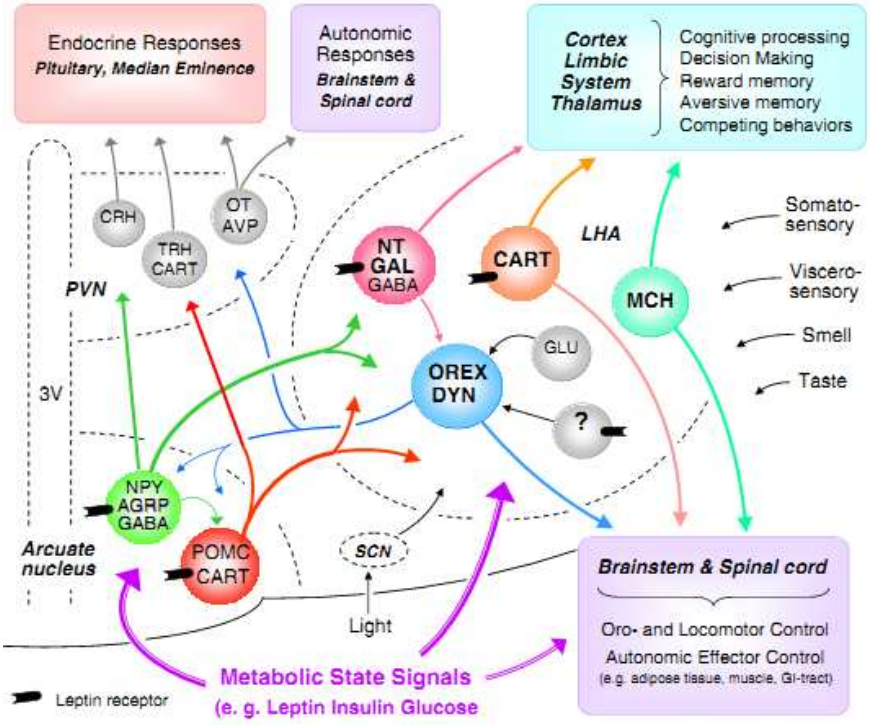

Fig. 8: *Interactions of lateral hypothalamic neurons with other hypothalamic areas and major behavioral, autonomic, and endocrine output pathways and functions. This highly simplified diagram does not show the relationship with other important hypothalamic nuclei such as the dorsomedial and ventral hypothalamic nuclei. Also not shown are the massive reciprocal connections from cortex and limbic structures to the lateral hypothalamic area. Arrows entering the three nuclei but not contacting individual neurons signifies potential input to all the different neuron types in that area. Abbreviations: AgRP, agouti-related protein; AVP, arginine-vasopressin; CART, cocaine and amphetamine-regulated transcript; CRH, corticotrophin-releasing hormone; DYN, dynorphin; GABA, gamma-aminobutyric acid; Gal, galanin, Glu, glutamate; MCH, melanin-concentrating hormone; NPY, neuropeptide Y; NT, neurotensin; ORX, orexin/hypocretin; OT, oxytocin; POMC, proopio-melanocortin; TRH, Thyrotropin-releasing hormone; LHA, lateral hypothalamic area; PVN, paraventricular nucleus of the hypothalamus; SCN, suprachiasmatic nucleus; 3V, third ventricle.*

Leptin

In 1950 the Jackson Laboratory identified a mouse line displaying profound hyperphagia, obesity, infertility and severe hyperglycemia resulting in diabetes. Nearly five decades later the genetic deficit underlying this phenotype was found to be a mutation on chromosome 6 in the obese (ob) gene and its gene product, leptin (137). It is a hormone produced by adipocytes and secreted into the circulation. Importantly, leptin is produced in proportion to peripheral energy reserves (i.e. fat), so leptin concentration indicates how much energy the body has on board (138). The crucial role of leptin in energy homeostasis is revealed by the hyperphagic and obese phenotypes of leptin-deficient rodents and humans, which are normalized with leptin treatment (139, 140). Leptin is thought to act in the CNS to regulate food intake and energy expenditure (141, 142).The secretion of leptin is reduced during periods of fasting and increased after meals, and is influenced by several metabolic and hormonal factors (140). Leptin also has an important role in the regulation of glucose homeostasis, reproduction, growth, the immune response and motivated behaviors, such as intake of food and drugs of abuse and locomotor activity (143-145). Another obese mouse was discovered in 1965, with a genetic mutation that mapped to chromosome 4: this became known as the db/db mouse (146-148). This obese phenotype was not due to lack of circulating leptin but perhaps something necessary to transduce the leptin signal and later experiments verified that the db gene encodes the long form of the leptin receptor (LepRb) (146-149), the only leptin receptor isoform containing the intracellular motifs required to convey leptin signals (148,150-152]. The central action of leptin is mediated via distributed populations of LepRb-expressing neurons throughout the brain (153-156). The LepRb is highly expressed in hypothalamic nuclei particularly ARC nucleus, ventro-medial, dorso-medial, and LHA. Upon the identification of LepRb much attention was devoted to understanding leptin action via the dense populations of LepRb-expressing neurons in the ARC and VMH. By comparison, much less was known about the nearby population of LepRb-expressing neurons in the LHA. In 1998 Elmquist et al. first reported a substantial number of LepRb neurons lying within the LHA (154), and an high leptin concentrations lead to a reduction of appetite via negative feedback mainly via the hypothalamus (157). Over the subsequent decade, many reports described leptin effects upon various LHA neuronal populations that altered energy homeostasis, but the role of leptin action via LepRb neurons in the LHA remained unclear. Neuroanatomical studies have suggested that the

majority of leptin’s anti-obesity effects are mediated by leptin receptors (LepRb) in the arcuate nucleus (ARC) of hypothalamus (158-160), in which leptin regulates the activity of two oppositely acting sets of lepRb-exspressing neurons by stimulating anorexigenic neurons that express POMC and CART, and inhibiting orexigenic neurons that express NPY and AgRP. After its binding to LepRb, leptin stimulates a specific signaling cascade that results in the inhibition of NPY neurons (161, 162) while stimulating POMC neurons (123, 161).These primary targets of leptin action communicate with the second-order neurons in other hypothalamic nuclei (especially PVN, dorso-medial, ventro-medial and LHA), where peripheral information on energy depots is integrated with behavioural, hormonal, and nutritional inputs coming from the periphery and higher cortical centres. Several hypothalamic neurotransmitters produced in these regions, including corticotropin releasing hormone (CRH), thyrotropin releasing hormone (TRH), MCH, brain-derived neurotrophic factor (BDNF), oxytocin, and OX, are physiologically involved in energy homeostasis. Leptin indirectly inhibits or stimulates these peptides, contributing to the regulation of energy intake and thermogenesis. Recent papers show that leptin modulates also the axonal growth and synaptic plasticity within the hypothalamus (6, 7). In particular, leptin increases neurite extension in the ARC during mouse perinatal development, thus playing an early trophic role within those circuits that will be the target of leptin physiological actions in adult life (6). Infact, ARC projections to each of its targets are markedly reduced in leptin-deficient Lep ob/ob (ob/ob) mice, and exogenous leptin can rescue these projections if administered during neonatal life (although not in adulthood) (6). It has been proposed that the leptin surge occurring in the perinatal period (163) promotes the maturation of hypothalamic circuits, which will be later functionally responsive to the hormone itself (6). The data presented by Bouret et al. indicate that distinct LepRb signaling pathways are required for normal development of hypothalamic neural projections that later convey the effects of leptin on energy balance (164). Leptin acts via multiple intracellular signaling pathways, including STAT3, ERK, and PI3-K→Akt, to modulate cellular and organismal physiology (145). Many data suggest important roles for LepRb →ERK and LepRb →STAT3 signaling in initial axonal outgrowth during ARC circuit formation. Leptin receptors are members of the cytokine receptor superfamily that interact with JAK/STAT via specific intracellular docking sites. Leptin's interaction with its receptor causes the activation of JAK2, which in turn can lead to the activation of other downstream kinase cascades, including MAPK and phosphatidylinositol 3-kinase (PI 3-K). This

activation induces a central signaling pathway that involves activation of signal transducer and activator of transcription 3 (STAT3) (151). In particular, leptin acts as a trophic factor in the elaboration of cortical growth cones by modulating MEK/ERK, PI3K/Akt, and PKC signaling pathways that converge in the inhibition of glycogen synthase kinase-3β (GSK3β). GSK3β is known to be a target of PI3K/Akt-mediated phosphorylation at Ser-9 (165). It is well established that phosphorylation of Ser9 on GSK3 β hinhibits its activity and leads to the inactivation of the enzyme which results in the reduction of tau phosphorylation (166). Tau is a group of neuronal microtubule-associated proteins which stabilize axonal microtubules and maintains neuronal processes. Tau plays a key role in regulating microtubule dynamics, axonal transport and neurite outgrowth, and all these functions of Tau are modulated by site-specific phosphorylation. Tau is a phosphoprotein and its phosphorylation negatively regulates its ability to stimulate microtubule assembly (167-169). It was demonstrated that primed phosphorylation of Tau at Thr 231 by GSK3β played a critical role in decreasing Tau's ability to both bind and stabilize microtubules (170). Treatment of cells with lysophosphatidic acid results in activation of GSK3β, increased Tau phosphorylation and neurite retraction (171, 172).

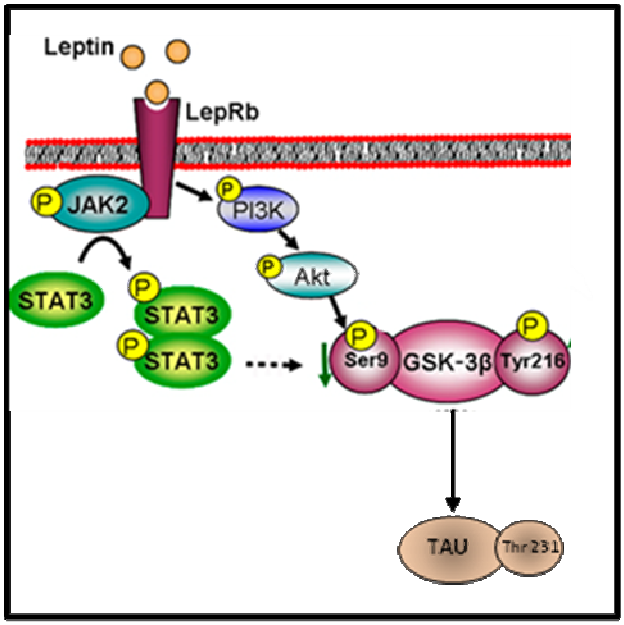

Fig. 9: *Leptin signaling patways.*

Hypothalamic endocannabinoids, orexin and leptin interaction in the control of food intake

Feed intake is a critical process for the normal growth and reproduction of mammals. Current studies on the regulation of food intake suggest that there are many central mediators that control the appetite. In recent years, the central regulation of energy balance has become even more fascinating and complex with the characterization of new mechanisms of control. The process leading to alterations in feed intake result from a complicated interplay between a large variety of factors, such as feed availability and quality, circulating concentrations of hormones and metabolites, as well as physical responses of the gastrointestinal system, all integrated by the CNS to yield the final physical act of eating. Although it is the CNS that regulates energy homeostasis, the CNS is responding in part to signals produced peripherally in proportion to the status of adipose tissue reserves, and in response to the presentation and ingestion of feed and the products of digestion. The hypothalamus has a central role in the integration of the various signals, resulting in activation of feeding or inhibition of feeding responses. A major location for the processing of these appetite regulatory signals is the ARC nucleus. Both stimulatory and inhibitory signals originate from the ARC and influence other secondary appetite neurons within the LHA, DMH, VMN, and PVN and subsequently other areas of the CNS, with those signals emerging from the LHA-DMH being stimulatory to feed intake and those from the VMN and PVN being inhibitory (173). With the discovery of leptin and the recent findings in the molecular genetic studies of several hypothalamic neuropeptides a new light has been shed in the molecular mechanism involving the feeding behavior and energy homeostasis. These studies suggested that leptin might diametrically regulate the LHA, which had initially been considered as a “feeding center”. Leptin administered selectively into the LHA inhibits food intake and promotes weight loss in rats. Furthermore, fasting (which decreases circulating leptin) and diet-induced obesity (in which neurons no longer respond normally to leptin) increase neuronal activation in the LHA — these data suggested that leptin normally acts to suppress the LHA “feeding center” (174,175). Leptin also may act by suppressing the activity of OX neurons, the biosynthesis of OX or both. OX have an important role in the hypothalamic central regulation of feeding behavior and many data indicate that OX neurons are involved in an appetite regulatory circuit that includes the circulating hormone leptin. Patch-clamp measurements in isolated OX neurons indicate that leptin can directly decrease the neuronal firing rate and intracellular Ca^{2+} concentrations (176). Recent study also showed that the

OX contents in the LH are increased in ob/ob mice. In addition, leptin has been shown to directly as well as to indirectly (via the α-MSH pathways originating in the ARC) inhibit gene expression for OX (177). Moreover, an OX_1R-selective antagonist reduced food intake and ameliorated obesity of leptin-deficient ob/ob mice (134), suggesting that leptin deficiency at least partly activates the orexin pathway to increase food intake. Several studies reported a major role of the EC system in this central regulation of food intake. More recently, increasing evidence supports the view that the activation of the EC system plays important regulatory roles in the control of food intake, energy balance and body mass through central and peripheralmechanisms at multiple levels including the brain, gastrointestinal tract, liver, pancreas, muscle and adipose tissue. The binding of ECs to CB1 receptors results in increased appetite, weight gain and lipogenesis. In the hypothalamus, ECs increase the production of orexigenic neurotransmitters and reduce the anorexigenic signals (178). The peripheral signals are able to determine changes within the activity of the central EC receptor. Nevertheless, if ECs stimulate eating by actions at central CB1 receptors, reciprocally, brain levels of ECs are in direct relation to feeding or changing nutritional status. Such a negative regulation of the EC production after feeding may be under the control of leptin secreted as an anorexigenic factor (2, 179). The notion that leptin and ECs participate in crosstalk was first suggested by the observation in mice in which leptin signaling was impaired. Impairment of leptin signaling (db/db mice expressing a defective leptin receptor), leptin deficiency (ob/ob), and leptin resistance (acquired resistance due to diet-induced obesity) in mice showed elevated levels of ECs in the hypothalamus and in adipose tissue (5). Central effects of leptin result in reduced levels of endocannabinoids due to interference with 2-AG synthesis and increased AEA degradation (4, 178). Administration of leptin in leptin-deficient ob/ob mice led to significantly down-regulate hypothalamic levels of ECs (2). Furthermore CB1 has been shown to colocalize with the food intake inhibiting the neuropeptide corticotropin-releasing hormone in the PVN of the hypothalamus, with melanin-concentrating hormone in the LH and pre-pro-orexin in the ventromedial hypothalamus (178, 180, 181). There is evidence that the LH could be an important site for the endocannabinoid action on energy balance. Another LH neuronal entity liable to play a significant role in the regulation of energy balance, and which could be implicated in the metabolic effect of endocannabinoids, is the OX system. That there could be some cross-talk between the OX and EC system to regulate energy balance is supported by the apparent co-localization of the CB1 and OX-A receptors in the ARC and

PVH (182). These new findings on the neuroendocrine mechanisms controlling energy homeostasis and body weight show the complexity of these integrating systems and the existence of many unravelled mysteries. Nevertheless, each mystery unveiled opens new opportunities for the development of novel therapies for obesity and nutritional disorders (Fig.10).

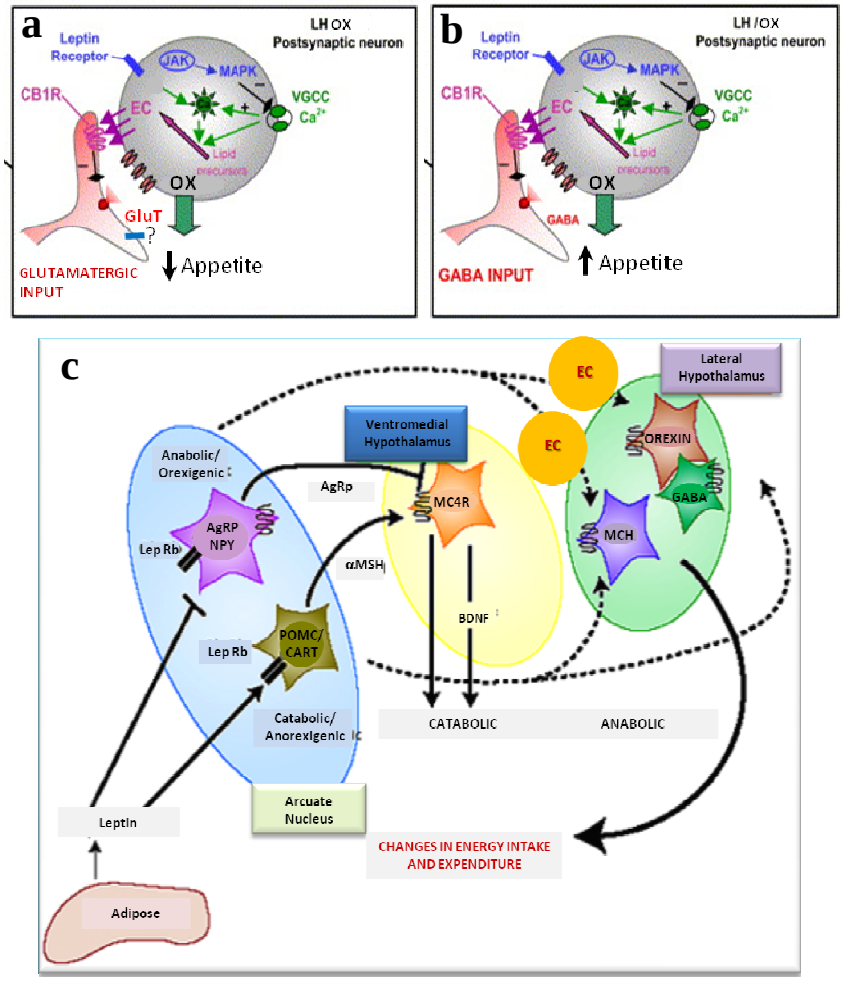

Fig. 10: ***a,b)*** *Model for mechanisms of endocannabinoid and leptin signaling and modulation of GABAergic and Glutammatergic transmission in the perifornical LH neurons of the LH.* ***c)*** *Hypothalamic endocannabinoids, orexin and leptin interaction in the control of food intake with leptin actions and downstream effects in the arcuate nucleus, ventromedial hypothalamus (VH) and lateral hypothalamus.*

AIMS

AIMS

Short-term food deprivation induces a “rewiring” of several hypothalamic nuclei that may underlie changes in the release of hypothalamic and peripheral orexigenic and anorexigenic mediators. In the ARC, neurons expressing pro-opiomelanocortin (POMC) and cocaine and amphetamine responsive transcript, on the one hand, and those expressing neuropeptide Y (NPY) and the agouti-related peptide (AgRP), on the other hand, undergo reciprocal changes in excitatory vs. inhibitory input, thus decreasing the activity of the former and increasing the activity of the latter, and facilitating food consumption (6,7). Food deprivation-induced enhancement of excitatory inputs also occurs on one of the two major subsets of neurons of the LH (12), i.e. orexinergic neurons (8, 79). These neurons send projections throughout the brain, thereby modulating not only food intake, but also more generally arousal and reward (79, 83, 183, 184). All of these changes are attenuated by re-feeding, are attributable to reduced leptin levels, and are reversed when leptin is administered to food-deprived mice (6, 7, 12). This “rewiring” of hypothalamic nuclei is scantily investigated in animal models of obesity. Perhaps even more surprisingly, given the prominent role of the endocannabinoid system in modulating both inhibitory and excitatory neurotransmission, its sensitivity to altered leptin and its dysregulation in obesity (4), it is not known if obesity-induced “rewiring” of the hypothalamus affects endocannabinoid system and its crucial neuromodulatory function. Furthermore, recent papers show that leptin modulates axonal growth and synaptic plasticity within the hypothalamus (6, 7). Bouret et al. report that dinstinct LepRb signaling pathways are required for normal development of hypothalamic neural projections (164), but the role of leptin action via LepRb neurons in the LHA remained unclear. Leptin acts by modulating MEK/ERK, PI3K/Akt, and PKC signaling pathways that converge in the inhibition of glycogen synthase kinase-3β (GSK3β). The phosphorylation of Ser9 on GSK3β inhibits its activity and leads to the reduction of Tau phosphorylation (166). Tau phosphorylation negatively regulates its ability to stimulate microtubule assembly (167-169).

The present study was primarily aimed at assess if obesity-induced rewiring of hypothalamic neurons occurs in the LH and its impact on the neuromodulatory function of the endocannabinoid system. In particular, we investigated if remodeling of orexinergic neuronal wiring also occurs during a prolonged nutritional perturbation caused by, or resulting in, leptin signalling deficiency, as in ob/ob and HFD mice, respectively, and its

impact on endocannabinoid signalling. We will test the hypothesis that the activity of orexin neurons could be modulated by a CB1-receptor-mediated inhibitory effect on the GABA inhibitory and/or Glutammate excitatory projections (by means of DSI and DSE) controlling the activity of the LH orexin neurons and the hypothesis that leptin-deficiency modifies the distribution of CB1 receptors between excitatory and inhibitory terminals leading to a switch from excitatory to inhibitory projections, which would alter endocannabinoid-control of neuronal activity.

At this purpose we will provide evidences in order to:

A. Ascertain the localization of the endocannabinoid system in the LH and in particular in the OX circuit.

B. To define the exact localization of CB1 receptor on GABAergic or glutamatergic fibers targeting the OX neurons.

C. To define if remodeling of CB1 receptor distribution on excitatory/inhibitory inputs onto OX neurons occurs during disorders of food-intake.

D. To define if a switch from excitatory to inhibitory wiring dependent from leptin deficiency occurs on OX neurons during disorders of food-intake and its impact on the neuromodulatory function of the endocannabinoid system.

Therefore, we employed electrophysiological, immunohistochemical, ultrastructural, biomolecular and biochemical methods to assess the changes in endocannabinoid signaling in LH orexinergic neurons and the role of leptin deficiency in this rewiring, in ob/ob mice at different postnatal ages, and in mice made obese by a high fat diet (HFD).

MATERIALS AND METHODS

Experimental procedures

Experiments were performed according to the guidelines of the institutional ethical code and the Italian (D.L. 116/92) and EEC (O.J. of E.C. L358/1 12/18/1986) regulations for the care and use of laboratory animals. In our study we employed the following animals:

a) Male leptin knockout *ob/ob* mice (JAK® mouse strain) B6.V-Lepob/J and *wt* leptin gene expressing homozygous siblings, of various ages, were obtained from breeding *leptin* gene heterozygouts, and genotyped with PCR. The pups were housed together with their dam up to weaning and consumed maternal milk only. After weaning, all these animals were fed *ad libitum* with a standard laboratory regimen (3.5 kcal/g, 14.5% of energy as fat).

b) Nine week old male C57BL/6J were made obese by being fed 7 weeks of high fat diet (n=6; HFD TD97366 Harlan, 4.7 kcal/g: 49% fat, 18% protein and 33% carbohydrate). Lean mice received a standard fat diet (SFD, n=6; 3.5 kcal/g, 14.5% of energy as fat). Serum leptin (Quantikine M; R&D Systems) levels were determined using commercial sandwich ELISA assays (B-Bridge International) in accordance with the manufacturer's instructions. All animals were maintained on a 12 h light/dark cycle (light off at 9 p.m) and fed *ad libitum*

Perfusion and preparation of tissue sections

For immunofluorescence and peroxidase based immunohistochemistry all the animals (n=10 per group) were deeply anesthetized with a mixture of ketamine–xylazine (25 mg/ml ketamine, 5 mg/ml xylazine, 0.1% w/w pipolphen in H2O; 1 ml/100 g, i.p.). Animals were then perfused transcardially with 0.9% saline for 5 min, followed by 100 ml of fixative containing 4% paraformaldehyde in 0.1 M phosphate buffer (PB), pH 7.4, for 20 min. At the end of this procedure conducted at a controlled temperature of 4°C and constant flow (10ml x min), the brain was removed from the skull, post-fixed for 2 hours in the perfusion fluid at 4°C, washed in PB and finally soaked for cryoprotection in 30% sucrose in PB at 4°C until it sank. After the time necessary for the brain to sink in

the liquid cryopreservation, the same has been frozen rapidly in liquid nitrogen and was cut with a Leica CM3050S cryostat (Leica, St. Louis, MO, Germany) in serial coronal frozen sections (10 µm-thick) collected onto electrostatic charged Menzel Super frost slides (Menzel Thermo Fisher Scientific, Germany) in three alternate series. For electron microscopy, the fixative contained 3% paraformaldehyde and 0.5% glutaraldehyde and The brains for double immunogold histochemistry were cut as 50-µm-thick coronal sections by a Leica VTS-1000 Vibratome (Leica, St. Louis, MO, Germany).
For RT-PCR analysis and Lipid extraction and endocannabinoid measurement the animals were sacrificed by cervical dislocation and the brains were quickly removed. Then the area corresponding to the hypothalamus has been micro-dissected, excised, frozen in liquid nitrogen and stored at -80 ° C until the biochemical assay.

Leptin injection

Recombinant murine leptin (Sigma) was reconstitueted in 10 mM pathogen-free Tris-HCl buffer pH 7.4 and 300 µl of this solution (10 mg/kg) was injected intraperitoneally in adults wt and ob/ob mice. The animals were rapidely sacrified or perfused and processed for electrophysiology or immunohistochemistry respectively.

Immunofluorescence and peroxidase based immunohistochemistry

For the single antibody immunoperoxidase procedure, sections were incubated with specific normal serum-diluted primary polyclonal antibodies of rabbit or guinea pig anti-DAGLα (all supplied from Prof. Mackie with respective blocking peptides) or rabbit anti-CB1 (supplied from Prof-Mackie or from Chalbiochem, Merck KGaA, Darmstadt, Germany), or goat anti-OX-A or anti-MAGL (Abcam Cambridge, UK) or anti-VGAT (Synaptic Systems, Goettingen, Germany) or anti-VGluT2 (Synaptic Systems, Goettingen, Germany) or anti-MCH (Abcam, Cambridge, UK) (range 1:200 - 1:400). Each primary antibody was revealed by specific biotinylated secondary anti- IgGs (Vector Laboratories, Burlingame, CA) followed by incubation with the avidin-biotin complex (ABC Kit;

Vectastain, Vector) and revealed by 3-3'-diaminobenzidine (DAB Sigma Fast, Sigma-Aldrich, Louis, MO U.S.A.). For multiple immunofluorescence the sections were incubated in a mixture of anti-OX-A combined with DAGLα or CB1 or CB1/Synaptophisin or CB1/VGluT2 or CB1/VGAT or MAGL/VGAT or MAGL/VGluT2. Multiple immunofluorescence was revealed by specific Alexa488/546/350 secondary donkey anti-IgGs. Controls of specificity of immunolabeling in multiple fluorescence experiments were performed by omission of primary and/or secondary antibodies or by preadsorbtion of primary antibodies with respective blocking peptides. Since DAGLα or MAGL immunostaining have not previously been described in the LH, we also ran single immunohistochemistry analyses by using pre-absorption of DAGLα antibody with its immunizing peptide or incubation of MAGL antibody with brain sections prepared from MAGL-/- mice. In no immunostaining was detected in these controls. The sections processed for immunofluorescence were examined using confocal laser scanning microscopy (LSM510 Meta, Zeiss) or a conventional fluorescent microscope equipped with the appropriate filters and equipped with a deconvolution system (Leica DMI6000B). Images were acquired using a digital camera (Leica DFC420). Image analysis was performed using the Leica MM AF Analisi Offline software including the *Z*-stack acquisition and deconvolution processing (Leica, Germany). For quantitative analysis of the ratio of CB1/VGluT2 or CB1/VGAT terminals onto OX-A neurons, merged excitatory or inhibitory puncta were counted in n=500 orexinergic neurons for each genotype and diet group. No labeling was detected in each control performed for reaction of multiple immunofluorescence. Quantitative analysis of CB1/VGAT- *vs.* CB1/VGluT2-immunolabeled axon terminals were acquired from CB1/VGAT/MCH or CB1/VGluT2/MCH or CB1/VGAT/OX-A or CB1/VGluT/OX-A sections in the *Z*-stack mode and reconstructed by application of MMOffline© Leica software for cell imaging and signal colocalization counting. n=60±6 OX-A neurons per group at 3, 5 and 9 weeks of *wt*, *ob/ob*, and at 16 weeks of SFD and HFD mice were used.

Pre-embedding immunogold-silver labeling

Pre-embedding double immunogold-silver labeling was performed according to the procedure of Yi and coworkers (185). Sections of 50μm from the LH of three obese (*ob/ob* or HFD) and three lean (*wt* or SFD) mice were prepared using a VTS-1000 vibratome (Leica, St. Louis, MO, Germany). Sections of obese and lean mice were washed in PB, placed for 15 min in PB containing 0.1% sodium borohydride to inactivate residual aldehyde groups in the tissue sections and then washed four times for 10 min each in PB. Sections were incubated in a blocking solution (2% BSA and 0.02% saponin in PBS) for 1 hour and then with the mixtures of two primary antibodies from different species at a working dilution of 1:200 in the blocking solution overnight at 4°C. Primary antibodies were: 1) a mixture of rabbit anti-CB1 and guinea pig anti-DAGLα; 2) a mixture of goat anti-OX-A and rabbit anti-CB1; 3) a mixture of goat anti-OX-A and guinea pig anti-DAGLα. After 6 washes of 10 min with PBS, sections were incubated, for 4 hours in gentle agitation at +4°C, with each first ultrasmall gold conjugate secondary antibody of donkey anti-IgG (Aurion, The Netherlands), specific for the respective first antibody of the mixture, diluted 1:50 in the blocking solution. The secondary antibodies were both affinity-purified F(ab')2 fragments of anti-Rabbit IgG (Aurion, The Netherlands) or anti-goat or guinea pig (Nanoprobes, NY, USA) conjugates to ultrasmall gold particles. Sections were washed with PBS six times for 10 min and PB two times for 10 min. The enhancement by silver was performed with a R-Gent SE-EM kit (Aurion, The Netherlands): sections were washed four times for 10 min with ECS (Enhancement Conditioning Solution) and then incubated with R-Gent SE-EM silver enhancement solution, at room temperature for 90 min shielded from bright light. The enhancement was stopped with 0.03 M sodium thiosulfate in ECS for 10 min. After four washes in ECS for 10 min each and two washes in PB for 10 min each, sections were incubated with the second secondary antibody ultrasmall conjugate donkey anti guinea pig IgG (Aurion, The Netherlands) and anti rabbit IgG (Aurion, The Netherlands), specific for the respective second primary antibody of each mixture. The second secondary antibody was used at a working dilution of 1:50, for 4 hours, at +4°C in agitation. Sections were then washed with PBS six times for 10 min and PB two times for 10 min. To prevent loss of labeling during the silver enhancement, sections were fixed with 2.5% glutaraldehyde in PB for 2 hours at 4° C under gentle agitation. After two washes of 10 min in PB, the second silver enhancement was repeated with the R-gent SE-EM silver enhancement

solution, at room temperature for 60 min shielded from bright light. The enhancement was stopped with 0.03 M sodium thiosulfate in ECS for 10 min. Then, the sections were washed four times in ECS for 10 min each and two times in PB for 10 min each. Additional sections were processed in parallel as controls in which the mixtures of primary and/or secondary antibodies were omitted. No labeling was detected in each control reaction. The sections were post fixed with 0.5% OsO4 in PB for 20 min at 4°C, dehydrated in an ascending series of ethanol and propylene oxide, and embedded in TAAB 812 resin (TAAB, England). During dehydration, sections were treated with 1% uranyl acetate in 70% ethanol for 15 min at 4°C. Ultrathin (60 nm) sections were collected on Formvar-coated single- or multiple slot grids and stained with 0.65% lead citrate for 3 min. Electron micrographs were taken with the TEM microscope LEO 912AB (Zeiss, Germany).

Pre-embedding immunogold labeling

A double pre-embedding immunogold labeling with gold particles of 6 and 10 nm was applied on 50μm vibratome sections, cut perpendicularly to the surface of the sections, of the LH of obese and lean mice. Sections were pretreated with PB containing 0.1% sodium borohydride for 1 min, washed with PB three times for 15 min once and exposed to a blocking solution with 5% normal donkey serum and 0.1% saponin for 2 hour at room temperature under gentle agitation. Sections were exposed to the same mixtures of two primary antibodies from different species as used in the pre-embedding immunogold-silver labeling: 1) a mixture of rabbit anti-CB1 and guinea pig anti- DAGLα; 2) a mixture of goat anti-OX-A and rabbit anti-CB1; 3) a mixture of goat anti-OX-A and guinea pig anti-DAGLα. The sections were incubated in agitation for 24 hours at 4°C with a mixture of primary antibodies diluted 1:100 in the blocking solution with 0.02 % saponin as detergent in order to enhance antibody penetration. Then the sections were washed in PB for 1 hour (six washes of 10 min once), at room temperature under gentle agitation. Then sections were incubated in agitation overnight at +4°C in a mixture of gold conjugated secondary antibodies diluted 1:30 in blocking solution with 0.02 % saponin and specific for the mixture of the primary antibodies: 1) a mixture of donkey anti-rabbit IgG-gold of 10nm and anti-goat IgG-gold of 6nm specific to reveal CB1 and DAGLα, respectively ; 2) a mixture of donkey anti-goat

IgG–gold of 10nm and anti-rabbit IgG-gold of 6nm specific to reveal OX-A and CB1, respectively; 3) a mixture of donkey anti-goat IgG-gold of 10nm and anti-guinea pig IgG of 6nm specific to reveal OX-A and DAGLα, respectively. All the secondary antibodies were obtained from Aurion (The Netherlands). Sections were washed with PBS four times for 10 min and PB two times for 10 min with gentle agitation. Additional sections were processed in parallel as controls by omitting the mixtures of either both or one of the primary antibodies of the mixture and/or of the secondary antibodies. No labeling was detected in each control reaction. Sections were then treated with 0.5% OsO4 in PB for 10 min at 4°C, dehydrated in an ascending series of ethanol and propylene oxide, and embedded in TAAB 812 resin (TAAB, England). During dehydration, sections were treated with 1% uranyl acetate in 70% ethanol for 15 min at 4°C. Ultrathin (60 nm) sections, carried out perpendicularly to the surface of 50 µm vibratome sections, were collected on Formvar-coated single- or multiple-slot grids and 0.65% lead citrate for 3 min. Electron micrographs were taken with the TEM microscope LEO 912AB (Zeiss, Germany).

Quantitative analysis of immunogold labeling

The relative abundance of CB1 inhibitory and excitatory inputs to OX-A cells was calculated through unbiased electron microscopy analysis applied to sequential silver-enhanced OX-A/CB1 preembedding immunogold on ultrathin sections of pre-weaned, post-weaned and adult *ob/ob* mice and adult HFD mice as compared to the respective *wt* and SFD mice (n=3 per group). Through sequential silver-enhanced double immunogold the expression of OX-A antigen was unequivocally discriminate showing the larger size than CB1 because its ultra-small gold conjugates antibody was enhanced twice while the anti-CB1 second ultra small gold conjugates antibody was enhanced only once (see the pre-embedding immunogold-silver labeling method for details). In these experiments the inhibitory synapses were identified by their symmetrical morphology and excitatory synapses by their asymmetrical morphology. Metal particles were counted only in presynaptic and postsynaptic profiles that possessed clearly visible, anatomically defined symmetrical or asymmetrical synapses. Selected boutons of 5 orexinergic neurons per animal were followed through 24 consecutive LH serial ultrathin sections (n=3 mice per group). According to

the synaptological method applied in the LH by Horwath and Gao (12) we randomly sampled every element of the analysis as the bouton at high power magnification, the orexinergic-immunoreactive perikarya and the plane of each transected OX-A cell. In this assesment 20 CB1-expressing boutons contacting OX-A soma were analyzed per each animal (an average of 4 CB1-expressing boutons per neuron). Moreover, from a different ribbon of 24 consecutive LH serial ultrathin sections we analyzed 10 CB1-expressing axo-dendritic boutons to following 4 orexinergic neurons.

Pre-proorexin mRNA quantification by RT-PCR analysis

Tissue samples from LH were dissected, from three animals for each group, and collected in RNA later (Invitrogen) following manufacturer's instructions and were homogenized in 1.0 ml of Trizol® (Invitrogen). Total RNA was extracted according to manufacturer recommendations, dissolved in RNAase-free water, and further purified by spin cartridge using the PureLink-micro RNA purification system (Invitrogen). Total RNA was dissolved in RNA storage solution (Ambion), UVquantified by a Bio-Photometer® (Eppendorf), and stored at −80°C until use. RNA aliquots (6 μg) were digested by RNAse-free DNAse I (Ambion DNA-free™ kit) in a 20 μl final volume reaction mixture to remove residual contaminating genomic DNA. After DNAse digestion, concentration and purity of RNAsamples were evaluated by the RNA-6000-Nano® microchip assay using a 2100 Bioanalyzer® equipped with a 2100 Expert Software® (Agilent) following the manufacturer's instructions. For all samples tested, the RNA integrity number was greater than 7 relative to a 0–10 scale. One microgram of total RNA, as evaluated by the 2100 Bioanalyzer, was reverse-transcribed in cDNA and analyzed as previously described (186). Optimized primers for SYBR-green analysis (GenBank accessions: Hypocretin Hcrt-NM_010410, hypoxanthine guanine phosphoribosyl transferase Hprt-NM_013556) and optimum annealing temperatures were designed by Allele-Id software version 7.0 (Biosoft International) and were synthesized (HPLC-purification grade) by MWG-Biotech. Relative gene expression calculation, corrected for PCR efficiency and normalized with respect to the reference gene *Hprt* was performed by the IQ5 software, as previously described.

Electrophysiology

Miniature Inhibitory Post Synaptic Currents (mIPSCs) were recorded in OX-A neurons of the lateral hypothalamic area from ob/ob, their wt siblings and *c57bl/6* mice (*n* of neurons/*n* of mice: 31/15, 27/9, 8/7, respectively). Two developmental stages were investigated: before weaning (range P18-23, average P21), and after weaning (range P30-39, average P34). In a subset of experiments, *ob/ob* and *wt* mice were fasted for 24 hr and received a single injection of recombinant leptin (50 μg i.p. at the beginning of food deprivation) before mIPSCs recording (*n* of neurons/*n* of mice: 13/4, 12/4, *ob/ob* and *wt*, respectively). Spontaneous Inhibitory Post Synaptic Currents (sIPSCs) were recorded after weaning (range P27-39, average P32,) in 29/13 *ob/ob* and 26/15 *wt* mice. Mice were anesthetized by inhalation of ether and depth of anesthesia was judged by lack of a righting reflex. The brain was perfused transcardially with ice-cold dissection media (DM), and the cerebral hemispheres quickly removed, placed in ice-cold DM and reduced to blocks. DM consisted of (in mM) 220 sucrose, 26 $NaHCO_3$, 1.23 NaH_2PO_4, 2.5 KCl, 6 $MgCl_2$, 1 $CaCl_2$, and 10 glucose, equilibrated with 95% O2/5% CO2. Hypothalamic coronal slices (200 μm thick) were cut in ice-cold DM and later collected in a holding chamber at 32oC for 45 min in artificial cerebrospinal fluid (ACSF) consisting of (in mM) 122 NaCl, 26 $NaHCO_3$, 1.23 NaH_2PO_4, 2.5 KCl, 2 $MgCl_2$, 2 $CaCl_2$, 1 Na-ascorbate, 3 Na-pyruvate and 10 glucose, equilibrated as above. Slices were subsequently transferred in a recording chamber perfused at 2-3 ml/min with ACSF at room temperature. Excitatory inputs were blocked with 10 μM NBQX and CPP (Sigma). At the end of each recording, 30 μM bicuculline (Sigma) was added to the bath, to confirm the inhibitory nature of the recorded synaptic activity. When appropriate, CB1-Receptors were activated by adding 5 μM WIN55,212-2 mesylate (WIN, Tocris), or blocked with 4 μM AM251 (AM, Tocris). Whole-cell recordings were performed with an Axopatch 200B amplifier (Axon Instruments), under a custom-made microscope equipped with an infrared video camera (Hamamatsu) and differential interference contrast optics. Neurons were functionally identified as orexinergic by recording, in current clamp mode, their typical responses to injected current pulses. Neurons were then voltage-clamped at -70 mV and the activity of inhibitory inputs recorded in the presence (mIPSC) or absence (sIPSC) of 1μM TTX (Sigma). With no TTX the pre-synaptic spiking activity was present and thus IPSCs due to both the stochastic and the spontaneous action potential-evoked GABA release were recorded. sIPSCs recording was performed when testing the effect of WIN and AM on CB1 receptors.

Recording electrodes (2-5 MΩ) were made with borosilicate glass (Warner Instruments) and filled with (in mM) 145 KCl, 10 HEPES, 0.2 EGTA, 2 Mg-ATP, 0.5 Na-GTP, pH 7.4 with KOH. Signals were filtered at 10 kHz by pClamp 9.2 and digitized at 20 kHz (Digidata 1322A, Axon Instruments). Series resistance (<30 MΩ in all analyzed recordings) and whole-cell capacitance were not compensated. The recording was terminated if series resistance changed more than 20%. To study Depolarization-induced Suppression of Inhibition (DSI), sIPSC were recorded before and after a step depolarization (5 s) from -70 to 0 mV. DSI was calculated as the sIPSC frequency measured in time intervals of 5 s after the depolarization and made relative to the frequency during 5 seconds before the depolarization. In each experiment, the responses to two successive depolarizations (separated by 90 s) were averaged together. In a subset of cells, DSI was tested also 4-5 minutes after the addition of 4μM AM. All measurements were performed at least 5 minutes from the establishment of the whole-cell, to let the cytosol equilibrate with the recording solution. The frequencies of mIPSCs and sIPSCs were measured over a 1 minute recording. The effect of AM and WIN on sIPSCfrequency and amplitude was measured 4-5 minutes after the addition of the drugs. Data were analyzed with Clampfit 9.2 (Axon Instruments). A subset of 17 neurons was injected with 2% FITC-Neurobiotin (Vector Lab) through the recording electrode. At the end of the recordings, the slices were fixed in 4% paraformaldheyde in 0.1M PB for 1h and kept in PB until they were incubated in a mixture of goat anti-OX-A/ rabbit anti-MCH primary antibodies (Santa Cruz Biotechnology, CA USA), labeled with anti-rabbit Alexa546/antigoat Alexa350 secondary antibodies.

Lipid extraction and endocannabinoid measurement

Tissue samples from the LH were homogenized in 5 volumes of chloroform/methanol/Tris HCl 50 mM (2:1:1 by volume) containing 10 pmol of d8-AEA and 50 pmol of d5-2AG19. Homogenates were centrifuged at 13,000 *g* for 16 min (4^{o}C), the aqueous phase plus debris were collected and four times extracted with 1 vol of chloroform. The lipid-containing organic phases were dried down and pre-purified by open bed chromatography on silica columns eluted with increasing concentrations of methanol in chloroform. Fractions for AEA and 2-AG measurements were obtained by eluting the columns with 9:1 (by vol.) chloroform/methanol and

then directly analyzed by liquid chromatography-atmospheric pressure chemical ionization-mass spectrometry (LC-APCIMS). LC-APCI-MS analyses were carried out in the selected ion monitoring (SIM) mode, as described (2), using *m/z* values of 356 and 348 (molecular ions +1 for deuterated and undeuterated anandamide), 384.35 and 379.35 (molecular ions +1 for deuterated and undeuterated 2-AG). AEA and 2-AG levels were therefore calculated on the basis of their area ratios with the internal deuterated standard signal areas, their amounts in pmols normalized per mg of lipids and compared by ANOVA followed by the Bonferroni's test.

Statistical analyses

Data are expressed as mean s.e.m. A repeated two-way ANOVA was performed using SPSS version 8.2. Student's or Bonferroni two tail *t* test were used to judge statistical significance between groups ($P<0.05$).

RESULTS

The endocannabinoid system is expressed in OX-A neurons

The distribution of CB1 receptors was recently determined in the LH of adult mice (187). We conducted multiple immunofluorescence studies to determine the distribution of other key elements of the endocannabinoid system in the LH of pre-weaned (i.e. 3 weeks, range: P19-23), weaned (5 weeks, range: P28-36) and adult (9 weeks old) mice (n=6 per group). First, using bright-field and fluorescence microscopy, as well as confocal laser scanning microscopy, we studied the expression of diacylglycerol lipase-α (DAGLα), the enzyme primarily responsible for the generation of 2-AG, in the LH. DAGLα-immunoreactivity was clearly detected on punctate structures corresponding to neuronal profiles in the LH (Fig 11)**.** Subsequently, we identified, by double DAGLα/OX-A immunofluorescence, orexinergic neurons expressing the 2-AG synthesizing enzyme (Fig. 12a) and observed, by means of triple CB1/OX-A/monoacylglicerol lipase (MAGL) immunofluorescence, the expression of CB1 receptors and of the 2-AG degrading enzyme, MAGL, in the neuropil surrounding OX-A neurons (Fig. 12b, c). MAGLimmunoreactivity was clearly detected on punctate structures surrounding neuronal profiles in the LH (Fig. 11)**.** When these experiments were quantified, we determined that DAGLα was detected post-synaptically in 68.5±8.4% of OX-A neurons receiving MAGL/CB1-bearing inputs. Using double immunogold electron microscopy, we confirmed that in lean and obese mice (n=3 per group), OX-A expressing neurons also expressed DAGLα, the corresponding immunoreaction product typically being concentrated in the cytoplasm just beneath the somatodendritic cell membrane (Fig. 13a-d arrowheads; Fig. 14a-c and e). In these neurons, most OX-A gold particles accumulated in dense vesicles (Fig. 13 a-b,e-f arrows; Fig. 14 c-d) in the cytoplasm of LH neurons, with a few being dispersed in low density vesicles and intracellularly around the endoplasmic reticulum or Golgi membrane. In the same OX-A neurons, DAGLα gold particles were mostly located near the internal surface of the plasma membrane (Fig. 13 a-b, arrowheads; Fig. 14 c,e). In the neuropil, labeling for DAGLα was also found in dendritic spines and CB1/DAGLα immunolabeling revealed a typical DAGLα expression selectively apposed to CB1-expressing terminals both in axo-somatic (Fig. 13 c,d) and in axo-dendritic asymmetric and symmetric synapses (Fig. 14 a,b). These data were obtained by preembedding double immunogold labeling of secondary antibodies conjugated with ultra small gold particles, revealed by two sequential steps of silver-enhancement according to the procedure of Yi et al (185) (Fig. 13), or using a preembedding double

immunogold labeling with gold particles of 6nm and 10nm (Fig. 14). Controls of antibody specificity were performed for both immmunogold methods by omission from the incubation mixture of either primary or secondary antibodies. No signal was observed in all performed controls obtained after omission of primary antibodies and after omission of secondary antibodies. DAGLα immunogold distribution was quantitatively evaluated in the DAGLα/OX-A double-immunolabeled LH of adult lean and obese mice (Fig. 15). The distribution was quantified after normalization to µm of plasma membrane of orexinergic neurons, since in the LH the enzyme is mainly expressed near the somatodendritic cytoplasmic surface of the plasma membrane, in agreement with previous findings in other brain regions (188, 189).

2-AG levels are upregulated in orexinergic neurons of *ob/ob* mice and mice with HFD-induced Obesity

LH concentrations of 2-AG were measured by isotope-dilution LC/MS mass spectrometry in 3, 5 and 9 weeks old *ob/ob vs. wt* mice and in adult (16 weeks old) mice after 7 weeks of HFD *vs.* Standard Fat Diet (SFD) (n=6 per group). 2-AG levels in the LH from 9 week old *ob/ob* mice were increased compared to 5 and 3 week old *ob/ob* mice. No difference was observed between 16 week old HFD mice and 9 week old *ob/ob* mice. Thus, a statistically significant increase of 2-AG was observed only in adult obese mice, either *ob/ob* or HFD, compared to the respective lean mice (Fig. 16 a,b). No differences were found between adult *ob/ob* or HFD mice and their lean counterparts for AEA levels (data not shown). Concurrently with the increase of 2-AG levels, a significant elevation of DAGLα immunoreactivity (DAGLα–ir) was observed in LH neurons of adult obese (*ob/ob* and HFD) mice compared to matched lean controls and younger mice, as assessed by densitometric analysis (Fig. 16c,d) carried out by comparing DAGLα staining in slides adjacent to those processed for DAGLα/OX-A.

Obesity is accompanied by increased pre-proorexin mRNA expression in the LH and increased OX-A signaling in the arcuate nucleus

To examine the consequences of altered endocannabinoid control over orexin signaling in obese mice, we measured the expression of pre-proorexin mRNA in the LH of adult and young *ob/ob* and *wt* mice by quantitative RT-PCR (n=6 mice per group). We found that pre-proorexin mRNA levels in the LH are increased in adult obese mice (Fig. 17a). By contrast, OX-A-ir in the soma of LH neurons, assessed by densitometric analysis, did not significantly differ between adult obese mice (*ob/ob* mice at all ages and adult HFD mice) and the respective controls (Fig. 17 b). However, a significant increase of OX-A immunoreactivity was found in the orexinergic projections to the ARC in 5 and 9 week old *ob/ob* mice as well as in adult HFD mice (Fig. 17c).

CB1–expressing fibers innervating orexinergic neurons are rearranged during obesity

An overall increase in immunoreactivity for the GABAergic marker, VGAT, *vs.* the glutamatergic marker, VGluT2, was observed in the LH of post-weaning obese mice as compared to lean mice of the same age**.** When we quantified CB1-expressing fibers, a statistically significant difference in the distribution of CB1 between excitatory (i.e. VGluT2-expressing) and inhibitory (i.e. VGAT-expressing) inputs onto OX-A neurons was observed when comparing the LH of lean mice at pre-, post-weaning and adult age, or of SFD mice, to that of age-matched *ob/ob* or HFD obese mice (Fig. 18a-d). By contrast, no difference in the general intensity of CB1-ir projections to OX-A neurons was observed between different ages of lean *vs.* obese mice. This was documented by densitometric analysis of CB1 staining in afferent fibers to OX-A neurons, the orexinergic nature of which was established in adjacent double-labeled CB1/OX-A sections (Fig. 19a,b). Moreover, the percentage of CB1- immunopositive afferents to OX-A neurons was calculated relative to the total number of synaptophysin positive axon terminals and there was no difference between lean and obese mice by genotype, diet or age (Fig. 19c,d). Quantitative analyses were carried out to assess the abundance of CB1/VGAT- *vs.* CB1/VGluT2-immunolabeled axon terminals in apposition to OX-A perikarya, (n=200 cells per LH; n=3 mice per group). This experiment revealed that in post-weaning and adult *ob/ob* or obese HFD mice CB1/VGAT inputs significantly outnumbered the

excitatory ones, contrary to the condition in the matched lean mice, where CB1/VGluT2 terminals were more abundant. Interestingly, no difference was found between the number of CB1/VGAT *vs.* CB1/VGluT2- expressing inputs in pre-weaning (3 weeks old) *wt* or *ob/ob* mice (Fig. 20). Finally, using double VGluT2/MAGL or VGAT/MAGL immunofluorescence, we observed that the 2-AG degrading enzyme, MAGL, was localized preferentially to LH inhibitory terminals compared to excitatory afferents onto OX-A neurons of adult obese HFD and *ob/ob* mice. The opposite situation was observed in lean controls (Fig. 21). The relative abundance of CB1-expressing inhibitory and excitatory inputs onto OX-A cells was further investigated through unbiased electron microscopic analysis. The analysis was applied to LH CB1/OX-A double immunogold labeled ultrathin sections of pre-weaned, weaned and adult *ob/ob* mice and adult HFD mice and compared to the respective *wt* and SFD mice (n=3 per group). In these blinded experiments, we identified inhibitory synapses by their symmetrical morphology and excitatory synapses by their asymmetrical morphology. Selected boutons of 5 orexinergic neurons per animal (n=3 mice per group) were followed through 24 consecutive LH serial ultrathin (60 nm) sections. According to the synaptological method used by Horvath and Gao3, we randomly sampled every element of the analysis as the bouton at high power magnification, the orexinergic-ir perikarya and the plane of each transected OX-A cell. Twenty CB1-expressing boutons contacting the soma of OX-A neurons were analyzed for each animal (i.e. an average of four CB1-expressing boutons per neuron). Furthermore, since the boutons contacting the dendritic spine proximal to the soma provide a further measure of the overall excitation/inhibition balance (given that a high number of synaptic inputs are received by proximal dendrites), we also analysed ten CB1-expressing axo-dendritic boutons for each mouse from another 24 consecutive LH ultrathin sections, different from those used for counting perisomatic CB1-expressing boutons. In post-weaning and adult *ob/ob* mice and in adult HFD mice, CB1-symmetric (inhibitory) synapses robustly outnumbered CB1-asymmetric (excitatory) contacts both in perisomatic and dendritic compartments. However, in pre-weaning *ob/ob* and *wt* mice an equivalent number of CB1-inhibitory and CB1-excitatory synapses were found in both perisomatic (Fig. 22a-d) and dendritic compartments (Fig. 22e-h). Finally, when analyzed as number of boutons per µm of plasma membrane, CB1-expressing boutons were found to be predominantly symmetric in the OX-A perikarya of adult *ob/ob* and HFD mice, as opposed to them being predominantly asymmetric in lean mice (Fig. 23).

Functional evidence for the stronger inhibitory innervation of *ob/ob* orexinergic neurons

To determine if our anatomical observation of a stronger inhibitory innervation of *ob/ob* orexinergic neurons had a functional consequence we performed whole-cell voltage-clamp recordings of miniature Inhibitory Post Synaptic Currents (mIPSCs) in neurons of the LH/perifornical area from murine brain slices at two developmental stages: before (3 weeks of age, n = 10 mice) and after (5 weeks of age, n = 7) weaning. mIPSCs are synaptic currents caused by the stochastic release of GABA when sodium-dependent action potentials are blocked (1 μM TTX in our case, with ionotropic glutamate receptors blocked by 10 μM CPP and NBQX) and provide a good estimate of the number of functional inhibitory inputs. In the LH/perifornical area about 70% of the neurons express orexins A or B. These neurons show a characteristic electrophysiological response to injected current, i.e.: 1) a tonic, non-adapting repetitive spiking evoked in response to a suprathreshold depolarizing pulse, 2) a rectifying potential change evoked in response to hyperpolarizing pulses, and 3) an abortive spike evoked in response to a sub-threshold depolarizing pulse (190). For our experiments we selected those neurons that showed at least two of the above responses, and confirmed the validity of these criteria in a subset of 17 orexinergic neurons (identified functionally) filled with neurobiotin through the recording electrode. With glutamate inputs blocked, we found no difference in the mean resting membrane potential of neurons from *ob/ob* and *wt* mice of the same age. Pooling data together from *ob/ob* and *wt* of the same age, a statistically significant difference was found in resting membrane potential between 3 *vs* 5 week-old neurons (- 52.6 ± 1.96 mV, n = 12, and -44.0 ± 1.08 mV, n = 44, 3 and 5 weeks respectively, $P < 0.005$). The mean input resistance was 154 ± 8.2 MΩ (n = 51), with no difference between *ob/ob* and *wt* mice at any developmental stage. With a high concentration of KCl in the recording solution and recording at a holding potential of -70 mV, a chloride-mediated mIPSC appears as an inward current (negative deflection on the recording trace). Before weaning, no difference was observed in mIPSC frequency betweeen *ob/ob* and *wt* neurons (0.8 ± 0.28 Hz, n = 8 and 0.8 ± 0.29 Hz, n = 5, *ob/ob* and *wt*, respectively). Interestingly, and consistent with our morphological data of more inhibitory synapses, in weaned *ob/ob* mice the mean mIPSCs frequency of orexinergic neurons was significantly higher than that of *wt* neurons (4.0 ± 0.74 Hz, n = 10; 1.6 ± 0.83 Hz, n = 10, in *ob/ob* and *wt* mice,

respectively, $P < 0.05$), and it was also higher than that of pre-weaning *ob/ob* neurons ($P < 0.005$) (Fig.24).

Modulation of inhibitory synaptic activity onto orexinergic neurons by CB1

We have presented morphological evidence for a higher expression of CB1 receptors in inhibitory terminals of *ob/ob* orexinergic neurons compared to their *wt* siblings. Thus we expected the CB1 agonist, WIN55,212-2 (WIN), to depress inhibitory synapses more effectively in *ob/ob* than in *wt* orexinergic neurons from 5 week old mice. To test this prediction we recorded spontaneous inhibitory activity in the absence of TTX. In this condition spontaneous action potentials are present, and thus two populations of IPSCs are simultaneously recorded, collectively named as "spontaneous Inhibitory Post Synaptic Currents" (sIPSCs): one population that is caused by the purely stochastic exocytosis of the neurotransmitter (which corresponds to mIPSCs), and a second one, evoked in response to a spontaneous pre-synaptic action potential. Since the activation of CB1 receptors is known to depress the action potential-evoked Ca^{2+} influx (22, 48), underlying synaptic vesicle release, sIPSCs may provide a more comprehensive measure of the effect of CB1 activation on synaptic transmission than just measuring mIPSCs. Similarly to mIPSCs, control sIPSC frequency was higher in post-weaning *ob/ob* orexinergic neurons than in *wt* neurons. Bath application of WIN (5 μM) reduced the frequency of sIPSCs both in *ob/ob* and in *wt*, although in the latter group the effect did not reach statistical significance (*ob/ob*: control condition 6.0 ± 1.4 Hz, WIN 1.5 ± 0.3 Hz, $n = 9$, $P < 0.01$; *wt*: control condition 4.7 ± 1.99 Hz, WIN 1.9 ± 0.84 Hz, $n = 9$, $P > 0.05$; Fig. 25). To better estimate a possible differential effects of WIN on sIPSC frequency between the two groups of neurons, for each experiment sIPSC frequency after WIN was normalized to sIPSC frequency before WIN. When data were expressed in this manner, the average inhibition was significantly larger in *ob/ob* compared to *wt* neurons (*ob/ob* sIPSC frequency after WIN relative to control: 33.1 ± 6.28%, $P < 0.001$; *wt*: 57.1 ± 8.04%, $P < 0.001$; difference between the two groups significant at $P < 0.05$). Two pieces of evidence are in favor of a CB1-mediated mechanism of action for WIN. First, the reduction of sIPSC frequency was not accompanied by a statistically significant reduction of their amplitude (relative *ob/ob* sIPSC amplitude with WIN: 89.5 ± 10.69%,

n = 9, *P* = 0.2; *wt*: 83.84 ± 8.04% *n* = 9, *P* > 0.1; absolute values in Fig. 25). This suggests that the primary site of WIN action was presynaptic, in agreement with the characteristic pre-synaptic location and function of CB1 receptors. Secondly, in the presence of the selective CB1 blocker AM251 (4 μM), WIN failed to significantly reduce sIPSC frequency (relative *ob/ob* sIPSC frequency with AM+WIN: 76.7 ± 9.67%, *n* = 6, *P* > 0.05; *wt*: 76.7 ± 14.11%, *n* = 4, *P* > 0.1; Fig. 26a). The application of AM251 alone did not affect sIPSC frequency, either in *ob/ob* neurons or their *wt* siblings (Fig. 26a). Finally, neither AM alone nor AM+WIN modified sIPSC amplitude (Fig. 26b).

Therefore, we have that *ob/ob* orexinergic neurons receive a strong inhibitory innervation which can be depressed by WIN, acting through presynaptic CB1 receptors. We have also shown that the same type of neurons express higher levels of DAGLα, which is central in the production of the endocannabinoid 2-AG, and that 2-AG itself is present at a higher concentration in the LH of *ob/ob* mice as compared to wt mice. Thus, it is likely that *ob/ob* orexinergic neurons, when stimulated, may release 2-AG, which in turn acts retrogradely on CB1-expressing inhibitory inputs to reduce their activity (a possible positive feed-back mechanism on the firing of *ob/ob* orexinergic neurons). A well known method to investigate this phenomenon is by evoking a Depolarization-induced Suppression of Inhibition (DSI). In a previous study examining orexinergic neurons from the LH of wt lean mice this type of retrograde inhibition by endocannabinoids was not observed (191). Interestingly, in the same study, a clear inhibitory effect was described on excitatory inputs (a negative feed-back mechanism on the firing of orexinergic neurons). These results can be reconciled by our present morphological observations of greater CB1 expression on the excitatory innervation of these neurons in *wt* and SFD lean mice. To test the hypothesis that DSI is increased in orexinergic neurons of *ob/ob* mice (5 weeks of age), we briefly (5 s) depolarized these neurons from -70 to 0mV and measured the frequency of sIPSCs before and after the depolarization. We found a significant 25-30% frequency reduction in *ob/ob* orexinergic neurons after the depolarization (frequency 5 and 10 s after the depolarization relative to 5 s before: 71% ± 0.05 and 74% ± 0.05, *n* = 11, P < 0.001; Fig. 27. Absolute values 5 s before and after the depolarization: 11.4 ± 3.33Hz and 8.5 ± 2.58Hz, *P* < 0.05). The DSI was: 1) short-lived, since it lasted about 10 seconds, by which time sIPSCs frequency had recovered to control values; and 2) mediated by the release of endocannabinoids acting at CB1 receptors, since, when repeating the experiment in the presence of AM251, DSI was not observed (frequency 5

and 10 s after the depolarization relative to 5 s before: 108% ± 0.13 and 90% ± 0.05, $n = 11$, P > 0.5 and > 0.1, respectively; Fig. 27. Absolute values 5 s before and after the depolarization: 3.6 ± 1.12 Hz, 3.4 ± 0.99 Hz, $n = 11$, $P > 0.1$).

The shift from excitatory to inhibitory CB1-expressing inputs onto OX-A neurons, and its stimulation of orexin release, are reversed by leptin administration in ob/ob mice

To test whether the altered synaptology of OX-A neuronal perikarya in adult obese mice is due to leptin deficiency or resistance, an analysis of the synaptic organization of these neurons was performed again in 9 week old wt and ob/ob mice, after a single injection of recombinant leptin at the beginning of 24h food deprivation. A general increase in immunoreactivity for VGluT2 and a decrease in VGAT immunoreactivity were observed in the LH of ob/ob mice after leptin injection, resembling the pattern observed in wt mice. This effect was accompanied by a shift of CB1 expression from inhibitory back to excitatory axon terminals (Fig. 28), as assessed by quantitative analysis of the abundance of CB1/VGAT-expressing vs. CB1/VGluT2-expressing axon terminals in close proximity to OX-A perikarya (Fig. 29). These leptin-induced morphological changes were paralleled by functional changes in inhibitory signaling onto orexinergic neurons. In fact, when we recorded mIPSCs from orexinergic neurons in 5 week old ob/ob and wt mice 24 hr after a single injection of recombinant leptin, we found no difference between ob/ob and wt mice (Fig. 30). This contrasts to what we observed in untreated animals, where ob/ob neurons had a higher mIPSC frequency. Specifically, after leptin administration, mIPSC frequency of ob/ob neurons was indistinguishable from the low level observed in wt neurons (ob/ob mIPSCs frequency: 1.35 ± 0.52 Hz, n = 13; wt: 1.71 ± 0.76 Hz, n = 12, P > 0.5). Finally, the above leptin treatment also reversed the changes in OX-A-ir in orexinergic neuron output to the ARC seen in obese adult mice. In these analyses also the effect of fasting alone was monitored (Fig. 31). Whilst no effect was observed in LH OX-A neurons, a substantial reduction of OX-A expression was observed in fibers of the ARC in leptin-injected ob/ob mice as compared to wt mice (Fig. 31).

DISCUSSION AND CONCLUSIONS

DISCUSSION

Based on the previously described role of leptin in food deprivation-induced "rewiring" of the hypothalamus, and the LH in particular (12), and on the important neuromodulatory roles of the endocannabinoid system in this area (191, 192), we investigated if remodeling of orexinergic neuronal wiring also occurs during a prolonged nutritional perturbation caused by, or resulting in, leptin signalling deficiency, as in ob/ob and HFD mice, respectively, and its impact on endocannabinoid signalling. First, through immunofluorescence and ultrastructural studies in the LH of lean mice, we found that, as in other brain nuclei, elements of the endocannabinoid system are well positioned to facilitate the retrograde action of post-synaptically produced 2-AG onto pre-synaptic CB1 receptors (193, 194). Specifically, orexinergic neurons express the 2-AG-biosynthesizing enzyme DAGLα in somatic and proximal dendritic compartments and receive afferents that express both CB1 receptors and the 2-AG-hydrolysing enzyme, MAGL. In lean mice these fibers are mostly glutamatergic/excitatory nature. This agrees with previous studies showing that DAGLα is mostly distributed in somatodendritic spines apposed to excitatory axon terminals (194), and indicating that orexinergic neurons mostly receive excitatory inputs (12, 191). These data provide for the first time the anatomical basis for the previously observed CB1-mediated inhibition of excitatory postsynaptic currents and for endocannabinoid participation in depolarization-induced suppression of excitation (DSE) in these neurons (191). More interestingly, we investigated a possible dysregulation of endocannabinoid neuromodulatory actions in the LH during obesity. Our next findings, based on a variety of experimental approaches, indicate that: 1) inhibitory axon terminals on orexinergic neurons become significantly more numerous than excitatory ones in adult and weaned, but not pre-weaned, ob/ob mice and adult HFD mice as compared to matched controls; 2) also CB1 and MAGL-expressing terminals onto orexinergic neurons become predominantly inhibitory in obese mice; 3) these rearrangements result in: a) higher mIPSC and sIPSC frequency, b) stronger presynaptic inhibition of sIPSC by CB1 agonists, and c) endocannabinoid-mediated DSI (as opposed to DSE of control mice), in orexinergic neurons; 4) 2-AG biosynthesis is elevated in the LH of adult ob/ob and HFD mice, thus potentially allowing for stronger endocannabinoid-mediated disinhibition of orexinergic neurons in these mice. These findings provide unprecedented evidence of a rapid and substantial functional rearrangement of endocannabinoid-mediated neuromodulation in the brain during obesity. In ob/ob mice, the shift from

excitatory to inhibitory transmission in LH orexinergic neurons occurs after weaning, i.e. when ob/ob pups stop receiving leptin from the milk of their heterozygote dams and become progressively leptin-depleted. This leads to the hypothesis that this rearrangement is directly due to lack of leptin, as previously suggested for the ARC (6, 7). Neuroanatomical studies have suggested that the majority of leptin's anti-obesity effects are mediated by LepRb in the ARC of hypothalamus (158-160), in which leptin regulates the activity of two oppositely acting sets of lepRb-exspressing neurons by stimulating anorexigenic neurons that express POMC and CART, and inhibiting orexigenic neurons that express NPY and AgRP (123, 161, 162). Leptin responsive POMC and NPY/AgRP neurons project to the LH and some of them make close anatomical contacts with OX neurons (123, 161, 162). Furthermore, recent papers show that leptin modulates also the axonal growth and synaptic plasticity within the hypothalamus (6, 7) and play a crucial role in the control of EC levels (2) and inhibitory or excitatory phenotype of arcuate projections to OX neurons (12) In particular, leptin increases neurite extension in the ARC during mouse perinatal development, thus playing an early trophic role within those circuits that will be the target of leptin physiological actions in adult life (6). Moreover, an OX1R-selective antagonist reduced food intake and ameliorated obesity of leptin-deficient ob/ob mice (134), suggesting that leptin deficiency at least partly activates the orexin pathway to increase food intake. Accordingly, we found that 24 h leptin administration to adult ob/ob mice was sufficient to reverse the observed rewiring of CB1-expressing afferents to OX neurons, as assessed by both immunohistochemical analyses and functional patch-clamp measurements. Furthermore, experiments in mice made obese and leptin resistant by prolonged HFD extend our findings to an animal model more relevant to human obesity. This provides further support for the involvement of leptin in the observed shift in synaptic populations and endocannabinoid signaling, and may suggest that the rearranged CB1-expressing afferents to LH neurons may originate in the ARC, since: 1) HFD mice exhibit leptin resistance in this nucleus, but not in other leptin-responsive hypothalamic and extra-hypothalamic nuclei (195); and 2) efferents to LH orexinergic neurons from the ARC were already known to undergo leptin-dependent reorganization following food deprivation in lean mice (12). However, in mice with HFD-induced obesity it is also possible that the alteration of CB1-mediated regulation of LH neuronal activity may have been due to the dysrupted nutritional regulation that follows a prolonged HFD. Due to their leptin resistance, it is not feasible to reverse the synaptic rearrangement observed in these mice by leptin injection, as

was possible for ob/ob mice. However, in HFD-mice we observed changes in synaptic function very similar to those of ob/ob mice. The increased levels of 2-AG that we found in adult ob/ob and HFD mice are unlikely to be due solely to defective leptin signaling (2). This is not only because leptin resistance may not have occurred in the LH of HFD mice40, but also because we found that increased 2-AG levels were paralleled by increased DAGLα expression, whereas leptin is thought to modify the activity of 2-AG synthesizing enzymes rather than their expression (2, 192, 196). Finally, we also found that the number of OX-A-expressing projections to the ARC was significantly elevated in ob/ob mice, from weaning onwards, and is also increased in adult HFD mice. One interpretation of this finding is that OX-A release is increased in the ARC, since increased release of a neuropeptide results in chronic upregulation of its trafficking to terminals. Accordingly, expression of pre-proorexin mRNA in the LH was increased with a later onset as compared to OX-A release into the ARC, whereas OX-A-ir in the LH did not change, possibly as a result of increased production in this area and increased release in output regions. These data suggest that the potentially enhanced endocannabinoid-mediated disinhibition of orexinergic neurons, described here, increases release of OX-A in the ARC, in which we found in both ob/ob and HFD obese mice, enhanced expression of OX-A. This plasticity could have obvious consequences on increasing appetite and body weight, thus possibly resulting in a vicious cycle in which the endocannabinoid 2-AG acts as both a trigger and enhancer of food intake. This possibility is also supported by the anorectic, thermogenic and anti-obesity activity of SB-334867-A, a selective orexin-A receptor antagonist, in ob/ob mice (9).

CONCLUSIONS

In conclusion, we provide here a unique example of how endocannabinoid neuromodulatory control over excitatory and inhibitory neurotransmission in the brain is profoundly altered as a consequence of leptin-dependent rewiring of glutamatergic and GABAergic synapses. In the LH this alteration may result in the disinhibition of orexinergic neurons via enhanced retrograde inhibition of their inhibitory vs. excitatory inputs. This data support our hypothesis that endocannabinoid signaling could really exert a powerful modulation of OX-A neurons in the LHA, playing a strategic role in feeding control. In particular, during feeding glutamate-induced hyperactivation of endocannabinoid synthesis may trigger a DSI via CB1 receptors which localize prevalently with GABAergic inputs, thus inducing disinhibition of OX1 release. A dishinibition of OX-A release could occur in the ARC of ob/ob mice as effect of 2-AG-mediated DSI on inhibitory inputs to orexinergic neurons thus increasing food-intake. The prolonged hypocretin disinhibition subsequent to overexpression of 2-AG as an effect of the altered rhythm of feeding may, in turn, trigger a vicious circle for feeding itself. Therefore, we have found a drastic rearrangement of the EC system, in all its elements, at the level of LH OX neurons during obesity, which seems to be explained at least in part by defective leptin signaling. In particular, the activity of OX neurons could be modulated by a CB1-receptor-mediated inhibitory effect on the GABA inhibitory and/or Glutammate excitatory projections (by means of DSI and DSE) controlling the activity of the LH OX neurons and the leptin-deficiency modifies the distribution of CB1 receptors between excitatory and inhibitory terminals leading to a switch from excitatory to inhibitory projections, which would alter endocannabinoid-control of neuronal activity.

FIGURES

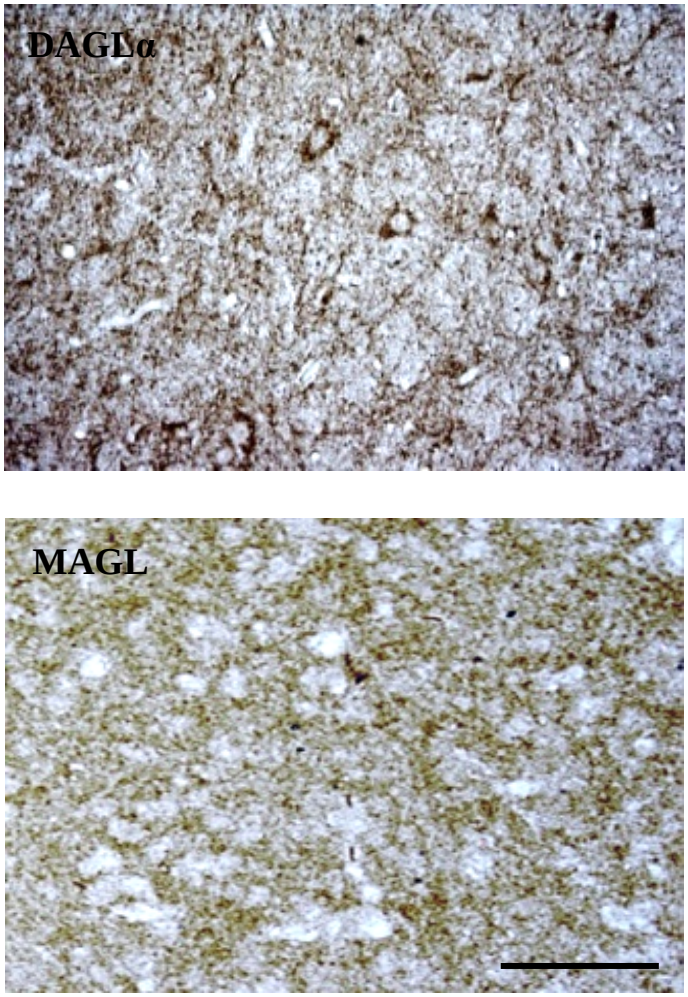

Fig. 11: *Peroxidase-based DAGLα and MAGL immunostaining showing DAGLα expression in the neuropil and perisomatic punctate structures and MAGL expression in punctate structures. Scale bars represent 100 µm.*

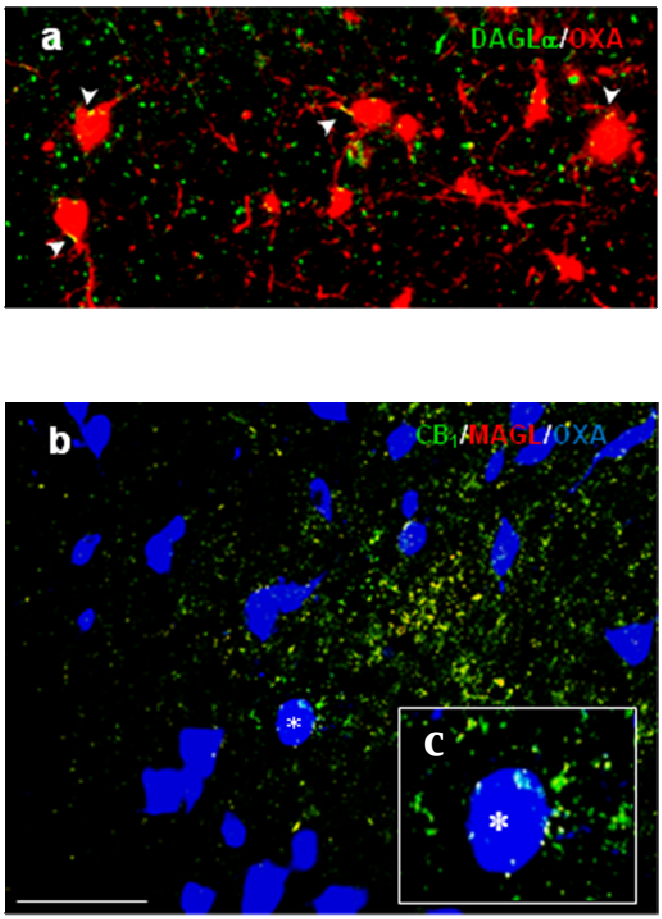

Fig. 12: *Expression of the endocannabinoid system at the level of OX-A neurons.* ***(a)*** *Distribution of DAGLα in OX-A neurons of the lateral hypothalamus perifornical area of adult wt mice. Perisomatic clustering of DAGLα in OX-A neurons (arrowheads) and in the neuropil.* ***(b)*** *CB1/MAGL co-localization in the neuropil of LH and on many OX-A neurons at the perisomatic level as it appears in the asterisk labeled neurons.Scale bars represent 60μm* ***(b, c),*** *and 25μm (insert* ***c****)*

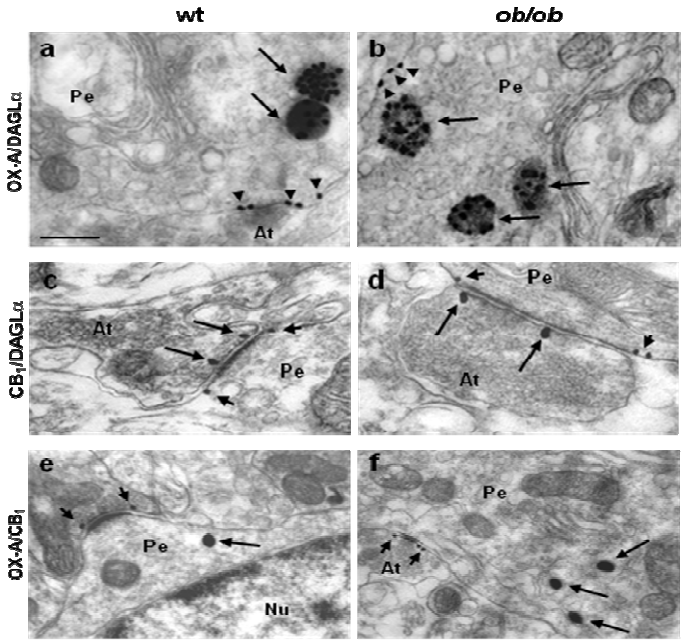

Fig. 13: *Sequential silver-enhanced double OX/DAGLα or CB_1/DAGLα or OX/CB_1 immunogold electron microscopy in the lateral hypothalamus of wt and ob/ob mice 9 week-old. Note that the first primary antibody of each adopted mixture generated a larger size than the second primary antibody because the corresponding ultra small gold antibody conjugate was enhanced twice whereas the second ultra small gold antibody conjugate was enhanced only once.* ***(a, b)*** *Intense accumulation of OX in dense vesicles (arrows) within the perikaryon (Pe) of cell expressing DAGLα concentrated on the somatic membrane (arrowheads) and forming an asymmetrical synapse with a putative excitatory terminal (At) (arrowheads).* ***(c)*** *Asymmetric, putative excitatory axo-somatic synapse and* ***(d)*** *symmetric, putative inhibitory axo-somatic synapse between an axonal terminal (At) expressing intense CB_1 accumulations (arrows) at presynaptic membrane opposite to DAGLα accumulations (arrowheads) at the edges of postsynaptic density.* ***(e, f)*** *Intense accumulation of OX immunogold in highly dense vesicles (arrows) in the perikaryon of neurons which receive an asymmetric putative excitatory CB_1-expressing synapse (arrowheads in* ***e****) or a symmetric putative inhibitory CB_1-expressing synapse (arrowheads in* ***f****). CB_1 labeling was detected intensely on edges of presynaptic membrane specializations. No differences in the ultrastructural expression and localization of each marker were found between the lateral hypothalamus of wt and ob/ob mice. Sp, dendritic spine; At, axonal terminal; Pe, perikaryon; Nu, nucleus. Scale bar represents 0.6 µm* ***(a,b)****, 0.5µm* ***(c)****, 0.4µm* ***(d,f)****, 0.3µm* ***(e)****.*

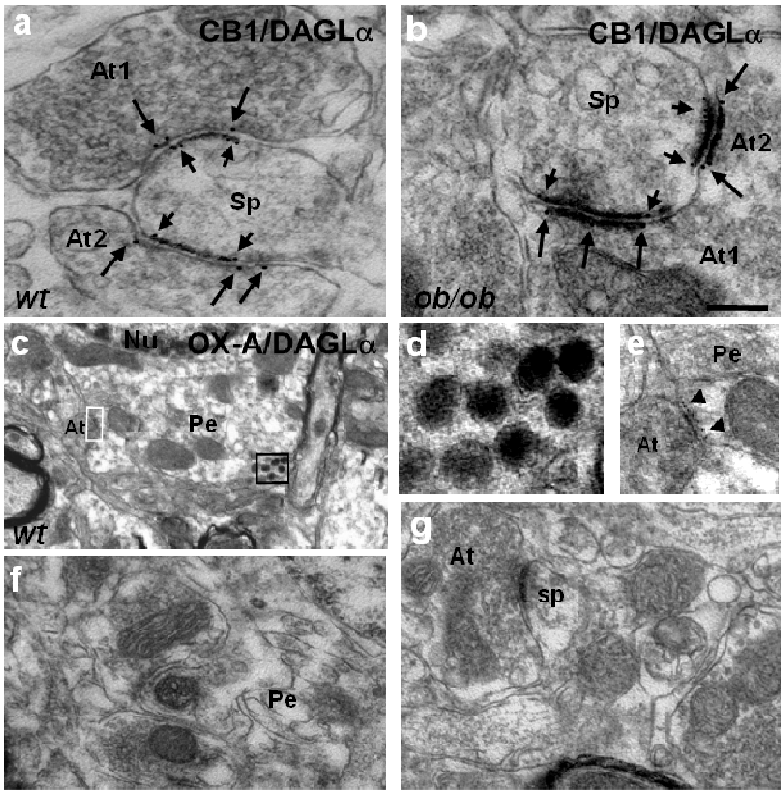

Fig. 15: *Double CB1/DAGLα or OX-A/DAGLα pre-embedding 6nm and 10 nm immunogold electron microscopy in wt and ob/ob mice.* ***(a)*** *Asymmetric, putative excitatory axo-dendritic synapses in the lateral hypothalamus of wt mice. 6nm DAGLα gold particles are selectively observed at a postsynaptic somatic perimembrane specialization of a dendritic spine (Sp, arrowheads). 10 nm CB1 particles are located in two different axonal terminals (At1 and At2, arrows) at the edges of each presynaptic site, opposite to DAGLα.* ***(b)*** *Symmetric, putative inhibitory axo-dendritic synapse in the lateral hypothalamus of ob/ob mice showing 6nm DAGLα and 10 nm CB1 particles distributed as in* ***(a)****.* ***(c)*** *6nm DAGLα gold particles are strictly located near the somatic perimembrane compartment including a postsynaptic side (white boxed) of a wt OX-A neuron with 10 nm OX-A gold particles piled in heavy dots within dense cytosolic vescicles (black boxed area).* ***(d)*** *High magnification of the black boxed area in "****c****" showing clusters of OX-A gold particles.* ***(e)*** *High magnification of white boxed area in "****c****" showing 6 nm DAGLα gold particles (arrowheads) near the internal surface of presynaptic plasma membrane. At, axonal terminal; Nu, nucleus; Pe, perikaryon, Sp, dendritic spine. Scale bars represent 0.1µm* ***(a,b)****, 1.4µm* ***(c)****, 0.2µm* ***(d)****, 0.12µm* ***(e)****.*

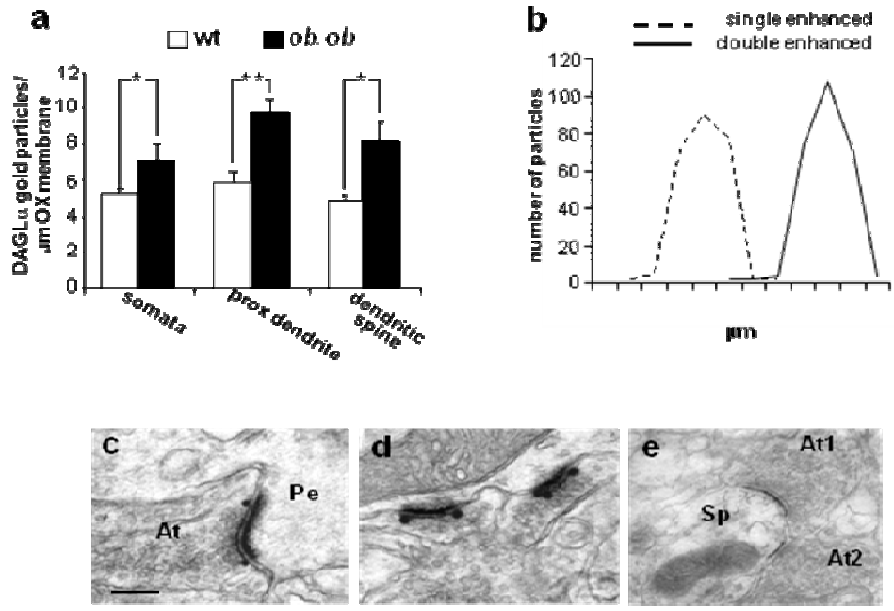

Fig. 15: ***(a)*** *Histogram showing the density of DAGLα gold particles in somata, proximal dendrites and dendritic spines of OX neurons. The distribution of DAGLα silver-enhanced immunogold labeling was normalized to µm of membrane length of orexinergic neurons by counting the number of particles on 5 neurons per animal followed through 24 consecutive lateral hypothalamus serial ultrathin sections (n=3 mice per group).* ***(b)*** *Histogram showing two distinct particle size distributions of gold particles silver enhanced, respectively, once vs twice. The mean diameter of n=250 particles was of 45.8 +8.50 nm when single enhanced; 92.5 +12.6 nm when double enhanced.* ***(c,d)*** *Controls of gold particle size growing performed by once* ***(c)*** *vs twice* ***(d)*** *silver enhancement of the secondary antibody against CB1 marker. Enhancing one of the gold labels once vs twice resulted in a doubling of size.* ***(e)*** *Negative controls obtained by omitting the mixture of primary antibodies. Note the absence of immunogold silver enhanced signal . Similar results were obtained by omission of the mixture of secondary ultra small antibodies (data not shown). Sp, dendritic spine; At, axonal terminal; Pe, perikaryon. Scale bar represents 0.7µm* ***(c,d)****.*

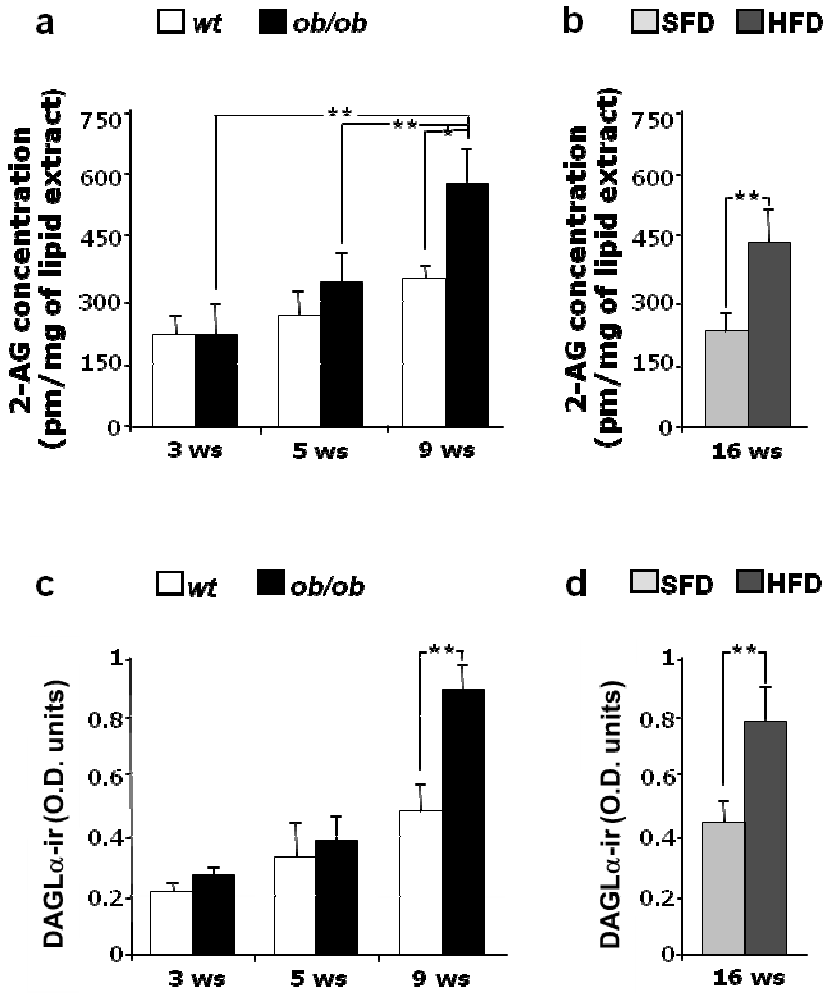

Fig. 16: *The levels of DAGLα protein expression and 2-AG in the lateral hypothalamus increase during obesity.* ***(a,b)*** *2-AG levels were evaluated by LC-MS on the lateral hypothalamus isolated from the brain of mice at different ages, genotypes and diets.* ***(c,d)*** *Quantitative analysis of DAGLα peroxidase-based immunostaining (optical density or O.D.) performed on orexinergic neurons identified on adjacent DAGLα/OX-A immunoreactive sections. Means ± s.e.m.; n=500 OX-A neurons per group of ages, genotypes and diets; * P < 0.05; ** P < 0.01.*

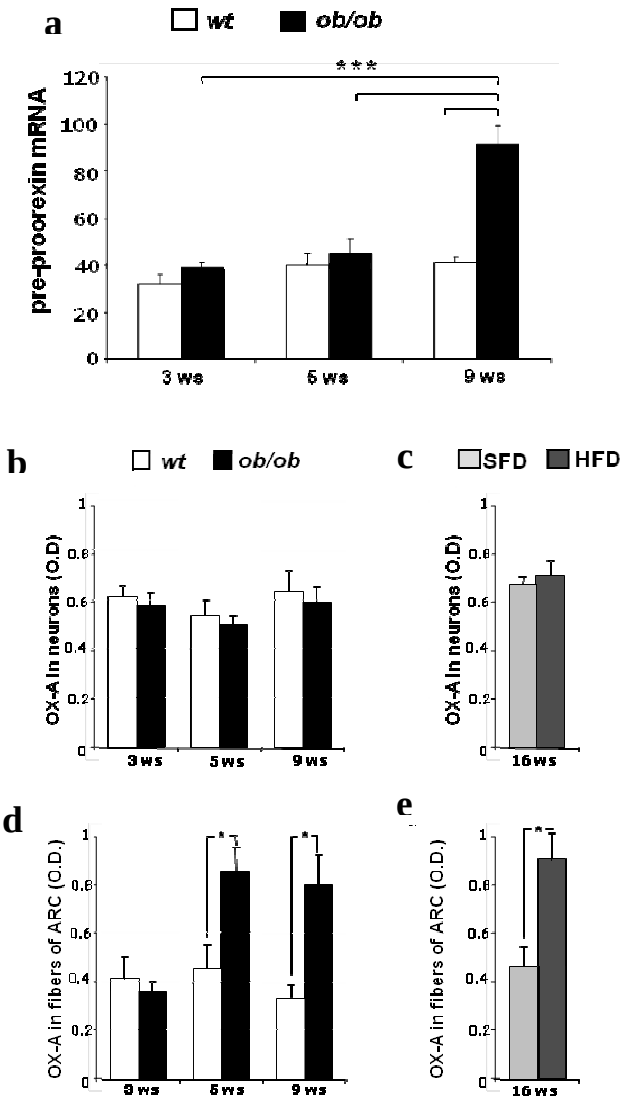

Fig. 17: ***(a)*** *Quantification of pre-proorexin mRNA expression in the lateral hypothalamus of 3, 5 and 9 weeks old ob/ob and wt mice, normalized to the reference gene Hprt; n=8 LH in each group; n= 4 animals per group; *** P < 0.001 for each comparison.* ***(b-e)*** *Histograms of quantitative densitometry scanning of optical density (O.D.) of peroxidase-based OX-A immunostaining during obesity compared to lean mice at each age both for genotype and diet.* ***(b,c)*** *Lateral hypothalamic orexinergic neurons showing no change in the intensity of OX-A expression;* ***(d,e)*** *fibers of the arcuate nucleus (ARC) showing the increase of expression in obese mice after weaning. Means ± s.e.m.; n>120 sections per area; n = 3 mice at each age for genotype and diet; *P < 0.05 for the comparison of post-weaning and adult ob/ob mice vs. the corresponding wt mice or of HFD vs. SFD mice.*

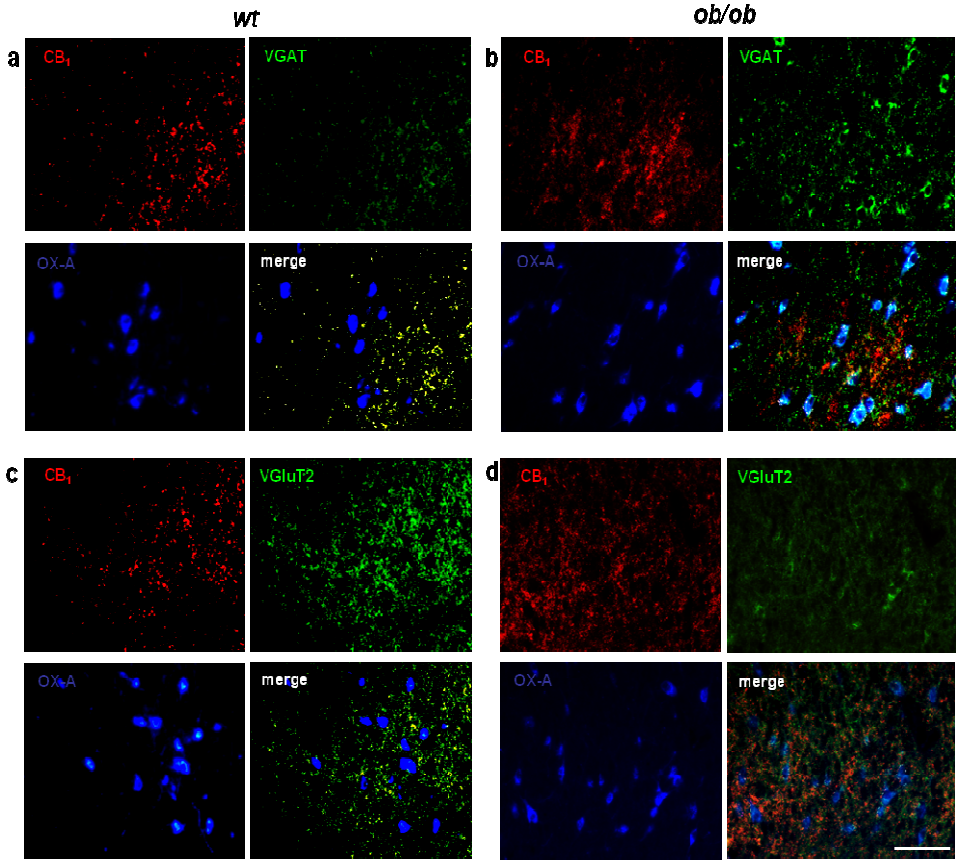

Fig. 18: *Abundance of glutamatergic CB1- or GABAergic CB1-expressing fibers onto OX-A-ir neurons of the lateral hypothalamus of adult (9 ws) wt* ***(a,c)*** *vs. ob/ob* ***(b,d)*** *mice, respectively.*

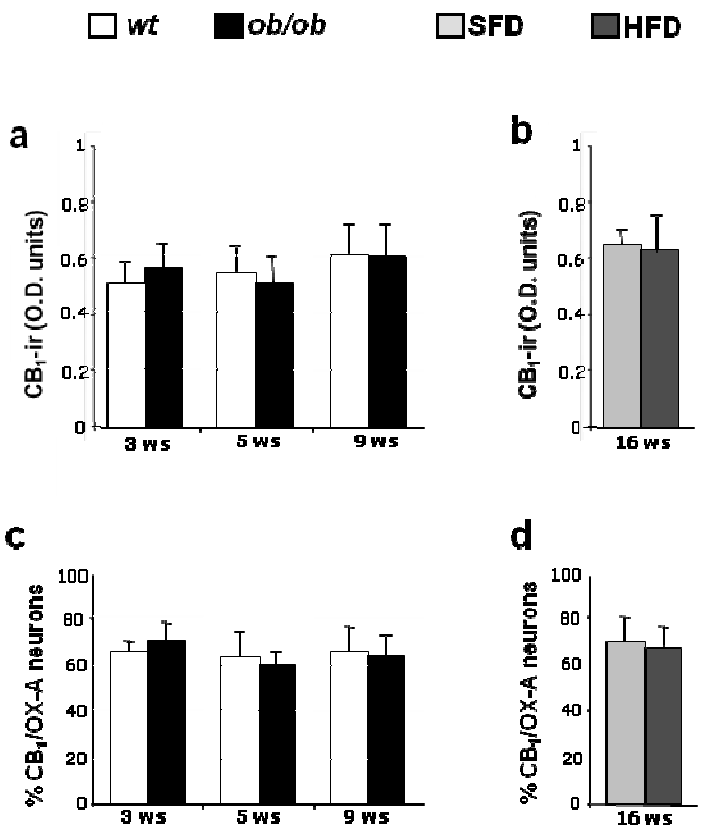

Fig. 19: ***(a, b)*** *Quantitative analysis of the optical density (O.D.) of CB1 peroxidase-based immunostaining of orexinergic neurons as identified on adjacent CB1/OX-A immunolabeled sections of the lateral hypothalamus. Means ± s.e.m.; n=500 OX-A neurons per group of ages, genotypes and diets.* ***(c,d)*** *Percentage of CB1-expressing fibers projecting to OX-A neurons, counted on the total of OX-A synaptophisin-labeled afferences. No statistically significant difference was found for mouse genotype, diet and age. n= 300 OX-A neurons per group. Means± s.e.m.*

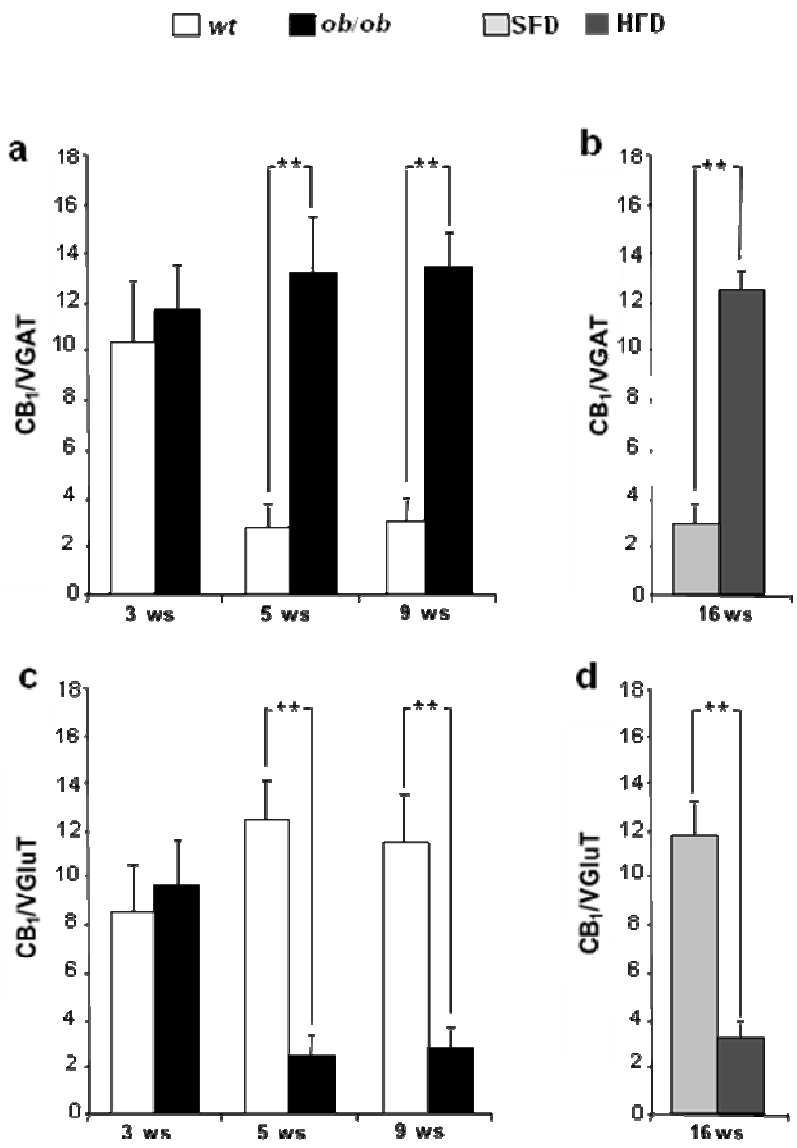

Fig. 20: *Quantitative analysis of CB1/VGAT- vs. CB1/VGluT2-immunolabeled axon terminals in apposition to OX-A perikarya in the lateral hypothalamus. n= 60 OX-A neurons per group, acquired from CB1/VGAT/OX-A or CB1/VGluT2/OX-A sections. In the lateral hypothalamus of post-weaning (5 ws) and adult (9 ws) ob/ob or HFD mice, CB1/VGAT inputs outnumbered CB1/VGluT2 imputs, contrary to what observed in lean mice. No difference was found in pre-weaning (3 ws) wt vs. ob/ob mice. Means± s.e.m.; ** P < 0.01 for the comparison of post-weaning and adult ob/ob mice vs. the corresponding wt mice or of HFD vs. SFD mice.*

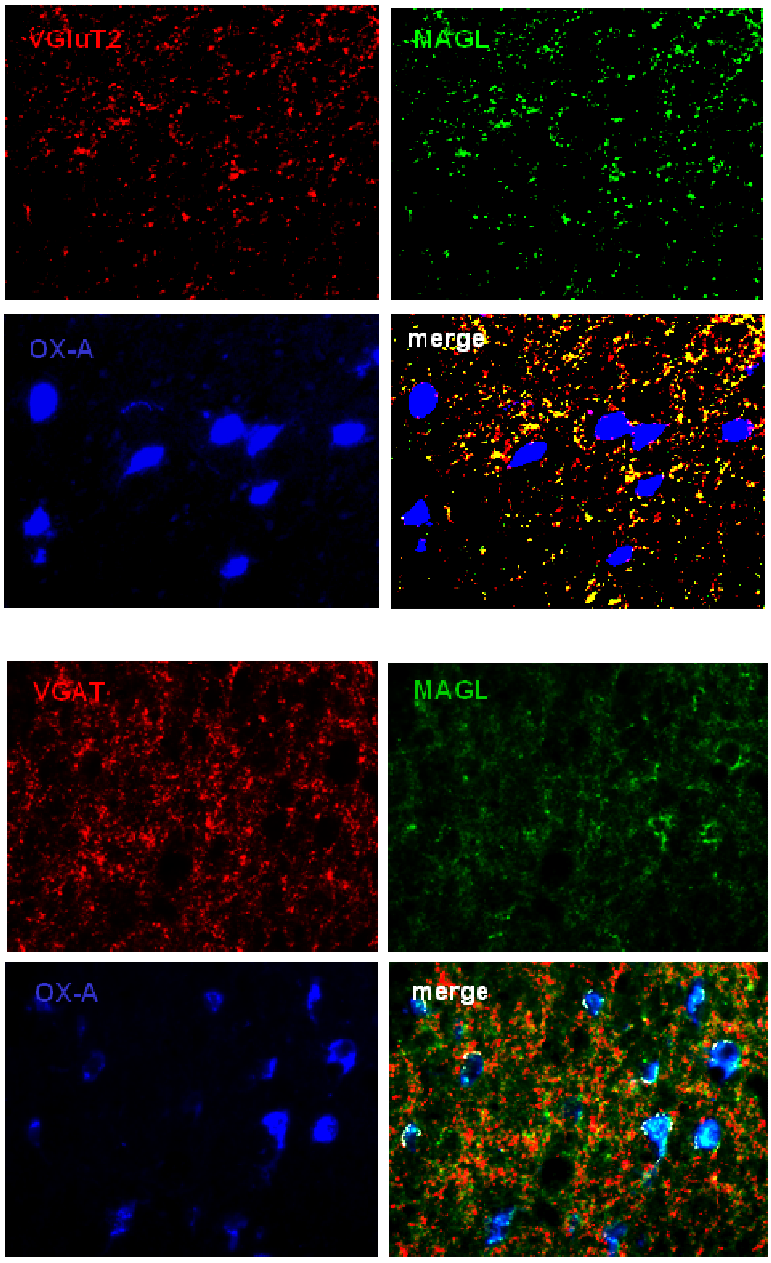

Fig. 21: *Triple VGluT2/MAGL/OX-A in wt and VGAT/MAGL/OX-A in ob/ob immunofluorescence showing the abundance of MAGL localization in glutamatergic vs. GABAergic fibers perisomatic to OX-A neurons in wt and ob/ob mice, respectively. Scale bars represent 50 µm.*

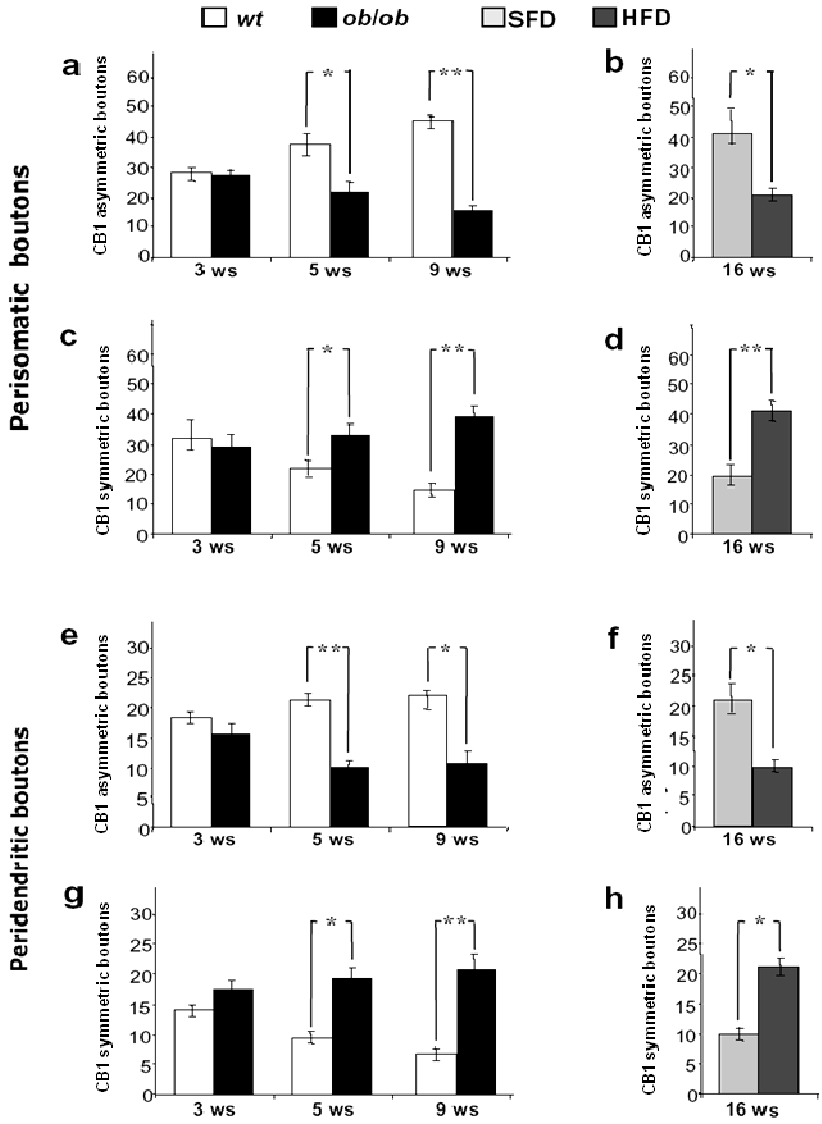

Fig. 22: *Quantitative analysis of perisomatic CB1-expressing boutons* ***(a-d)*** *and somato-proximal peridendritic CB1-expressing boutons* ***(e-h)*** *on OX-A cells in the lateral hypothalamus. The data were collected from 3 ws (pre-weaning), 5 ws (post-weaning) and 9 ws (adult) ob/ob and wt mice and from 16 ws HFD and SFD mice. Only CB1-expressing boutons with clearly identified symmetric or asymmetric morphology were selected for analysis. In post-weaning and adult ob/ob mice and in adult HFD mice, CB1 symmetric synapses outnumbered CB1 asymmetric contacts both in perisomatic and dendritic compartments. No difference was found in pre-weaning wt vs. ob/ob mice both in perisomatic and dendritic compartments. Means± s.e.m; * P< 0.05; ** P < 0.001.*

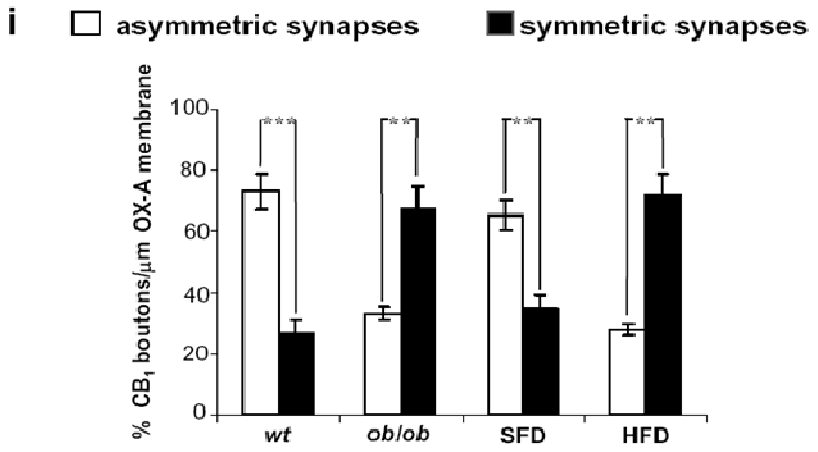

Fig. 23: *Percentage of asymmetric and symmetric CB1-expressing boutons per µm of OX-A membrane of adult (9 weeks old) lean and ob/ob mice. Asymmetric CB1-expressing boutons outnumbered symmetric ones per µm of OX-A membrane of wt and SFD adult mice. An opposite scenario was found in adult obese ob/ob and HFD mice. The value are expressed as mean percentage ± s.e.m ; ** P < 0.01, *** P < 0.001 for the comparison of adult ob/ob mice vs. the corresponding wt mice or of HFD vs. SFD mice.*

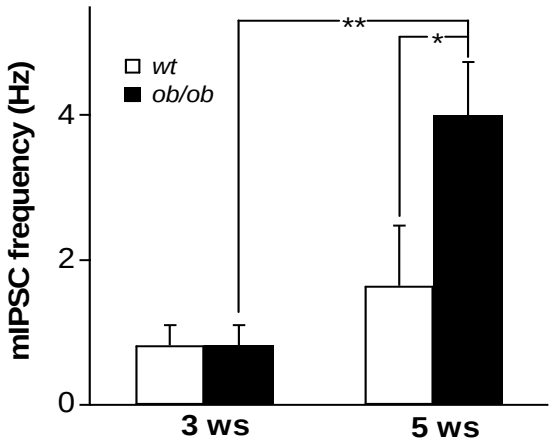

Fig. 24: *Orexinergic neurons of ob/ob mice become more inhibited then wt after weaning. Mean ± s.e.m. frequency of mIPSCs in ob/ob and wt orexinergic neurons before and after weaning. * P < 0.05, ** P < 0.005.*

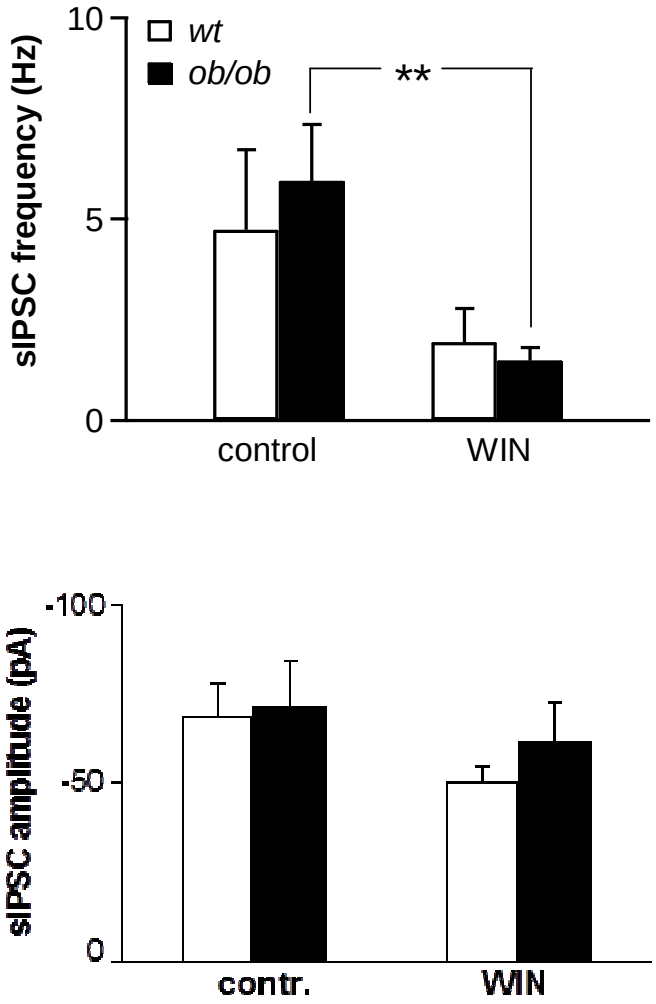

Fig. 25: *Absolute values of sIPSCs frequency and amplitude in ob/ob and wt orexinergic neurons in control condition and in the presence of WIN (5 μM, n = 9 in both groups). The inhibitory synapses acting on ob/ob orexinergic neurons are strongly depressed by the CB_1 agonist WIN55,212-22 (WIN). Data are expressed as mean ± s.e.m. ** P < 0.01.*

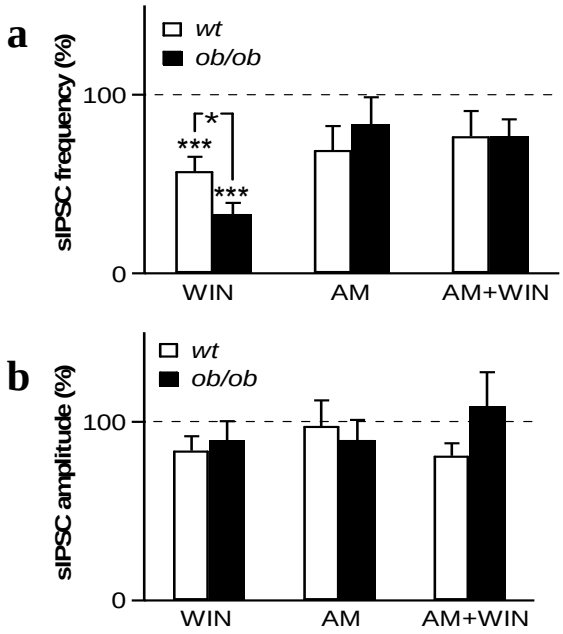

Fig. 26: ***(a)*** *Relative frequency of sIPSCs in the presence of: WIN (5 μM, n = 9 in both groups) or the CB1-receptor antagonist AM251 (AM, 4 μM, n = 6 and 5, ob/ob and wt respectively), and AM with 5 μM WIN (AM+WIN, n = 6 and 4, ob/ob and wt respectively). The dashed line marks the reference sIPSC frequency in control conditions.* ***(b)*** *Relative amplitude of sIPSCs in the presence of: WIN, AM251 and AM+WIN. Same neurons as in* ***(a)****. The dashed line marks the reference amplitude in control condition. Data are expressed as mean ± s.e.m. * P < 0.05, *** P < 0.001.*

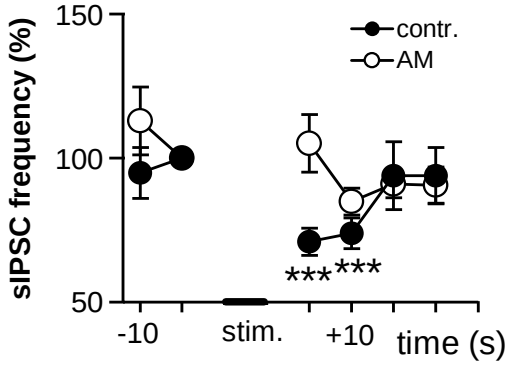

Fig. 27: *Mean ± s.e.m. frequency of sIPSCs as a function of time (5 s bin) after a 5 s step-depolarization to 0 mV ("stim." and the corresponding thicker portion of the abscissa), relative to the frequency 5 s before the depolarization in ob/ob orexinergic neurons before (contr.) and after (AM) the addition of AM. n = 11 in both groups. *** P < 0.001.*

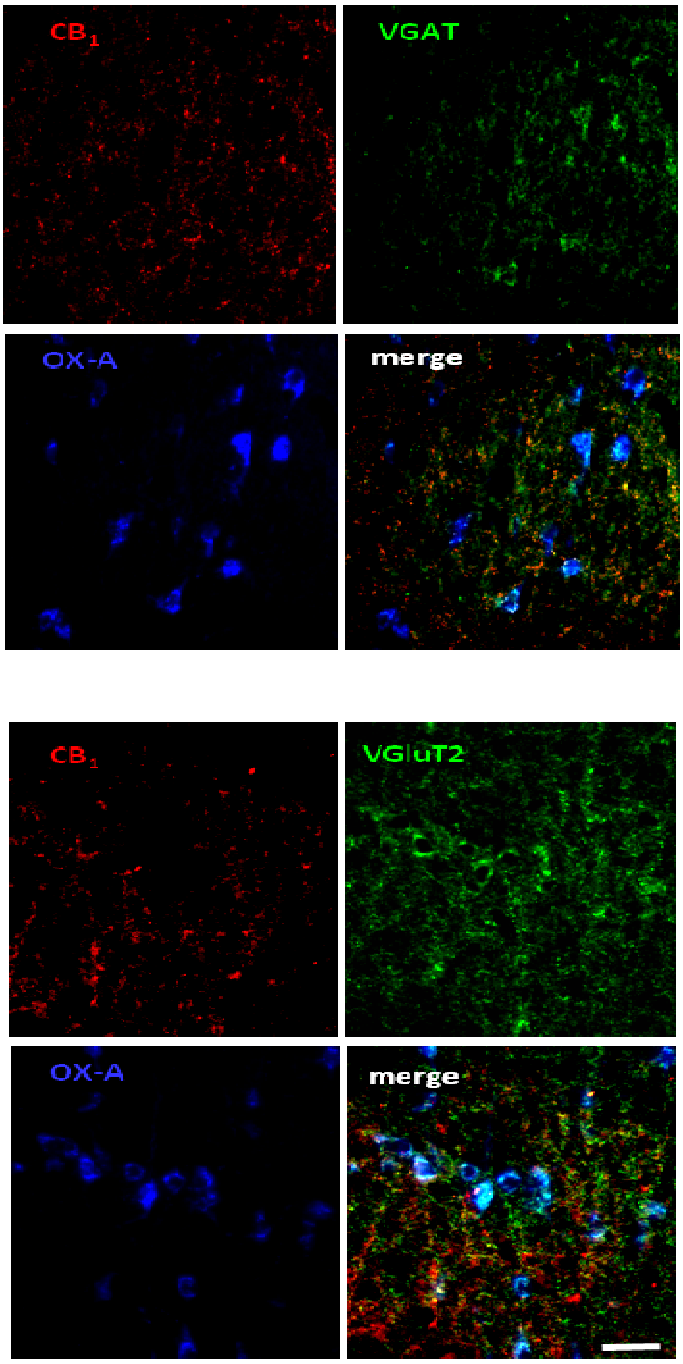

Fig. 28: *Effect of intraperitoneal leptin administration on the rewiring of OX-A neurons in the lateral hypothalamus of ob/ob mice. Triple CB1/VGAT/OX-A and CB1/VGluT2/OX-A immunofluorescence showing the scarcity of CB1 expression in inhibitory fibers and the abundance of CB1 expression in excitatory fibers, respectively, onto OX-A neurons in the lateral hypothalamus at the perisomatic level in adult ob/ob mice. Scale bars represent 50 µm.*

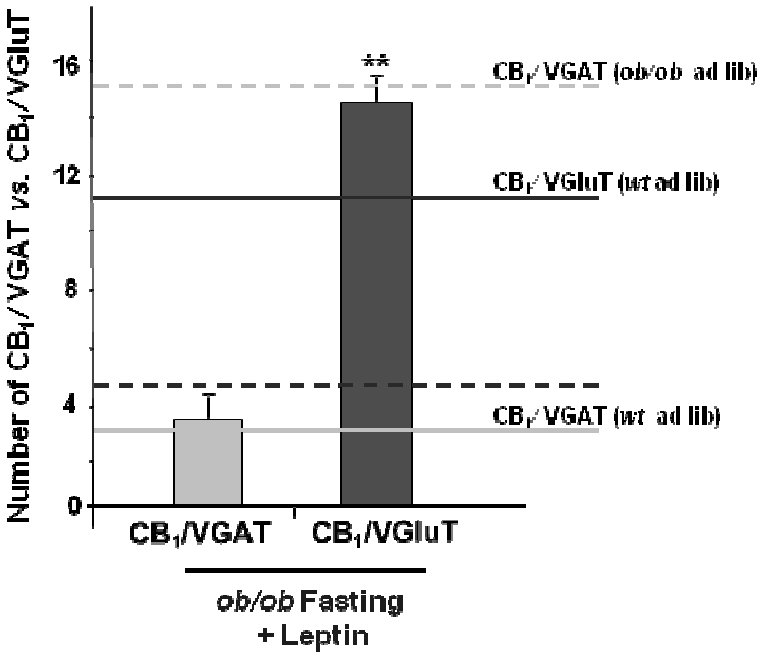

Fig. 29: *Quantitative analysis of CB1/VGAT- vs. CB1/VGluT2-immunolabeled axon terminals apposed to OX-A perikarya, performed after leptin injection plus fasting in adult ob/ob mice. Leptin administration reverses the synaptological alteration of OX-A neurons in the lateral hypothalamus of obese mice. Means± s.e.m; ** P < 0.001 for the comparison of CB1/VGAT- vs. CB1/VGluT2-immunolabeled axon terminals in leptin-injected adult ob/ob mice. Lines denote the amount of CB1/VGAT- vs. CB1/VGluT2-immunolabeled axon terminals in adult untreated wt ad ob/ob mice fed ad libitum.*

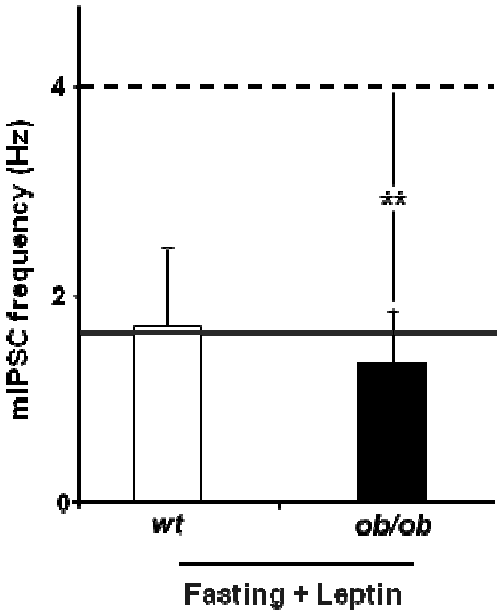

Fig. 30: *Leptin equalizes the number of functional inhibitory synapses of ob/ob orexinergic neurons to wt levels. Mean ± s.e.m. mIPSC frequency in neurons from 5 weeks old mice with 24h fasting + leptin administration. Dashed and solid lines are the mean frequency levels of, respectively, ob/ob and wt mice fed ad libitum. * P < 0.05, ** P < 0.01.*

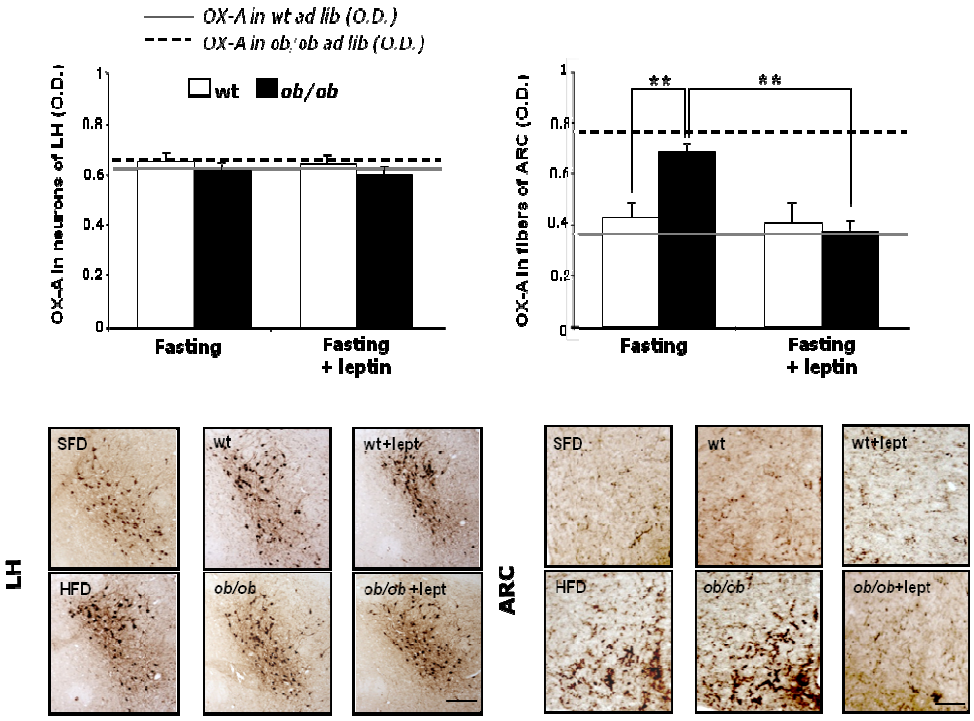

Fig. 31: *The amounts of OX-A in the ARC is increased in adult ob/ob mice in a manner reversed by leptin injection. The intensity of the OX-A signal (O.D.) in the lateral hypothalamus (LH) is not different between wt and ob/ob mice, whereas its intensity is enhanced in the ARC of adult ob/ob mice and reduced in ob/ob but not wt mice 24h after leptin administration plus fasting. Dashed and solid lines represent the mean OX-A optical density in untreated wt ad ob/ob mice fed ad libitum, respectively. Means ± s.e.m.; n=3 mice per group. *P < 0.05; **P < 0.01. The images show an high peroxidase-based OX-A immunoreactivity in neurons of the lateral hypothalamus and an higher peroxidase-based OX-A immunoreactivity in fibers projecting to the ARC in HFD and ob/ob mice compared to SFD and wt, respectively. This alteration is reversed by intra peritoneal treatment of leptin and fasting for 24 h, which instead did not affect wt mice. Scale bars represent 150 µm (LH) and 20 µm (ARC).*

BIBLIOGRAPHY

1. Kirkham T.C., Williams C.M., Fezza F., Di Marzo V. Endocannabinoid levels in rat limbic forebrain and hypothalamus in relation to fasting, feeding and satiation: stimulation of eating by 2-arachidonoyl glycerol. *Br. J. Pharmacol.* **136**, 550–557. (2002)

2. Di Marzo V., Goparaju S.K., Wang L., Liu J., Batkai S., Jarai Z., Fezza F., Miura G.I., Palmiter R.D., Sugiura T., Kunos G. Leptin-regulated endocannabinoids are involved in maintaining food intake. *Nature* **410**, 822–825. (2001)

3. Monteleone P., Matias I., Cardias V., De Petrocellis L., Maj M., Di Marzo V. Blood levels of the endocannabinoid anandamide are increased in anorexia nervosa and in binge-eating disorder, but not in bulimia nervosa. *Neuropsychopharmacology.* **30**, 1216-1221. (2005).

4. Di Marzo V. & Matias I. Endocannabinoid control of food intake and energy balance. *Nat Neurosci.* **8**, 585–589. (2005)

5. Matias I., Gonthier M.P., Orlando P., Martiadis V., De Petrocellis L., Cervino C. Petrosino S, Hoareau L, Festy F, Pasquali R, Roche R, Maj M, Pagotto U, Monteleone P, Di Marzo V. Regulation, function, and dysregulation of endocannabinoids in models of adipose and beta-pancreatic cells and in obesity and hyperglycemia. *J. Clin. Endocrinol. Metab.* **91**, 3171–80. (2006)

6. Bouret S. G., Draper S. J., & Simerly R. B. Trophic action of leptin on hypothalamic neurons that regulate feeding. *Science.* **304**, 108-10 (2004)

7. Pinto S., Roseberry A. G., Liu H., Diano S., Shanabrough M., Cai X., Friedman J. M., Horvath T. L. Rapid re-wiring of arcuate nucleus feeding circuits by leptin. *Science.* **304**, 110–115 (2004)

8. Sakurai T.**,** Amemiya A., Ishii M., Matsuzaki I., Chemelli R.M. Tanaka H, Williams SC, Richardson JA, Kozlowski GP, Wilson S, Arch JR, Buckingham RE, Haynes AC, Carr SA, Annan RS, McNulty DE, Liu WS, Terrett JA, Elshourbagy NA, Bergsma DJ, Yanagisawa M.Orexins and orexin receptors: a family of hypotalamic neuropeptides and G protein-coupled receptors that regulate feeding behavior. *Cell*. **92**, 573-585 (1998)

9. Haynes A.C., Chapman H., Taylor C., Moore G.B., Cawthorne M.A., Tadayyon M., Clapham J.C., Arch J.R. Anorectic, thermogenic and anti-obesity activity of a selective orexin-1

receptor antagonist in ob/ob mice. *Regul. Pept.* **104**, 153–159. (2002)

10. Crespo I.**,** Gómez de Heras R., Rodríguez de Fonseca F., Navarro M. Pretreatment with subeffective doses of Rimonabant attenuates orexigenic actions of orexin A-hypocretin. *Neuropharmacology*. **54(1)**, 219-25. (2008)

11. Huang Y., Huang Y.L., Lai B., Zheng P., Zhu Y.C., Yao T. Raloxifene acutely reduces glutamate-induced intracellular calcium increase in cultured rat cortical neurons via inhibition of high-voltage-activated calcium current. *Neuroscience*. **147(2)**, 334-41 (2007)

12. Horvath T.L. & Gao X.B. Input organization and plasticity of hypocretin neurons: possible clues to obesity's association with insomnia. *Cell Metab*. **1(4)**, 279-86 (2005)

13. Gaoni Y. & Mechoulam, R. Isolation, structure, and partial synthesis of an active constituent of hashish. *J. Am. Chem. Soc.* **86**, 1646−1647 (1964)

14. Gaoni Y. & Mechoulam R. The isolation and structure of delta-1-tetrahydrocannabinol and other neutral cannabinoids from hashish. *J. Am. Chem. Soc.* **93(1)**, 217-24. (1971)

15. Devane W.A., Dysarz F.A. 3rd, Johnson M.R., Melvin L.S., Howlett A.C. Determinationand characterization of a cannabinoid receptor in rat brain. *Mol Pharmacol.* **34(5)**, 605-13. (1988)

16. Elsohly M.A. & Slade D. Chemical constituents of marijuana: The complex mixture of natural cannabinoids. *Life. Sci.* **78**, 539–548. (2005)

17. Mechoulam R., Lander N., Varkony T.H. Kimmel I., Becker O., Ben-Zvi Z., Edery H., Porath G. Stereochemical requirements for cannabinoid activity. *J. of Med- Chem.* **23**, 1068–1072. (1980)

18. Mechoulam R., Feigenbaum J.J., Lander N. Segal M., Järbe T.U., Hiltunen A.J., Consroe P. Enantiomeric cannabinoids: stereospecificity of psychotropic activity. *Experientia.* **44**, 762–764. (1988)

19. Matsuda L.A., Lolait S.J., Brownstein M.J., Young A.C., Bonner T.I. Structure of a cannabinoid receptor and functional expression of the cloned cDNA. *Nature.* **346(6284)**, 561-4. (1990)

20. Munro S., Thomas K.L., Abu-Shaar M. Molecular characterization of a peripheral receptor for cannabinoids. *Nature.* **365(6441)**, 61-5. (1993)

21. Pertwee R.G. & Ross R.A. Cannabinoid receptors and their ligands. *Prostaglandins Leukot Essent Fatty Acids.* **66(2-3)**, 101-21. Review. (2002)

22. Mackie K. & Hille B. Cannabinoids inhibit N-type calcium channels in neuroblastoma glioma cells. *Proc Natl Acad Sci U S A.* **89(9)**, 3825-9. (1992)

23. Gebremedhin D., Lange A.R., Campbell W.B., Hillard C.J., Harder D.R.. Cannabinoid CB1 receptor of cat cerebral arterial muscle functions to inhibit L-type Ca^{2+} channel current. *Am J Physiol.* **276**, H2085-93. (1992)

24. Mackie K., Lai Y., Westenbroek R., Mitchell R. Cannabinoids activate an inwardly rectifying potassium conductance and inhibit Q-type calcium currents in AtT20 cells transfected with rat brain cannabinoid receptor. *J Neurosci.* **15(10)**, 6552-61. (1995)

25. Howlett A.C. Efficacy in CB1 receptor-mediated signal transduction. *Brit. J Pharmacol.* **142**, 1209-1218. Rewiew. (2004)

26. Osei-Hyiaman D., DePetrillo M., Pacher P. Liu J., Radaeva S., Bátkai S., Harvey-White J., Mackie K., Offertáler L., Wang L., Kunos G. Endocannabinoid activation at hepatic CB1 receptors stimulates fatty acid synthesis and contributes to diet-induced obesity. *J. of Clin. Inv.* **115**, 1298–1305. (2005)

27. Ashton J.C. & Glass M. The Cannabinoid CB2 Receptor as a target for inflammation-dependent neurodegeneration. *Current Neuropharmacology*. **5**, 73–80. (2007).

28. Van Sickle M.D., Duncan M., Kingsley P.J. Mouihate A., Urbani P., Mackie K., Stella N., Makriyannis A., Piomelli D., Davison J.S., Marnett L.J., Di Marzo V., Pittman Q.J.,Patel K.D., Sharkey K.A. Identification and functional characterization of brainstem cannabinoid CB2 receptors. *Science* **310**, 329–332. (2005)

29. Onaivi E.S., Ishiguro H., Gong J.P. Patel S., Meozzi P.A., Myers L., Perchuk A., Mora Z., Tagliaferro P.A., Gardner E., Brusco A., Akinshola B.E., Hope B., Lujilde J., Inada T., Iwasaki S., Macharia D., Teasenfitz L., Arinami T., Uhl G.R. Brain neuronal CB2 cannabinoid receptors in drug abuse and depression: from mice to human subjects. *PLoS ONE* **3**, e1640. (2008)

30. Guzma ´nM., Sa ´nchez C. & Galve-Roperh I. Cannabinoids and cell fate. Pharm. & Ther. **95**, 175–184. (2002)

31. Di Marzo V., Bifulco M. & De Petrocellis L. The endocannabinoid system and its therapeutic exploitation. *Nat. Rev. Drug Disc.* **3**, 771–784. (2004)

32. Pertwee R.G.. Pharmacological actions of cannabinoids. *Handbook of Exp. Pharmacol.* **168**, 1–51. (2005)
33. Pacher P., Ba ´ tkai S. & Kunos G. The endocannabinoid system as an emerging target of pharmacotherapy. *Pharmacol. Rev.* **58**, 389–462. (2006)
34. Pertwee R. Evidence for the presence of CB1 cannabinoid receptors on peripheral neurones and for the existence of neuronal non-CB1 cannabinoid receptors. *Life Sci*. **65**, 597–605. (1999)
35. Herkenham M., Lynn A., Johnson M.R., Melvin L.S., de Costa B.R., Rice K.C. Characterization and localization of cannabinoid receptors in rat brain: A quantitative in vitro autoradiographic study. *J Neurosci.* **11**, 563. (1991)
36. Farquhar-Smith W.P., Egertova M., Bradbury E.J., McMahon S.B., Rice A.S., Elphick M.R. Cannabinoid CB(1) receptor expression in rat spinal cord. *Mol Cell Neurosci.* **15(6)**, 510-21. (2000)
37. Cristino L., De Petrocellis L., Pryce G., Baker D., Guglielmotti V., Di Marzo V. Immunohistochemical localization of cannabinoid type 1 and vanilloid transient receptor potential vanilloid type 1 receptors in the mouse brain. *Neuroscience.* **139(4)**, 1405-15. (2006)
38. Cristino L., Starowicz K., De Petrocellis L., Morishita J., Ueda N., Guglielmotti V., Di Marzo V. Immunohistochemical localization of anabolic and catabolic enzymes for anandamide and other putative endovanilloids in the hippocampus and cerebellar cortex of the mouse brain. *Neuroscience.* **151(4)**, 955-68. (2008)
39. Parolaro D. Presence and functional regulation of cannabinoid receptors in immune cells. *Life Sci.* **65(6-7)**, 637-44. (1999)
40. Klein T.W., Newton C., Larsen K., Lu L., Perkins I., Nong L., Friedman H. The cannabinoid system and immune modulation. *J Leukoc Biol.* **74(4)**, 486-96. Rev. (2006)
41. Devane W.A., Hanus L., Breuer A. Pertwee R.G., Stevenson L.A., Griffin G., Gibson D., Mandelbaum A., Etinger A., Mechoulam R. Isolation and structure of a brain constituent that binds to the cannabinoid receptor. *Science.* **258**, 1946–1949. (1992)
42. Mechoulam R., Ben-Shabat S., Hanus L., Ligumsky M., Kaminski N.E., Schatz A.R., Gopher A., Almog S., Martin B.R., Compton D.R., et al. Identification of an endogenous 2-monoglyceride, present in canine gut, that binds to cannabinoid receptors. *Biochemical Pharmacology.* **50**, 83–90. (1995)
43. Sugiura T., Kondo S., Sukagawa A. Nakane S., Shinoda A., Itoh K., Yamashita A., Waku K. 2-Arachidonoylglycerol: a possible

endogenous cannabinoid receptor ligand in brain. *Biochemical and Biophysical Research Communications*. **215**, 89–97. (1995)

44. Burkey T.H., Quock R.M., Consroe P., Ehlert F.J., Hosohata Y., Roeske W.R., Yamamura H.I. Relative efficacies of cannabinoid CB1 receptor agonists in the mouse brain. *Eur J Pharmacol.* **336(2-3)**, 295-8. (1997)

45. Glass M. & Northup J.K. Agonist selective regulation of G proteins by cannabinoid CB(1) and CB(2) receptors. *Mol Pharmacol.* **56(6)**, 1362-9. (1999)

46. Wilson RI, Nicoll RA. Endocannabinoid signalling in the brin. *Science.* **296**, 678-682. (2002)

47. Alger B.E. Retrograde signaling in the regulation of synaptic transmission: focus on endocannabinoids. *Prog. Neurobiol.* **68**, 247–86. (2002)

48. Kano M., Ohno-Shosaku T., Hashimotodani Y., Uchigashima M., Watanabe M. Endocannabinoid mediated control of synaptic transmission. *Physiol Rev.* **89(1)**, 309-80. Review. **(**2009)

49. Ueda N., Okamoto Y., Morishita J. N-acyl phosphatidylethanolamine-hydrolyzing phospholipase D: a novel enzyme of the beta-lactamase fold family releasing anandamide and other N-acylethanolamines. *Life Sci.* **77(14)**, 1750-8. (2005)

50. Cadas H., di Tomaso E. & Piomelli D. Occurrence and biosynthesis of endogenous cannabinoid precursor, N-arachidonoyl phosphatidylethanolamine, in rat brain. *The Journal of Neuroscience*. **17**, 1226–1242. (1997)

51. Stella N., Schweitzer P. & Piomelli D. A second endogenous cannabinoid that modulates long-term potentiation. *Nature.* **388**, 773–778. (1997)

52. Bisogno T., Melck D., De Petrocellis L., Di Marzo V. Phosphatidic acid as the biosynthetic precursor of the endocannabinoid 2-arachidonoylglycerol in intact mouse neuroblastoma cells stimulated with ionomycin. *Journal of Neurochemistry*. **72**, 2113–2119. (1999)

53. Bisogno T., Howell F., Williams G., Minassi A., Cascio M.G., Ligresti A., Matias I., Schiano-Moriello A., Paul P., Williams E.J., Gangadharan U., Hobbs C., Di Marzo V, Doherty P. Cloning of the first sn1-DAG lipases points to the spatial and temporal regulation of endocannabinoid signaling in the brain. *J Cell Biol*. **163**, 463-8. (2003)

54. Cravatt B.F., Giang D.K., Mayfield S.P. Boger D.L., Lerner R.A., Gilula N.B. Molecular characterization of an enzyme that degrades neuromodulatory fatty-acid amides. *Nature.* **384**, 83–87. (1996)

55. Karlsson M., Contreras J.A., Hellman U., Tornqvist H., Holm C. cDNA cloning, tissue distribution, and identification of the catalytic triad of monoglyceride lipase. Evolutionary relationship to esterases, lysophospholipases, and haloperoxidases. *The Journal of Biological Chemistry* **272**, 27218–27223. (1997)

56. Dinh T.P., Carpenter D., Leslie F.M., Freund T.F., Katona I., Sensi S.L., Kathuria S., Piomelli D. Brain monoglyceride lipase participating in endocannabinoid inactivation. *The Proceedings of National Academy of Sciences of the United States of America* **99**, 10819–10824. (2002)

57. Thomas E.A., Cravatt B.F., Danielson P.E., Gilula N.B., Sutcliffe J.G. Fatty acid amide hydrolase, the degradative enzyme for anandamide and oleamide, has selective distribution in neurons within the rat central nervous system. *J Neurosci Res.* **50**, 1047-1052. (1997)

58. Goparaju S.K., Ueda N., Taniguchi K., Yamamoto S. Enzymes of porcine brain hydrolyzing 2-arachidonoylglycerol, an endogenous ligand of cannabinoid receptors. *Biochem Pharmacol.* **57(4)**, 417-23. (1999)

59. Di Marzo V., Bisogno T., De Petrocellis L., Melck D., Orlando P., Wagner J.A., Kunos G. Biosynthesis and inactivation of the endocannabinoid 2-arachidonoylglycerol in circulating and tumoral macrophages. *Eur J Biochem.* **264(1)**, 258-67. (1999)

60. Cox M.L. & Welch S.P. The antinociceptive effect of Delta9-tetrahydrocannabinol in the arthritic rat. *Eur J Pharmacol.* **493(1-3)**, 65-74. (2004)

61. Mechoulam R. & Hanus L. A historical overview of chemical research on cannabinoids. *Chem Phys Lipids.* **108(1-2)**, 1-13. Review. (2000)

62. Pertwee R.G. Cannabinoid receptors and pain. *Prog Neurobiol.* **63(5)**, 569-611. Review. (2001)

63. Check W.A. Marijuana may lessen spasticity of MS. *JAMA.* **241(23)**, 2476. (1979)

64. Baker D., Pryce G., Croxford J.L., Brown P., Pertwee R.G., Makriyannis A., Khanolkar A., Layward L., Fezza F., Bisogno T., Di Marzo V. Endocannabinoids control spasticity in a multiple sclerosis model. *FASEB J.* **15(2)**, 300-2. (2001)

65. Smith P.F. Cannabinoids in the treatment of pain and spasticity in multiple sclerosis. *Curr Opin Investig Drugs.* **3(6)**, 859-64. Review. (2002)

66. Mestre L., Correa .F, Arevalo-Martin A., Molina-Holgado E., Valenti M., Ortar G., Di Marzo V., Guaza C. Pharmacological modulation of the endocannabinoid system in a viral model of multiple sclerosis. *J Neurochem.* **92(6),** 1327-39. (2005)

67. Pertwee R.G. Cannabinoids and multiple sclerosis. *Pharmacol Ther.* **95(2)**, 165-74. Review. (2002)

68. Di Marzo V., Hill M.P., Bisogno T., Crossman A.R., Brotchie J.M. Enhanced levels of endogenous cannabinoids in the globus pallidus are associated with a reduction in movement in an animal model of Parkinson's disease. *FASEB J.* **14(10)**, 1432-8. (2000)

69. Van der Stelt M., Fox S.H., Hill M., Crossman A.R., Petrosino S., Di Marzo V., Brotchie J.M. A role for endocannabinoids in the generation of parkinsonism and levodopa-induced dyskinesia in MPTP-lesioned non-human primate models of Parkinson's disease. *FASEB J.* **19(9)**, 1140-2. (2005)

70. Pazos M.R., Nunez E., Benito C., Tolon R.M., Romero J. Role of the endocannabinoid system in Alzheimer's disease: new perspectives. *Life Sci.* **75(16)**, 1907-15. Review. (2004)

71. Milton N.G. Anandamide and noladin ether prevent neurotoxicity of the human amyloid-beta peptide. *Neurosci Lett.* **332(2)**, 127-30. (2002)

72. Milton N.G. Phosphorylated amyloid-beta: the toxic intermediate in alzheimer's disease neurodegeneration. *Subcell Biochem.* **38**, 381-402. Review. (2005)

73. Lastres-Becker I., Gomez M., De Miguel R., Ramos J.A., Fernandez-Ruiz J. Loss of cannabinoid CB(1) receptors in the basal ganglia in the late akinetic phase of rats with experimental Huntington's disease. *Neurotox Res.* **4(7-8)**, 601-608. (2002)

74. Lastres-Becker I., Bizat N., Boyer F., Hantraye P., Brouillet E., Fernandez-Ruiz J. Effects of cannabinoids in the rat model of Huntington's disease generated by an intrastriatal injection of malonate. *Neuroreport.* **14(6)**, 813-6. (2003)

75. D'Souza D.C., Abi-Saab W.M., Madonick S., Forselius-Bielen K., Doersch A., Braley G., Gueorguieva R., Cooper T.B., Krystal J.H. Delta-9-tetrahydrocannabinol effects in schizophrenia: implications for cognition, psychosis, and addiction. *Biol Psychiatry.* **57(6)**, 594-608. (2005)

76. Rodriguez de Fonseca F., Gorriti M.A., Bilbao A., Escuredo L., Garcia-Segura L.M., Piomelli D., Navarro M. Role of the endogenous cannabinoid system as a modulator of dopamine transmission: implications for Parkinson's disease and schizophrenia. *Neurotox Res.* **3(1)**, 23-35. (2001)

77. De Marchi N., De Petrocellis L., Orlando P., Daniele F., Fezza F., Di Marzo V. Endocannabinoid signalling in the blood of patients with schizophrenia. *Lipids Health Dis*. **2**, 5. (2003)

78. Matias I., Leonhardt M., Lesage J., De Petrocellis L., Dupouy J.P., Vieau D., Di Marzo V. Effect of maternal under-nutrition on pup body weight and hypothalamic endocannabinoid levels. *Cell Mol Life Sci.* **60(2)**, 382-9. (2003)

79. De Lecea L., Kilduff T.S., Peyron C., Gao X., Foye P.E., Danielson P.E., Fukuhara C., Battenberg E.L., Gautvik V.T., Bartlett F.S. 2nd, Frankel W.N., van den Pol A.N., Bloom F.E., Gautvik K.M., Sutcliffe J.G. The hypocretins: hypothalamus-specific peptides with neuroexcitatory activity. *Proc Natl Acad Sci U S A* **95**, 322–327. (1998)

80. Willie J.T. Chemelli R.M., Sinton C.M., Yanagisawa M. To eat or to sleep? Orexin in the regulation offeeding and wakefulness. *Annu. Rev. Neurosci.* **24**, 429–458 (2001)

81. Soppet D.R., Li Y., and Rosen C.A., inventors; Human Genome Sciences Inc., assignees. Human neuropeptide receptor. World Patent no. WO9634877. (1996)

82. Zhu Y., Miwa Y., Yamanaka A., Yada T., Shibahara M., Abe Y., Sakurai T., and Goto K. Orexin receptor type-1 couples exclusively to pertussis toxin-insensitive G-proteins, while orexin receptor type-2 couples to both pertussis toxin-sensitive and -insensitive G-proteins. *J Pharmacol Sci.* **92**, 259–266. (2003)

83. Peyron C., Tighe D.K., van den Pol A.N., de Lecea L., Heller H.C., Sutcliffe J.G., Kilduff T.S. Neurons containing hypocretin (orexin) projectto multiple neuronal systems. *J. Neurosci.* **18**, 9996–10015. (1998)

84. Nambu T., Sakurai T., Mizukami K., Hosoya Y., Yanagisawa M., Goto K. Distribution of orexin neurons in the adult rat brain. *Brain Res.* **827**, 243–260. (1999)

85. Date Y., Ueta Y., Yamashita H., Yamaguchi H., Matsukura S., Kangawa K., Sakurai T., Yanagisawa M., Nakazato M. Orexins, orexigenic hypothalamic peptides,interact with autonomic,

neuroendocrine and neuroregulatory systems. *Proc. Natl. Acad. Sci. U.S.A.* **96**, 748–753. (1999)

86. Chen C.T., Dun S.L., Kwok E.H., Dun N.J. & Chang J.K. Orexin A-like immunoreactivity in the rat brain. *Neurosci Lett.* **260**, 161–164. (1999)

87. Yoshida K., McCormack S., Espana R.A., Crocker A., Scammell T.E. Afferents to the orexin neurons of the rat brain. *J Comp Neurol.* **494**, 845–861. (2006)

88. Sakurai T., Nagata R., Yamanaka A., Kawamura H., Tsujino N., Muraki Y., Kageyama H., Kunita S., Takahashi S., Goto K., Koyama Y., Shioda S., Yanagisawa M. Input of orexin/hypocretin neurons revealed by a genetically encoded tracer in mice. *Neuron.* **46**, 297–308. (2005)

89. Broberger C., De Lecea L., Sutcliffe J.G., Ho¨kfelt T. Hypocretin/orexin- and melanin-concentrating hormone-expressing cells form distinct populations in the rodent lateral hypothalamus: relationship to the neuropeptide Y and agouti gene-related protein systems. *J Comp Neurol*. **402**, 460–474. (1998)

90. Elias C.F., Saper C.B., Maratos-Flier E., Tritos N.A., Lee C., Kelly J., Tatro J.B., Hoffman G.E., Ollmann M.M., Barsh G.S., Sakurai T., Yanagisawa M., Elmquist J.K. Chemically defined projections linking the mediobasal hypothalamus and the lateral hypothalamic area. *J Comp Neurol.* **402**, 442–459. (1998)

91. Cutler D.J., Morris R., Sheridhar V., Wattam T.A., Holmes S., Patel S., Arch J.R.,Wilson S., Buckingham R.E., Evans M.L., Leslie R.A., Williams G. Differential distribution of orexin-A and orexin-B immunoreactivity in the rat brain and spinal cord. *Peptides*. **20**, 1455–1470. (1999)

92. Nixon J.P. & Smale L. A comparative analysis of the distribution of immunoreactive orexin A and B in the brains of nocturnal and diurnal rodents. *Behav Brain Funct.* **3**, 28. (2007)

93. Trivedi P., Yu H., MacNeil D.J., Van der Ploeg L.H., Guan X.M. Distribution of orexin receptor mRNA in the rat brain. *FEBS Lett.* **438,** 71–75. (1998)

94. Lu X.Y., Bagnol D., Burke S., Akil H., Watson S.J. Differential distribution and regulation of OX1 and OX2 orexin/hypocretin receptor messenger RNA in the brain upon fasting. *Horm Behav***. 37**, 335–344. (2000)

95. Marcus J.N., Aschkenasi C.J., Lee C.E., Chemelli R.M., Saper C.B., Yanagisawa M., Elmquist J.K. Differential expression of orexin receptors 1 and 2 in the rat brain. *J Comp Neurol*. **435**, 6–25. (2001)

96. Jo¨hren O., Neidert S.J., Kummer M., Dendorfer A., Dominiak P. Prepro-orexin and orexin receptor mRNAs are differentially expressed in peripheral tissues of male and female rats. *Endocrinology*. **142**, 3324–3331. (2001)

97. Edwards C.M., Abusnana S., Sunter D., Murphy K.G., Ghatei M.A., Bloom S.R. The effect of the orexins on food intake: comparison with neuropeptide Y, melanin-concentrating hormone and galanin. *J Endocrinol.* **160**, R7–12. (1999)

98. Haynes A.C., Jackson B., Chapman H., Tadayyon M., Johns A., Porter R.A., Arch J.R. A selective orexin-1 receptor antagonist reduces food consumption in male and female rats. *Regul Pept.* **96**, 45–51. (2000)

99. Yamada H., Okumura T., Motomura W., Kobayashi Y., Kohgo Y. Inhibition of food intake by central injectionof anti-orexin antibody in fasted rats. *Biochem. Biophys. Res. Commun.* **267**, 527–531. (2000)

100. Yamanaka A., Kunii K., Nambu T., Tsujino N., Sakai A., Matsuzaki I., Miwa Y., Goto K., Sakurai T. Orexin-induced food intake involves neuropeptide Y pathway. *Brain Res.* **24**, 404–409. (2000)

101. Muroya S., Funahashi H., Yamanaka A., Kohno D., Uramura K., Nambu T., Shibahara M., Kuramochi M., Takigawa M., Yanagisawa M., Sakurai T., Shioda S., Yada T. Orexins (hypocretins) directly interact with neuropeptide Y, POMC and glucose-responsive neurons to regulate Ca^{2+} signaling in a reciprocal manner to leptin: orexigenic neuronal pathways in the mediobasal hypothalamus. *Eur. J. Neurosci.* **19**, 1524–1534. (2004)

102. Thorpe A.J. & Kotz C.M. Orexin A in the nucleus accumbens stimulates feeding and locomotor activity. *Brain Res.* **1050**, 156–162. (2005)

103. Baldo B.A., Gual-Bonilla L., Sijapati K., Daniel R.A., Landry C.F., Kelley A.E. Activation of a subpopulation of orexin/hypocretin-containing hypothalamic neurons by GABAA receptor-mediated inhibition of the nucleus accumbens shell, but not by exposure to a novel environment. *Eur. J. Neurosci.* **19**, 376–386. (2004)

104. Shiuchi T., Haque M.S., Okamoto S., Inoue T., Kageyama H., Lee S., Toda C., Suzuki A., Bachman E.S., Kim Y.B., Sakurai T.,

Yanagisawa M., Shioda S., Imoto K., Minokoshi Y. Hypothalamic orexin stimulates feeding-associated glucose utilization in skeletal muscle via sympathetic nervous system. *Cell Metab.* **10**, 466–480. (2009)

105. Anaclet C., Parmentier R., Ouk K., Guidon G., Buda C., Sastre J.P., Akaoka H., Sergeeva O.A., Yanagisawa M., Ohtsu H., Franco P., Haas H.L., Lin J.S. Orexin/ hypocretin and histamine: distinct roles in the control of wakefulness demonstrated using knock-out mouse models. *J Neurosci.* **29**, 14423–38. (2009)

106. Blouin A.M., Thannickal T.C., Worley P.F., Baraban J.M., Reti I.M., Siegel J.M. Narp immunostaining of human hypocretin (orexin) neurons: loss in narcolepsy. *Neurology.* **65**, 1189–92. (2005)

107. Hara J., Beuckmann C.T., Nambu T., Willie J.T., Chemelli R.M., Sinton C.M., Sugiyama F., Yagami K., Goto K., Yanagisawa M., Sakurai T. Genetic ablation of orexin neurons in mice results in narcolepsy, hypophagia, and obesity. *Neuron*. **30**, 345–54. (2001)

108. Huang H., Ghosh P., van den Pol A.N. Prefrontal cortex-projecting glutamatergic thalamic paraventricular nucleus-excited by hypocretin: a feedforward circuit that may enhance cognitive arousal. *J Neurophysiol*. **95**, 1656–68. (2006)

109. Kirouac G.J., Parsons M.P., Li S. Orexin (hypocretin) innervation of the paraven- tricular nucleus of the thalamus. *Brain Res*. **1059**, 179–88. (2005)

110. Kerman I.A., Akil H., Watson S.J. Rostral elements of sympatho-motor circuitry: a virally mediated transsynaptic tracing study. *J Neurosci*. **26**, 3423–33. (2006)

111. Kerman I.A., Bernard R., Rosenthal D., Beals J., Akil H., Watson S.J. Distinct populations of presympathetic-premotor neurons express orexin or melanin-concentrating hormone in the rat lateral hypothalamus. *J Comp Neurol.* **505**, 586–601. (2007)

112. Oldfield B.J., Allen A.M., Davern P., Giles M.E., Owens N.C. Lateral hypothalamic 'command neurons' with axonal projections to regions involved in both feeding and thermogenesis. *Eur J Neurosci.* **25**, 2404–12. (2007)

113. Baldo B.A., Daniel R.A., Berridge C.W., Kelley A.E. Overlapping distributions of orexin/hypocretin- and dopamine-beta-hydroxylase immunoreactive fibers in rat brain regions mediating arousal, motivation, and stress. *J Comp Neurol*. **464**, 220–37. (2003)

114. Espana R.A., Reis K.M., Valentino R.J., Berridge C.W. Organization of hypocretin/orexin efferents to locus coeruleus and

basal forebrain arousal-related structures. *J Comp Neurol*. **481**, 160–78. (2005)

115. Abrahamson E.E., Leak R.K., Moore R.Y. The suprachiasmatic nucleus projects to posterior hypothalamic arousal systems. *Neuroreport*. **12**, 435–440. (2001)

116. Haas H.L., Sergeeva O.A., Selbach O. Histamine in the nervous system. *Physiol Rev*. **88**, 1183–1241. (2008)

117. Abizaid A., Liu Z.W., Andrews Z.B., Shanabrough M., Borok E., Elsworth J.D., Roth R.H., Sleeman M.W., Picciotto M.R., Tschöp M.H., Gao X.B., Horvath T.L. Ghrelinmodulates the activity and synaptic input organization of midbrain dopamine neurons while promoting appetite. *J Clin Invest*. **116**, 3229–3239. (2006)

118. Swanson L.W., Sanchez-Watts G.,Watts A.G. Comparison ofmelanin-concentrating hormone and hypocretin/orexin mRNA expression patterns in a new parceling scheme of the lateral hypothalamic zone. *Neurosci Lett.* **387(2),** 80–4. (2005)

119. Saper C.B., Swanson L.W., Cowan W.M. An autoradiographic study of the efferent connections of the lateral hypothalamic area in the rat. *J Comp Neurol.* **183 (4)**, 689–706. (1979)

120. Simerly R.B. Anatomical substrates of hypothalamic integration. In: Paxinos G, editor. The rat nervous system. Second Edition. San Diego: Academic Press; p. 353–76. (1995)

121. Ter Horst G.J., de Boer P., Luiten P.G., van Willigen J.D. Ascending projections from the solitary tract nucleus to the hypothalamus. A Phaseolus vulgaris lectin tracing study in the rat. *Neuroscience*. **31(3)**, 785–97. (1989)

122. Ter Horst G.J., Luiten P.G. Phaseolus vulgaris leuco-agglutinin tracing of intrahypothalamic connections of the lateral, ventromedial, dorsomedial and paraventricular hypothalamic nuclei in the rat. *Brain Res Bull.* **18(2)**, 191–203. (1987)

123. Elias C.F., Aschkenasi C., Lee C., Kelly J., Ahima R.S., Bjorbaek C., Flier J.S., Saper C.B., Elmquist J.K. Leptin differentially regulates NPY and POMC neurons projecting to the lateral hypothalamic area. *Neuron*. **23(4**), 775–86. (1999)

124. Bittencourt J.C., Presse F., Arias C., Peto C., Vaughan J., Nahon J.L., Vale W., Sawchenko P.E. The melanin- concentrating hormone system of the rat brain: an immuno- and hybridization histochemical characterization. *J Comp Neurol*. **319(2**), 218–45. (1992)

125. Bittencourt J.C., Frigo L., Rissman R.A., Casatti C.A., Nahon J.L., Bauer J.A. The distribution of melanin-concentrating hormone in the monkey brain (Cebusapella). *Brain Res.* **804(1)**, 140–3. (1998)

126. Luttinger D., King R.A., Sheppard D., Strupp J., Nemeroff C.B., Prange Jr A.J. The effect of neurotensin on food consumption in the rat. *Eur J Pharmacol*. **81(3)**, 499–503. (1982)

127. Kristensen P., Judge M.E., Thim L., Ribel U., Christjansen K.N., Wulff B.S., Clausen J.T., Jensen P.B., Madsen O.D., Vrang N., Larsen P.J., Hastrup S. Hypothalamic CART is a new anorectic peptide regulated by leptin. *Nature.* **393(6680)**, 72–6. (1998)

128. Zheng H, Patterson LM, Morrison C, Banfield BW, Randall JA, Browning KN, Travagli R.A., Berthoud H.R. Melanin concentrating hormone innervation of caudal brainstem areas involved in gastrointestinal functions and energy balance. *Neuroscience*. **135(2)**, 611–25. (2005)

129. Kokkotou E.G., Tritos N.A., Mastaitis J.W., Slieker L., Maratos-Flier E. Melanin- concentrating hormone receptor is a target of leptin action in the mouse brain. *Endocrinology.* **142(2)**, 680–6. (2001)

130. Tritos N.A., Mastaitis J.W., Kokkotou E., Maratos-Flier E. Characterization ofmelanin concentrating hormone and preproorexin expression in the murine hypothalamus. *Brain Res.* **895(1–2)**, 160–6. (2001)

131. Tritos N.A., Vicent D., Gillette J., Ludwig D.S., Flier E.S., Maratos-Flier E. Functional interactions between melanin-concentrating hormone, neuropeptide Y, and anorectic neuropeptides in the rat hypothalamus. *Diabetes*. **47(11)**, 1687–92. (1998)

132. Ludwig D.S., Tritos N.A., Mastaitis J.W., Kulkarni R., Kokkotou E., Elmquist J., Lowell B., Flier J.S., Maratos-Flier E. Melanin-concentrating hormone overexpression in transgenic mice leads to obesity and insulin resistance. *J Clin Invest.* **107(3)**, 379–86. (2001)

133. Sakurai T. Orexins and orexin receptors: implication in feeding behavior. *Regul Pept.* **85(1)**, 25–30. (1999)

134. Haynes A.C., Chapman H., Taylor C., Moore G.B., Cawthorne M.A., Tadayyon M., Clapham J.C., Arch J.R. Anorectic, thermogenic and anti-obesity activity of a selective orexin-1 receptor antagonist in ob/ob mice. *Regul Pept.* **104(1–3)**, 153–9. (2002)

135. Leinninger G.M., Jo Y.H., Leshan R.L., Louis G.W., Yang H., Barrera J.G., Wilson H., Opland D.M., Faouzi M.A., Gong Y., Jones J.C., Rhodes C.J., Chua S. Jr, Diano S., Horvath T.L., Seeley R.J., Becker J.B., Münzberg H., Myers M.G. Jr. Leptin acts via leptin

receptor-expressing lateral hypothalamic neurons to modulate the mesolimbic dopamine system and suppress feeding. *Cell Metab*. **10(2)**, 89–98. (2009)

136. Louis G.W., Leinninger G.M., Rhodes C.J., Myers Jr M.G. Direct innervation and modulation of orexin neurons by lateral hypothalamic LepRb neurons. *J Neurosci.* **30(34)**, 11278–87. (2010)

137. Zhang Y., Proenca R., Maffei M., Barone M., Leopold L., Friedman J.M. Positional cloning of the mouse obese gene and its human homologue. *Nature*. **372**, 425–32. (1994)

138. Maffei M., Halaas J., Ravussin E., Pratley R.E., Lee G.H., Zhang Y., Fei H., Kim S., Lallone R., Ranganathan S., et al. Leptin levels in human and rodent: measurement of plasma leptin and ob RNA in obese and weight-reduced subjects. *Nat Med.* **1**:1155–61. (1995)

139. Farooqi I.S., Jebb S.A., Langmack G., Lawrence E., Cheetham C.H., Prentice A.M., Hughes I.A., McCamish M.A., O'Rahilly S. Effects of recombinant leptin therapy in a child with congenital leptin deficiency. *N Engl J Med*. **341**, 879–84. (1999)

140. Halaas J.L., Gajiwala K.S., Maffei M., Cohen S.L., Chait B.T., Rabinowitz D., Lallone R.L., Burley S.K., Friedman J.M. Weight-reducing effects of the plasma protein encoded by the obese gene. *Science*. **269**, 543–6. (1995)

141. Campfield L.A., Smith F.J., Guisez Y., Devos R., Burn P. Recombinant mouse OB protein: evidence for a peripheral signal linking adiposity and central neural networks. *Science.* **269(5223)**, 546-9. (1995)

142. Schwartz M.W., Seeley R.J., Campfield L.A., Burn P., Baskin D.G. Identification of targets of leptin action in rat hypothalamus. *J Clin Invest.* **98(5)**, 1101-6. (1996)

143. Leinninger G.M.. Location, location, location: the CNS sites of leptin action dictate its regulation of homeostatic and hedonic pathways. *Int J Obes.* **33** (Suppl 2), S14–7. (2009)

144. Myers Jr M.G., Munzberg H., Leinninger G.M., Leshan R.L. The geometry of leptin action in the brain: more complicated than a simple ARC. *Cell Metab*. **9**, 117–23. (2009)

145. Robertson S.A., Leinninger G.M., Myers Jr M.G. Molecular and neural mediators of leptin action. *Physiol Behav*. **94**, 637–42. (2008)

146. Chua Jr S.C., Chung W.K., Wu-Peng X.S., Zhang Y., Liu S.M., Tartaglia L., Leibel R.L. Phenotypes of mouse diabetes and rat fatty due to mutations in the OB (leptin) receptor. *Science*. **271**, 994–6. (1996)

147. Coleman D.L.A. Historical perspective on leptin. *Nat Med*. **16**, 1097–9. (2010)

148. White D.W., Kuropatwinski K.K., Devos R., Baumann H., Tartaglia L.A. Leptin receptor (OB-R) signaling. Cytoplasmic domain mutational analysis and evidence for receptor homo-oligomerization. *J Biol Chem*. **272**, 4065–71. (1997)

149. Bahary N., Leibel R.L., Joseph L., Friedman J.M. Molecular mapping of the mouse db mutation. *Proc Natl Acad Sci U S A*. **87**, 8642–6. (1990)

150. Kloek C., Haq A.K., Dunn S.L., Lavery H.J., Banks A.S., Myers Jr M.G. Regulation of Jak kinases by intracellular leptin receptor sequences. *J Biol Chem*. **277**, 41547–55. (2002)

151. Vaisse C., Halaas J.L., Horvath C.M., Darnell Jr J.E., Stoffel M., Friedman J.M. Leptin activation of Stat3 in the hypothalamus of wild-type and ob/ob mice but not db/db mice. *Nat Genet*. **14**, 95–7. (1996)

152. Tartaglia L.A. The leptin receptor. *J Biol Chem.* **272**, 6093–6. (1997)

153. Cohen P., Zhao C., Cai X.,Montez J.M., Rohani S.C., Feinstein P., Mombaerts P., Friedman J.M. Selective deletion of leptin receptor in neurons leads to obesity. *J Clin Invest.* **108**, 1113–21. (2001)

154. Elmquist J.K., Bjorbaek C., Ahima R.S., Flier J.S., Saper C.B. Distributions of leptin receptor mRNA isoforms in the rat brain. *J Comp Neurol*. **395**, 535–47. (1998)

155. Leshan R.L., Bjornholm M., Munzberg H., Myers Jr M.G. Leptin receptor signaling and action in the central nervous system. *Obesity (Silver Spring).* **14**(Suppl 5), 208S–12S. (2006)

156. Scott M.M., Lachey J.L., Sternson S.M., Lee C.E., Elias C.F., Friedman J.M., Elmquist J.K. Leptin targets in the mouse brain. *J Comp Neurol*. **514**, 518–32. (2009)

157. Elmquist J.K., Elias C.F., Saper C.B. From lesions to leptin: hypothalamic control of food intake and body weight. *Neuron*. **22**, 221–232. (1999)

158. Saper C.B., Chou T.C., Elmquist J.K. The need to feed: homeostatic and hedonic control of eating. *Neuron.* **36(2)**, 199-211. Review. (2002)

159. Schwartz M.W., Porte D. Jr. Diabetes, obesity, and the brain. *Science.* **307(5708)**, 375-9. (2005)

160. Spiegelman B.M., Flier J.S. Obesity and the regulation of energy balance. *Cell.* **104(4)**, 531-43. (2001)

161. Cowley M.A., Smart J.L., Rubinstein M., Cerdán M.G., Diano S., Horvath T.L., Cone R.D., Low M.J. Leptin activates anorexigenic

POMC neurons through a neural network in the arcuate nucleus. *Nature.* **411(6836)**, 480-4. (2001)

162. Van den Top M., Lee K., Whyment A.D., Blanks A.M., Spanswick D. Orexigen-sensitive NPY/AgRP pacemaker neurons in the hypothalamic arcuate nucleus. *Nat Neurosci.* **7(5)**, 493-4. (2004)

163. Ahima R.S., Prabakaran D., Flier J.S. Postnatal leptin surge and regulation of circadian rhythm of leptin by feeding. Implications for energy homeostasis and neuroendocrine function. *J Clin Invest.* **101(5)**, 1020-7. (1998)

164. Bouret S.G., Bates S.H., Chen S., Myers M.G. Jr, Simerly R.B. Distinct roles for specific leptin receptor signals in the development of hypothalamic feeding circuits. *J Neurosci.* **32(4)**, 1244-52. (2012)

165. Cross D. A., Alessi D. R., Cohen P., Andjelkovich M., Hemmings B. A. Inhibition of glycogen synthase kinase-3 by insulin mediated by protein kinase B. *Nature*. **378**, 785–789. (1995)

166. Ryder J., Su Y., Ni B., Akt/GSK3beta serine/threonine kinases: evidence for a signalling pathway mediated by familial Alzheimer's disease mutations. *Cell. Signal.* **16**, 187–200. (2004)

167. Cleveland D.W., Hwo S.Y., Kirschner M.W. Physical and chemical properties of purified tau factor and the role of tau in microtubule assembly. *J. Mol. Biol.* **116**, 227-247. (1977)

168. Jameson L., Frey T., Zeeberg B., Dalldorf F., Caplow, M. Inhibition of microtubule assembly by phosphorylation of microtubule-associated proteins. *Biochemistry.* **19**, 2472-2479. (1980)

169. Lindwall G. & Cole R. D. Phosphorylation affects the ability of tau protein to promote microtubule assembly. *J. Biol. Chem.* **259**, 5301-5305. (1984)

170. Cho J.H. & Johnson G.V. Primed phosphorylation of tau at Thr231 by glycogen synthase kinase 3beta (GSK3beta) plays a critical role in regulating tau's ability to bind and stabilize microtubules. *J. Neurochem.* **88**, 349– 358. (2004)

171. Sayas C.L., Avila J., Wandosell F. Glycogen synthase kinase-3 is activated in neuronal cells by Galpha12 and Galpha13 by Rho-independent and Rho-dependent mechanisms. *J. Neurosci.* **22,** 6863–6875. (2002)

172. Sayas C.L., Avila J., Wandosell F. Regulation of neuronal cytoskeleton by lysophosphatidic acid: role of GSK-3. *Biochim. Biophys. Acta.* **1582,** 144–153. (2002)

173. Sartin J.L., Daniel J.A., Whitlock B.K., Wilborn R.R. Selected hormonal and neurotransmitter mechanisms regulating feed intake in sheep. *Animal*. **4**, 1781–1789. (2010)

174. Xi Y., Ryan J., Noble S., Yu M., Yilbas A.E., Ekker M. Impaired dopaminergic neuron development and locomotor function in zebrafish with loss of pink1 function. *Eur J Neurosci.* **31**, 623–33. (2010)

175. Fulton S., Woodside B., Shizgal P. Modulation of brain reward circuitry by leptin. *Science.* **287,** 125–8. (2000)

176. Muroya S., Uramura K., Sakurai T., Takigawa M., Yada T. Lowering glucose concentrations increases cytosolic Ca2+ in orexin neurons of the rat lateral hypothalamus. *Neurosci. Lett.* **309**, 165-168. (2001)

177. Qi Y., Henry B.A., Oldfield B.J., Clarke I.J. The action of leptin on appetite-regulating cells in the ovine hypothalamus: Demonstration of direct action in the absence of the arcuate nucleus. *Endocrinology.* **151**, 2106–2116. (2010)

178. Horvath T.L. Endocannabinoids and the regulation of body fat: the smoke is clearing. *J Clin Invest.* **112**, 323–326. (2003)

179. Buettner C., Muse E.D., Cheng A., Chen L., Scherer T., Pocai A., Su K., Cheng B., Li X., Harvey-White J., Schwartz G.J., Kunos G., Rossetti L., Buettner C. Leptin controls adipose tissue lipogenesis via central, STAT3-independent mechanisms. *Nat Med.* **14**, 667–75. (2008)

180. Inui A. Feeding and body-weight regulation by hypothalamic neuropeptides mediation of the actions of leptin. *TrendsNeurosci*. **22**, 62–7. (1999)

181. Cota D., Marsicano G., Tschop M., Grubler Y., Flachskamm C., Schubert M., Auer D., Yassouridis A., Thöne-Reineke C., Ortmann S., Tomassoni F., Cervino C., Nisoli E., Linthorst A.C., Pasquali R., Lutz B., Stalla G.K., Pagotto U. The endogenous cannabinoid system affects energy balance via central orexigenic drive and peripheral lipogenesis. *J Clin Invest.* **112**, 423–31. (2003)

182. Matias I., Cristino L., Di Marzo V. Endocannabinoids: some like it fat (and sweet too). *J Neuroendocrinol.* **20 (**Suppl 1), 100-9. Review. (2008)

183. Horvath T.L., Diano S., Van Den Pol A.N. Synaptic interaction between hypocretin (orexin) and neuropeptide Y cells in the rodent and primate hypothalamus: a novel circuit implicated in metabolic and endocrine regulations. *J. Neurosci.* **19**, 1072–1087 (1999)

184. Horvath T.L., Peyron C., Diano S., Ivanov A., Aston-Jones G., Kilduff T.S., van Den Pol A.N. Hypocretin (orexin) activation and synaptic innervation of the locus coeruleus noradrenergic system. *J. Comp. Neurol.* **415**, 145–159 (1999)

185. Yi H., Leunissen J., Shi G., Gutekunst C., Hersch S. A novel procedure for pre-embedding double immunogold-silver labeling at the ultrastructural level. *J Histochem Cytochem.* **49**, 279-84. (2001)

186. Keimpema E. et al. Differential subcellular recruitment of monoacylglycerol lipase generates spatial specificity of 2-arachidonoyl glycerol signaling during axonal pathfinding. *J Neurosci.* **30,** 13992-14007 (2010).

187. Wittmann G., Deli L., Kalló I., Hrabovszky E., Watanabe M., Liposits Z., Fekete C. Distribution of type 1 cannabinoid receptor (CB1)-immunoreactive axons in the mouse hypothalamus. *J Comp Neurol.* **503**, 270-9 (2007)

188. Yoshida T., Uchigashima M., Yamasaki M., Katona I., Yamazaki M., Sakimura K., Kano M., Yoshioka M., Watanabe M. Unique inhibitory synapse with particularly rich endocannabinoid signaling machinery on pyramidal neurons in basal amygdaloid nucleus. *Proc. Natl. Acad. Sci. U S A.* **108**, 3059-3064. (2011)

189. Uchigashima M., Narushima M., Fukaya M., Katona I., Kano M., Watanabe M. Subcellular arrangement of molecules for 2-Arachidonoyl-glicerol-mediated retrograde signaling and its physiological contribution to Synaptic modulation in the striatum. *J.Neurosci.* **27**, 3663-3676. (2007)

190. Eggermann E., Bayer L., Serafin M., Saint-Mleux B., Bernheim L., Machard D., Jones B.E., Mühlethaler M. The wake-promoting hypocretin-orexin neurons are in an intrinsic state of membrane depolarization. *J Neurosci.* **23**, 1557-62. (2003)

191. Huang H., Acuna-Goycolea C., Li Y., Cheng H.M., Obrietan K., van den Pol A.N. Cannabinoids excite hypothalamic melanin-concentrating hormone but inhibit hypocretin/orexin neurons: implications for cannabinoid actions on food intake and cognitive arousal. *J Neurosci.* **27**, 4870-81 (2007)

192. Jo Y.H., Chen Y.J., Chua S.C. Jr, Talmage D.A., Role L.W. Integration of endocannabinoid and leptin signaling in an appetite-related neural circuit. *Neuron.* **48**, 1055-66. (2005)

193. Di Marzo V. Endocanabinoid signaling in the brain: biosynthetic mechanisms in the limelight. *Neurosci.* **14**, 9-15. (2011)

194. Alger B.E. & Kim J. Supply and demand for endocannabinoids. *Trends Neurosci.* **34**, 304-315. (2011)

195. Münzberg H., Flier J.S., Bjørbaek C. Region-specific leptin resistance within the hypothalamus of diet-induced obese mice. *Endocrinology*. **145**, 4880-9. (2004)

196. Malcher-Lopes R., Di S., Marcheselli V.S., Weng F.J., Stuart C.T., Bazan N.G., Tasker J.G.. Opposing crosstalk between leptin and glucocorticoids rapidly modulates synaptic excitation via endocannabinoid release. *J Neurosci.* **26**, 6643-50. (2006)

RINGRAZIAMENTI

Nel giorno del conseguimento di un importante obiettivo della mia vita personale e lavorativa, non posso esimermi dal ringraziare le molte persone che con la loro presenza mi hanno accompagnato e mi hanno permesso di terminare con successo il Dottorato di Ricerca.

In primis un ringraziamento particolare va al mio Tutor, la Dott.ssa Luigia Cristino, per aver creduto in me e per la pazienza e lo spirito critico con cui mi ha sostenuto, consigliato ed aiutato, sia in ambito lavorativo che personale, durante tutto lo svolgimento degli esperimenti e la stesura della tesi e per avermi trasmesso la passione per la ricerca. La ringrazio per la stima e l'affetto dimostratomi e per avermi trasmesso il suo entusiasmo nello spingersi oltre le proprie conoscenze, nel porsi sempre nuove domande, cercando le risposte nella sperimentazione, in una disciplina affascinante quale la Neurobiologia.

Ringrazio inoltre il Prof. Giuseppe Busetto, dell'Università di Verona, per avermi trasmesso con la sua passione e la sua dedizione, sempre conditi con un pizzico di ironia e col sorriso, l'amore per l'elettrofisiologia, senza di lui questo lavoro non sarebbe stato completo e le mie avventure Veronesi non sarebbero state così interessanti e piacevoli.

Ringrazio tutte le persone che hanno reso possibile la stesura di questo lavoro, in particolare la Dott.ssa Stefania Petrosino, dell'istituto di chimica biomolecolare (ICB) del C.N.R. di Pozzuoli, Il Dott. Pierangelo Orlando dell'istituto di chimica biomolecolare (ICB) del C.N.R. di Pozzuoli e il Dott. Vincvenzo Di Marzo "Boss" dell'Endocannabinoid Research group del C.N.R. di Pozzuoli.

Un lavoro di tesi è fatto anche della quotidianità del laboratorio e per questo sento di dover ringraziare tutti quelli che mi hanno accompagnato nel cammino di ogni giorno. Infinite grazie a Mari Antonietta Di Grazia per tutte le volte che mi ha ascoltato, incoraggiato e sostenuto fuori e dentro il laboratorio e per essere sempre riuscita a strapparmi un sorriso anche nelle situazioni peggiori. Grazie a tutti i ragazzi dell'Endocannabinoid Research group del C.N.R. di Pozzuoli.per la loro disponibilità.

Un grazie di cuore va ai miei genitori ed alla mia famiglia per il bene smisurato che continuamente mi dimostrano e per tutti i sacrifici che continuano a fare per me e per aver sempre mostrato per ciò che faccio una fiducia cieca e priva di incertezze, spronandomi sempre ad andare avanti per la mia strada. Con questo lavoro spero di poter ripagare almeno in parte tutti i sacrifici fatti affinché questo giorno da me tanto desiderato arrivasse.

Ringrazio, infine, tutti coloro che hanno creduto in me, più che mai nei momenti in cui il cammino diventava difficile, e le energie per affrontare le difficoltà sembravano esaurirsi.

Roberta Imperatore